SANDIA REPORT
SAND2020-11145
Printed October 2020

Sandia National Laboratories

Early-Time (E1) High-Altitude Electromagnetic Pulse Effects on Transient Voltage Surge Suppressors

Rodrigo E. Llanes — Sandia National Laboratories
Nikita D. Dougan — University of New Mexico
Ken V. Le — University of New Mexico
Matt Halligan — Sandia National Laboratories
Ross Guttromson — Sandia National Laboratories
Jane Lehr — University of New Mexico
David E. Sanabria-Diaz — University of New Mexico

Prepared by
Sandia National Laboratories
Albuquerque, New Mexico
87185 and Livermore,
California 94550

Issued by Sandia National Laboratories, operated for the United States Department of Energy by National Technology & Engineering Solutions of Sandia, LLC.

Available to DOE and DOE contractors from
U.S. Department of Energy
Office of Scientific and Technical Information
P.O. Box 62
Oak Ridge, TN 37831

Telephone: (865) 576-8401
Facsimile: (865) 576-5728
E-Mail: reports@osti.gov
Online ordering: http://www.osti.gov/scitech

Available to the public from
U.S. Department of Commerce
National Technical Information Service
5301 Shawnee Rd
Alexandria, VA 22312

Telephone: (800) 553-6847
Facsimile: (703) 605-6900
E-Mail: orders@ntis.gov
Online order: https://classic.ntis.gov/help/order-methods/

ABSTRACT

Determining the effectiveness of surge and pulse protection devices in the United States power grid against effects of a High-Altitude Electromagnetic Pulse (HEMP) is crucial in determining the present state of grid resilience. Transient Voltage Surge Suppressors (TVSS) are used to protect loads in substations from transient overvoltages. Designed to mitigate the effects of lightning, their response to a HEMP event is unknown and was determined. TVSSs were tested in two unique configurations using a pulser that generates pulses in the tens of nanoseconds scale to determine their protective capability as well as to determine their self-resilience against HEMP pulses. Testing concluded that TVSS devices adequately protect against microsecond scale pulses like lightning but do not protect against pulses resembling HEMP events. It suggests that TVSS devices should not be relied upon to mitigate the effects of HEMP pulses.

ACKNOWLEDGEMENTS

The authors would like to thank Dr. Andrew Fierro for his input and advisement throughout the conduction of this research. The authors would also like to thank Mike Dinallo for his services providing a peer review for this paper.

CONTENTS

LIST OF FIGURES

LIST OF TABLES

This page left blank

EXECUTIVE SUMMARY

Transient Voltage Surge Suppressors (TVSS) are devices used throughout the United States to protect sensitive loads from high voltage pulses that may be seen in electrical systems. Their ability to protect loads against pulses generated from a high-altitude nuclear detonation as well as their ability to withstand those types of overvoltages was evaluated in this report.

The protection devices were subjected to conducted pulse testing in two unique configurations using an energized circuit meant to replicate real-world conditions. The devices' responses to the tests were evaluated to determine their effectiveness in providing proper protection against a conducted E1 HEMP pulse. Their ability to withstand pulses without incurring damage was also evaluated.

The proper function of the devices was first verified by testing them with a conducted pulse similar in timescale to those which they were designed to protect against, lightning. Conducted pulse testing emulating a coupled E1 HEMP pulse was then commenced and the TVSS devices' responses were evaluated. Testing on each device was conducted at increasing pulse magnitudes and the state of health of each device after each test increment was evaluated. A total of eight devices were tested at three different voltage increments in two different test configurations.

The conclusion of the conducted tests demonstrated that the devices did not respond to the E1 HEMP pulse . This response is due to the time required for the protection circuitry inside of the devices to activate and properly protect against an overvoltage. The state of health evaluation for each device determined that they incurred no damage from the conducted pulse test.

ACRONYMS AND DEFINITIONS

Abbreviation	Definition
CVT	Current Viewing Transformer
DUT	Device Under Test
E1	Early-Time
FFT	Fast Fourier Transform
FWHM	Full-Width Half-Maximum
HEMP	High-altitude electromagnetic pulse
I-V	Current-Voltage
LTG	Line-to-Ground
LTN	Line-to-Neutral
MCOV	Maximum Continuous Operating Voltage
MOV	Metal Oxide Varistor
NTG	Neutral-to-Ground
PCB	Printed Circuit Board
SOH	State of health
TVSS	Transient Voltage Surge Suppressor
VPR	Voltage Protection Rating
ZnO	Zinc Oxide

1. INTRODUCTION

Effects of High-Altitude Electromagnetic Pulses (HEMP) have been studied since their discovery in early nuclear weapons testing during the mid-20th century. The early-time (E1) of a HEMP event poses concern with its potential impact to the power grid of the United States. The generated electromagnetic fields can couple to conductors in a variety of locations, including substations, creating a high magnitude voltage pulse [1]. The large voltage pulse travelling through the conductors has a potential to cause upset or damage to the devices connected to them. The devices this report is concerned with are substation components such as low voltage circuit breakers and digital protective relays. These components are essential for the proper function of the national power grid and damage to these components would hinder the operation of the substations in which they're located.

Transient Voltage Surge Suppressors (TVSS) potentially mitigate the effects of high voltage pulses and are already installed in some power systems to protect against other forms of high voltage pulses such as lightning strikes or other switching transients. The TVSS' were subjected to conducted pulse testing with a representative HEMP E1 waveform to evaluate their ability to withstand protect against E1. This document outlines the methodology used in the development of the test, reports on the results, and makes a final determination on the device's response.

2. TEST DESCRIPTION

2.1. Components

2.1.1. Transient Voltage Surge Suppressor

A TVSS is used to protect substation equipment from high voltage pulses such as lighting strikes and other switching events. The TVSS is placed between the protected device and the electrical source of the potential impulse and, under standard operating conditions, behaves as a high impedance in parallel with the protected device. When an overvoltage is detected, the TVSS behaves as a low impedance and provides a shunt to ground, diverting energy and clamping the voltage.

TVSS' use a network of metal oxide varistors (MOV) to provide protection for loads. An MOV is a device made of Zinc Oxide (ZnO) and other oxides that operates as a bi-polar, non-linear voltage-clamping device [2]. MOVs conduct minimal current until a voltage threshold, known as its clamping voltage, is reached. The MOV then conducts current rapidly as the voltage across it increases slowly. The passive voltage-clamping characteristics make MOVs a popular choice for overvoltage circuit protection because, under normal operating conditions, little impact to overall circuit performance is seen.

The TVSS tested is a SolaHD® STV25K Series, single phase device rated for operation in a 240 VAC circuit. It has a Maximum Continuous Operating Voltage (MCOV) rating of 300 V, an operating frequency range of 47-63 Hz, a 20 A input current rating and a voltage protection rating (VPR) of 900 V. It contains six terminals: the line side of the TVSS has a line, neutral, and ground terminal and the load side of the TVSS has a load, neutral, and ground terminal. The device contains three protection circuits each comprised of a network of MOVs that offer protection for line-to-neutral (LTN), line-to-ground (LTG), and neutral-to-ground (NTG) Figure 2-1 and Figure 2-2 contain images of the TVSS and the printed circuit board (PCB) within it and Figure 2-3 contains a circuit model for the TVSS device.

Figure 2-1. Photo of the Front Face of the SolaHD® TVSS

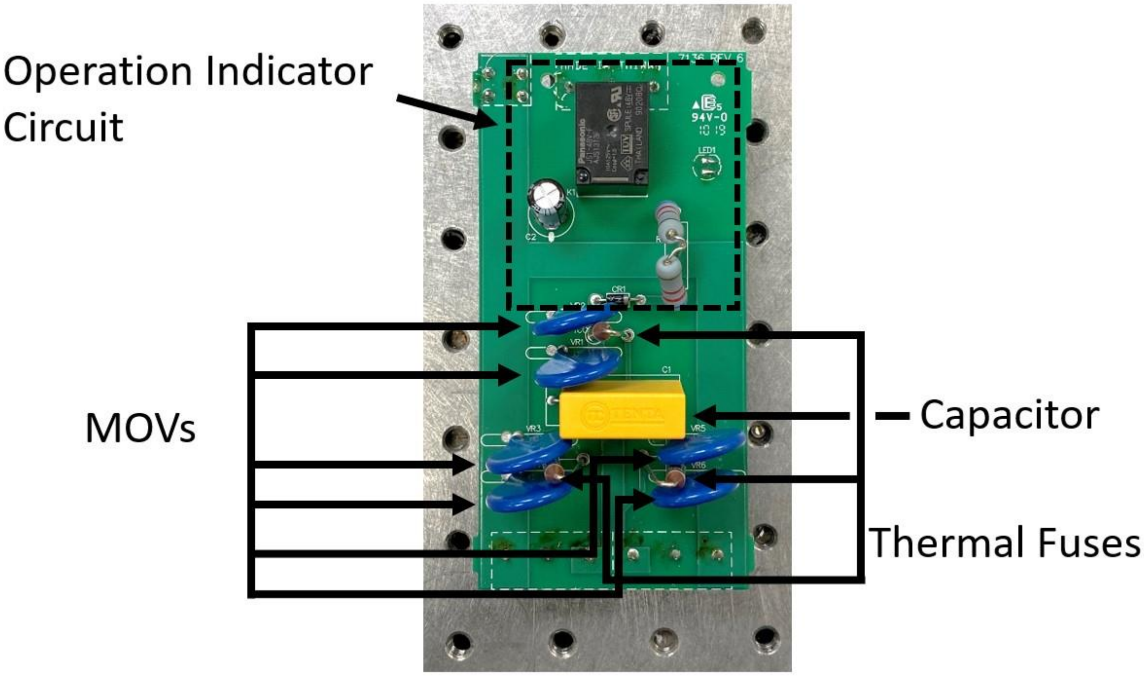

Figure 2-2. Photo of the Exposed PCB of the SolaHD® TVSS

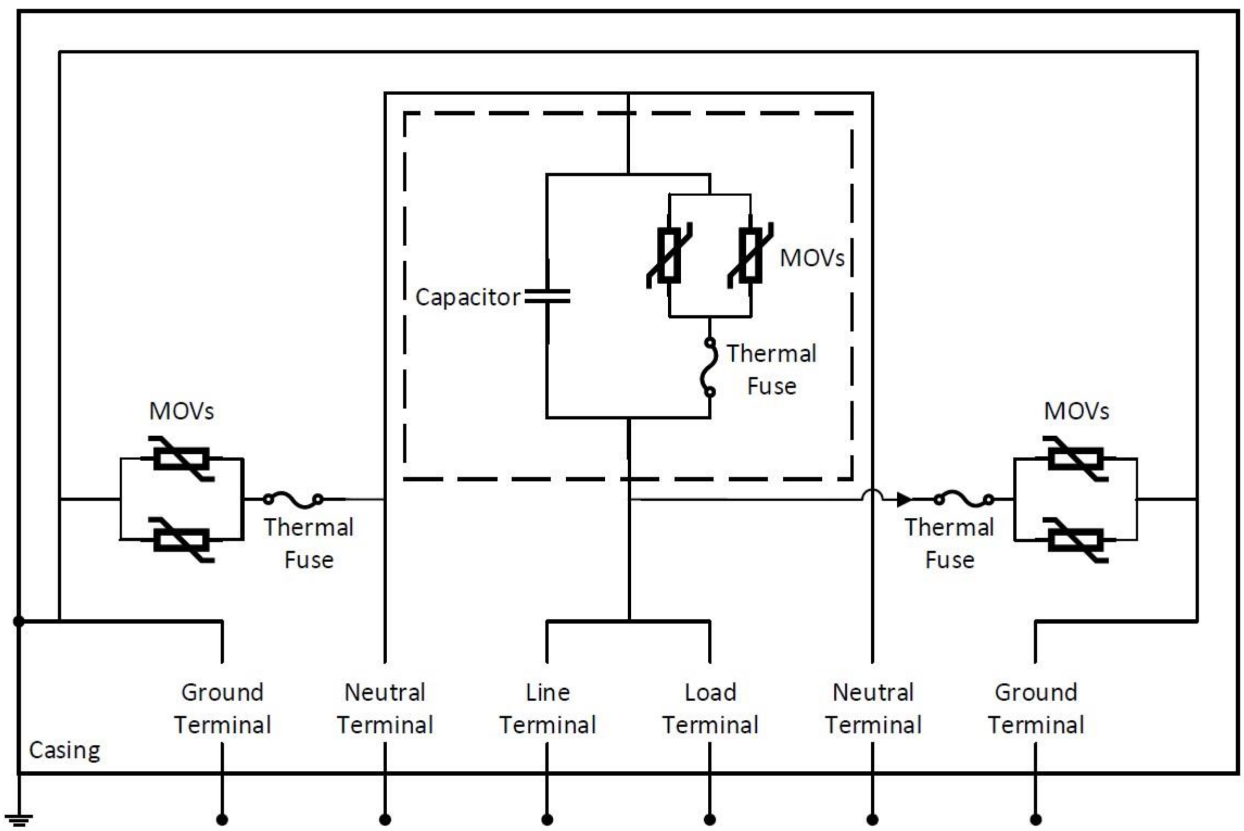

Figure 2-3. Circuit Diagram for SolaHD® TVSS

2.1.2. *University of New Mexico Pulser*

A pulser designed by The University of New Mexico (UNM) [3] was used to generate the insult pulse for the test. It outputs a double exponential pulse with a risetime of 10-15 ns and a full width half maximum (FWHM) pulsewidth of approximately 30-75 ns. Figure 2-4 contains an image of the pulser.

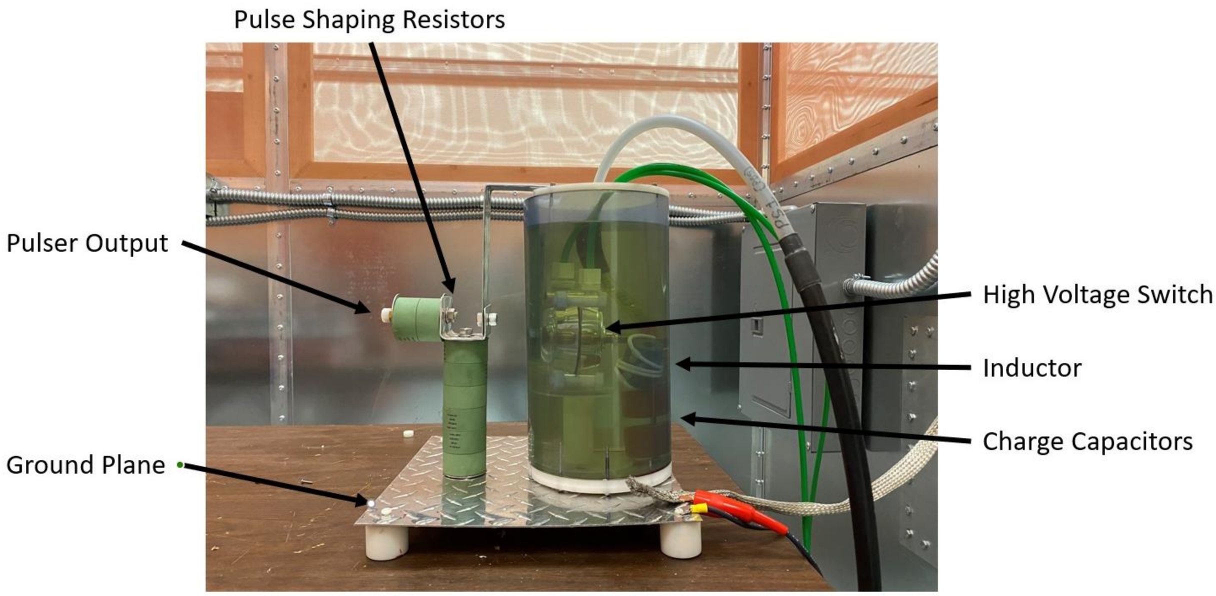

Figure 2-4. Pulser Designed by UNM for Conducted Pulse Testing

The pulser output can be adjusted by varying the charge voltage on the capacitors and the gas pressure in the air spark gap switch. Figure 2-5 shows the relationship between output voltage and pulse shape. The voltage is measured "open circuit" with a Northstar® high impedance voltage probe connected between the output and ground plane of the pulser.

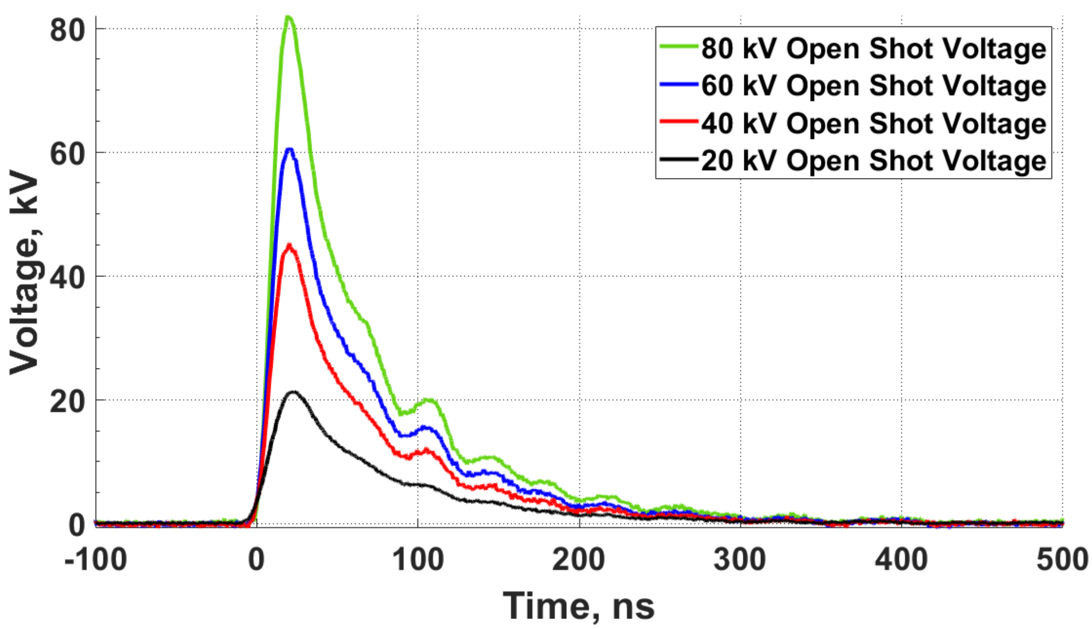

Figure 2-5. UNM Pulser Open Circuit Output Incremented Voltages, 10pt. Rolling Average

Table 2-1. Waveform Characteristics from Open Configuration Pulser Output

Open Circuit Voltage	Risetime (10%-90%)	Pulsewidth (FWHM)
20 kV	18 ns	54 ns
40 kV	14 ns	44 ns
60 kV	13 ns	42 ns
80 kV	12 ns	41 ns

2.2. Test Configurations

Each TVSS was subjected to the conducted pulse test in two different configurations. Both were conducted with the TVSS connected to a 240 V AC, 60 Hz circuit terminated with a 150 Ω resistor. A step-up transformer connected to a 120 V wall receptable was used as the voltage source. The TVSSs are always in an operating circuit when placed in a substation. Typically, they protect digital protective relays and circuit breakers that are part of the substation metering network. Determining their response to a conducted E1 pulse while in an energized circuit ensures that the response observed in the test resembles the response that would likely occur in a real HEMP event. The subsequent sections detail the configurations.

2.2.1. Common-Mode Testing

The first configuration determined the TVSS response to an E1 pulse coupling to a two-conductor circuit in a substation yard. During a HEMP event, a two-conductor circuit would experience overvoltage spikes on both conductors due to their equal exposure to the radiated field from E1. The test was conducted by injecting a pulse into the line and neutral terminals of the TVSS which simulates the generation of an overvoltage spike on each conductor. This is known as a common mode configuration. The TVSS was evaluated by its ability to withstand and protect against the injected pulses.

The pulser output was connected to the line and neutral terminals of the TVSS. The pulser ground plane was connected to the grounded casing of the device via a DIN rail which is the industry standard for connecting rack-mounted equipment. The TVSS was also connected to the 240 V AC circuit mentioned previously. Connections from the transformer were made by connecting the energized and neutral conductors to the TVSS line and neutral terminals, respectively, and the ground conductor to the pulser ground plane. The 150 Ω resistor was connected between the TVSS load and neutral terminals. Figure 2-6 details the circuit model representation of the conducted pulse common mode configuration and Figure 2-7 contains a photo of the common mode test configuration. The configuration will be discussed in further detail in the subsequent paragraphs.

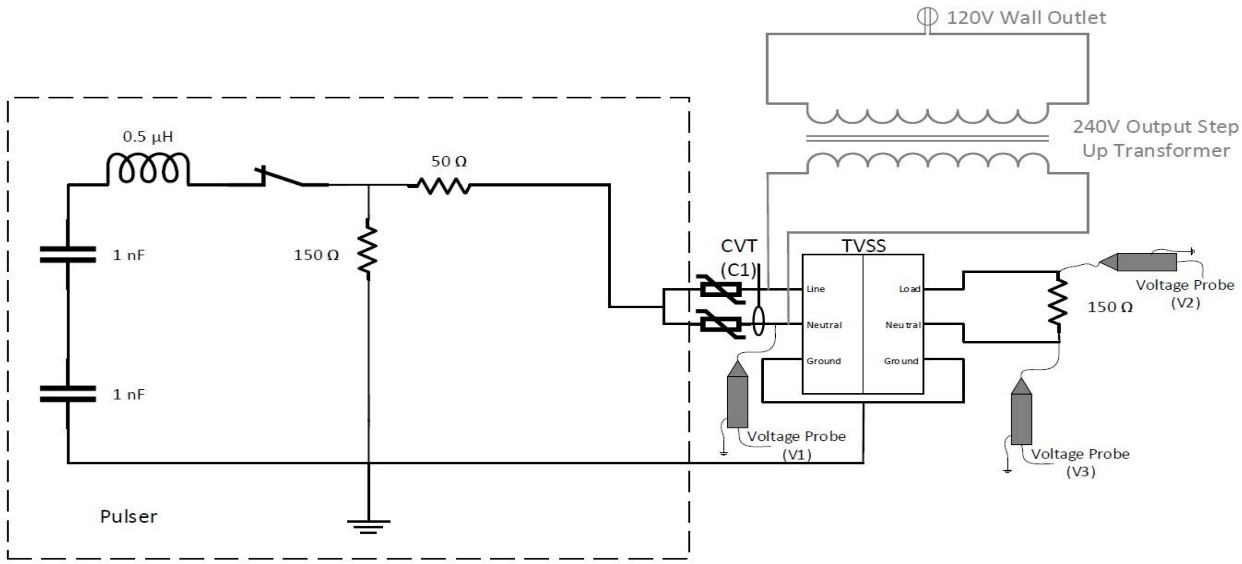

Figure 2-6. Common Mode Test Configuration

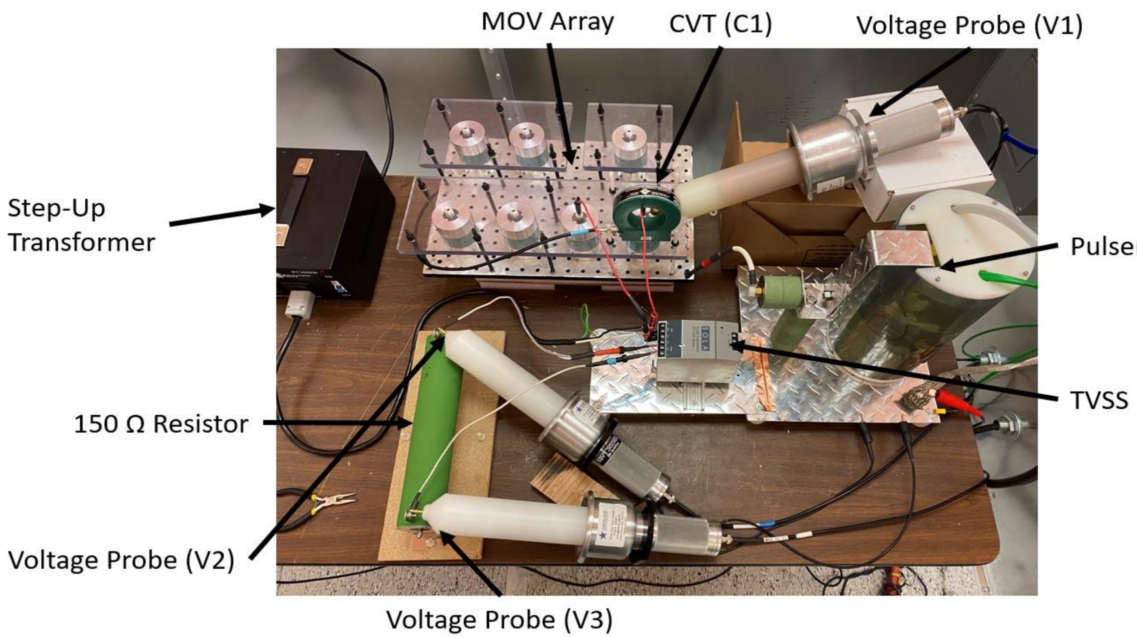

Figure 2-7. Photo of Common Mode Test Configuration

The pulser connections to the TVSS can result in a short circuit condition in the AC circuit. To mitigate this, a connection fixture of MOVs made by the EMP Grand Challenge team at Sandia National Laboratories (SNL) was used in the test configuration. The fixture was used to place an MOV in series between the pulser output and each TVSS terminal. The clamping voltage characteristics of the MOVs [4] ensured that the pulser connections appeared as a high impedance to the AC circuit, preventing a short circuit condition. The fixture consisted of a metal plate which was connected to the pulser output and seven MOVs electrically connected to the plate. A metal disk was placed on top of each MOV and served as the connection point between them and the TVSS terminals. Only two MOVs from the fixture were used for the common mode test configuration. Figure 2-8 contains a diagram of the pulser output through the MOV fixture and Figure 2-9 contains a photo of it.

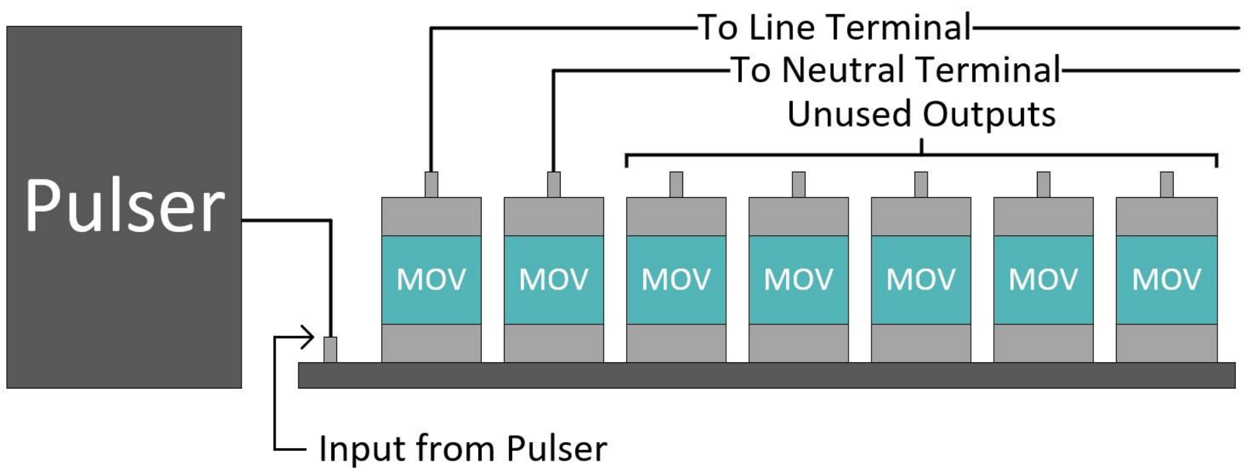

Figure 2-8. Pulser Output Through MOV Fixture

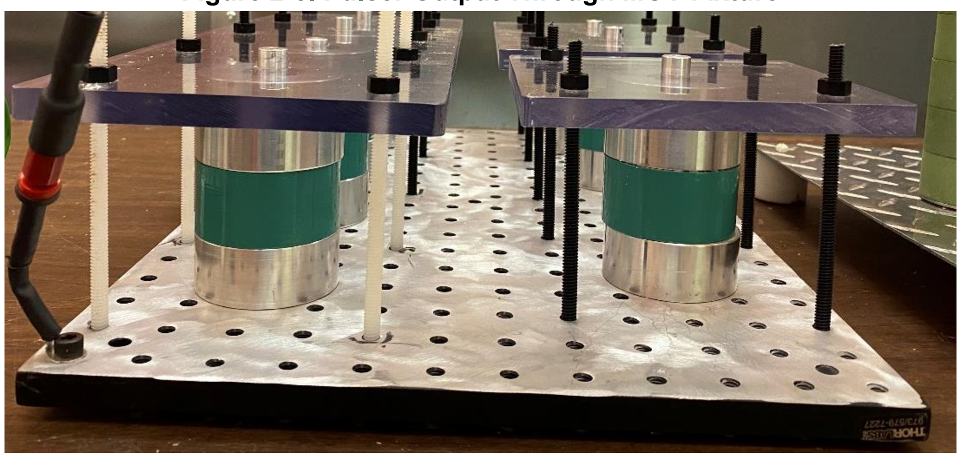

Figure 2-9. MOV Fixture

Comparisons between the pulser output with and without an MOV from the fixture in series were made to ensure that the MOV in series did not add any undesirable effects to the waveform. Comparisons were made at open circuit pulser output increments of 20 kV, 40 kV, 60 kV, and 80 kV. Voltages were measured using a Northstar® high-impedance voltage probe. Figure 2-10 contains the results of this test.

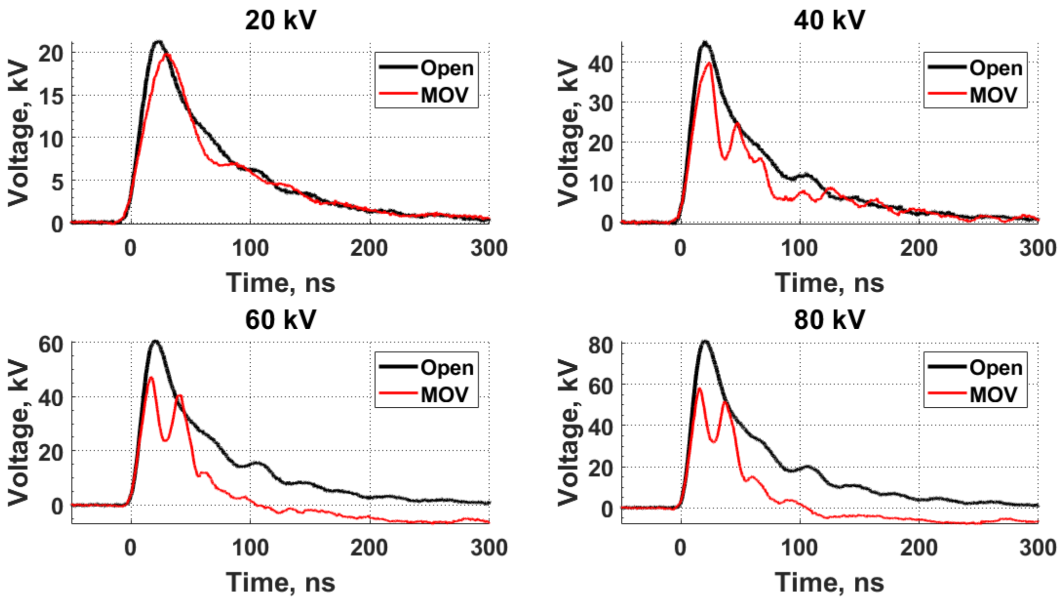

Figure 2-10. Pulser Open Circuit Output Comparison, Output vs. through MOV, 10pt. Rolling Average

The plots demonstrate an increased signal distortion and amplitude loss between the open circuit output and output through an MOV as the pulser voltage output is increased. This is due to the impedance introduced into the test by the MOVs. However, the output pulse through the MOV still demonstrated the appropriate risetime and FWHM for the conducted pulse testing on the TVSS devices as listed in Table 2-1.

Three Northstar® voltage probes and one Pearson® current viewing transformer (CVT) probe were used to monitor the circuit during testing. Probe V1 measured the voltage output through a terminal of the MOV fixture, probe V2 measured the voltage across the TVSS LTG protection circuit, and probe V3 measured the voltage across the TVSS NTG protection circuit. The CVT monitored the output current from one MOV fixture terminal. The total output current of the pulser per shot would be effectively double what was measured through the CVT.

2.2.2. Single-Ended Testing

The second configuration determined the TVSS response to an E1 pulse conducted into only the line terminal. In the common mode configuration discussed in Section 2.2.1, current does not flow through the boxed protection circuit in Figure 2-3 because both the line and neutral terminals are at an equal voltage potential. By conducting the pulse into only the line terminal, some current will flow through the boxed protection circuit. This test configuration in conjunction with the common mode configuration ensures that each protection circuit in each device is subjected to the conducted testing. The TVSSs were connected to the 240 V AC circuit for this test configuration as well. This ensured that they were tested in the same environmental conditions for both tests. The TVSS was evaluated by its ability to withstand and respond to the injected pulse.

The pulser output was connected to the TVSS line terminal. The pulser ground plane was connected to the grounded TVSS casing via a DIN rail. The connection from the pulser to the TVSS was made through the MOVs in the fixture mentioned in the previous section to ensure output consistency between the two test configurations. The TVSS was placed in the 240 V AC circuit by connected the energized output from the step-up transformer to the TVSS line terminal while leaving the neutral conductor disconnected. The ground conductor for the TVSS was connected to the pulser ground plane. The 150 Ω resistor was connected between the TVSS load terminal and the pulser ground plane.

Two voltage probes and a CVT were used to monitor the circuit during testing. Probe V1 measured the voltage output of the pulser after the MOV in the fixture and probe V2 measured the voltage across the load. The CVT (C1) measured the current output of the pulser through the MOV in the fixture. Figure 2-11 details the circuit model representation of the single-ended testing configuration and Figure 2-12 contains a photo depicting the test configuration.

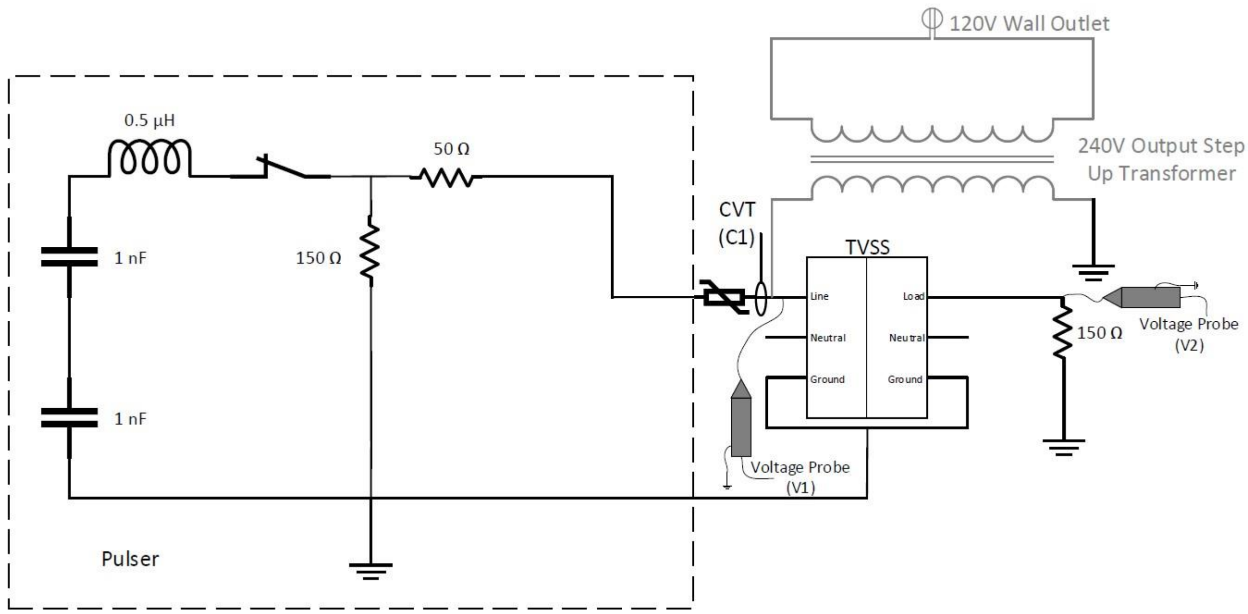

Figure 2-11. Single-Ended Test Configuration Circuit Model

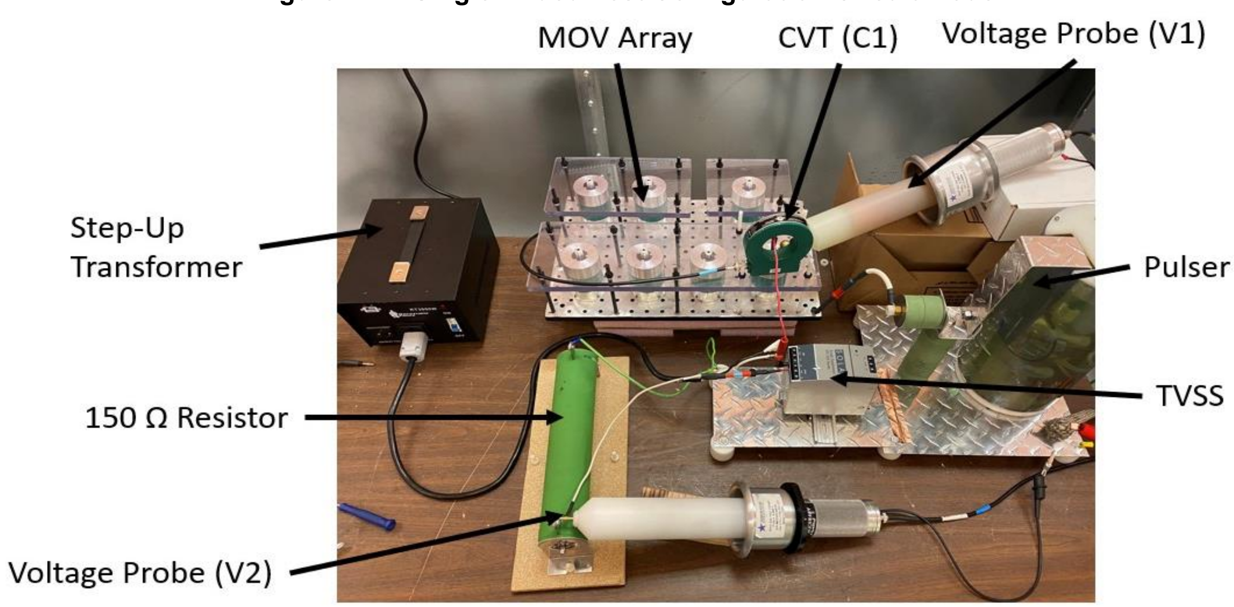

Figure 2-12. Photo of Single-Ended Test Configuration

2.3. State of Health

State of health (SOH) measurements were developed to determine the ability of each TVSS to withstand the conducted pulse tests. Three measurements were conducted on each device after each test iteration to determine if any damage had been incurred. The subsequent sections detail the measurements.

2.3.1. Impedance Characterization

Noting any change in the frequency dependent impedance characteristics of each TVSS was the first state of health metric conducted after each test iteration. A vector network analyzer (VNA) used in conjunction with a ground plane structure shown in Figure 2-13 were used to collect the impedance data. The ground plane fixture allows a device to be connected in series with the inner conductor of the VNA coax cables while still maintaining continuity of the outer conductors.

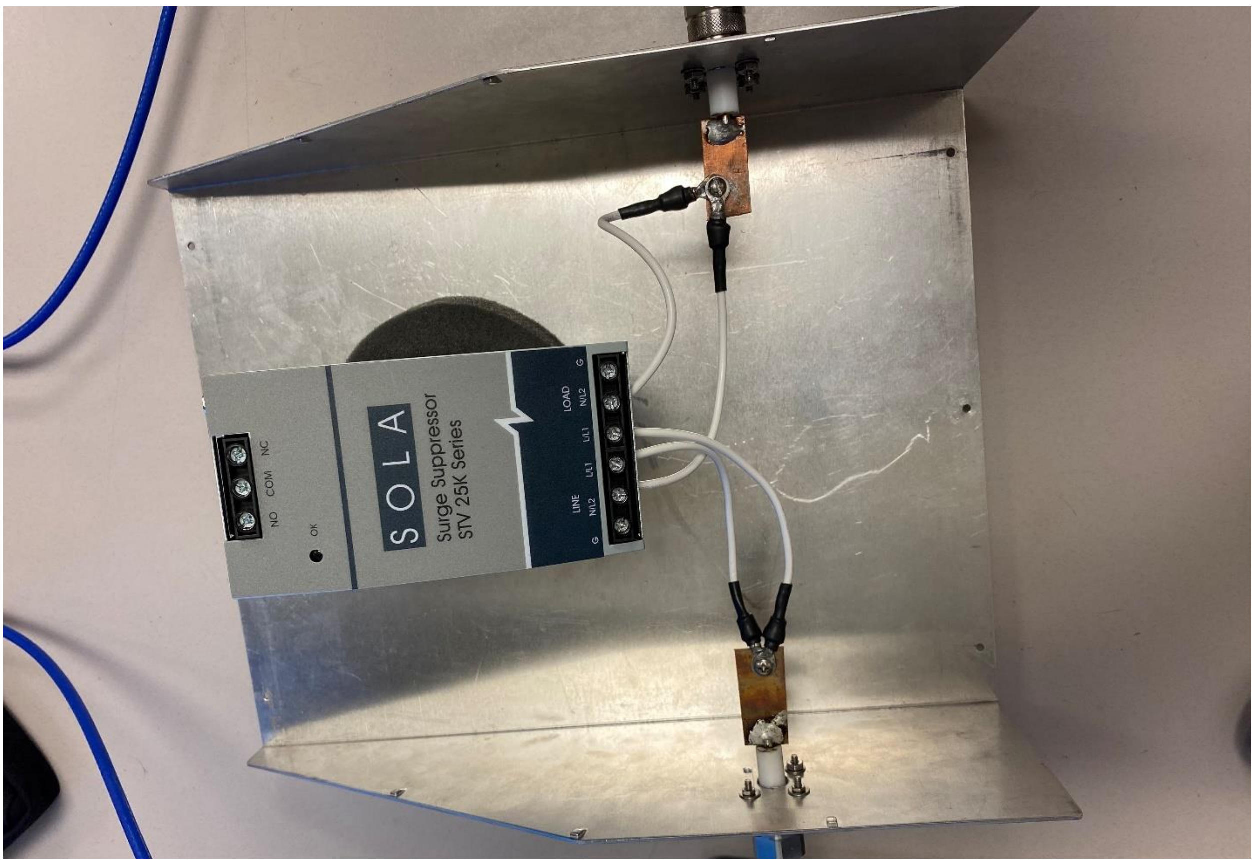

Figure 2-13. VNA Sweep Configuration

Each TVSS contained three unique circuits as noted in Figure 2-3. The ensure that the impedance characteristics of each circuit were being extracted, VNA sweeps were conducted in three different configurations: LTG, LTN, and NTG.

To extract impedance characteristics from the VNA frequency sweeps, the raw Touchstone files were converted to ABCD-Parameters using Matlab. The B-term was approximated to be the through impedance of the circuit [5] and capacitance and inductance were extracted using the through impedance. Any significant changes in the extracted capacitance and inductance values denoted that the injected pulse caused damage or degradation to the circuit.

All sweeps in subsequent sections were conducted across a frequency range of 100 kHz – 1 GHz. Baseline sweeps were performed on each device before any testing commenced. The values for capacitance and inductance after each test were compared with baseline measurements to determine if any changes were observed.

2.3.1.1. Line-to-Ground

To extract the network parameters for the circuit in the dashed box shown in Figure 2-14, its through impedance was measured using a VNA. The VNA's port 1 was connected to the TVSS' line and load terminals and port 2 to its ground.

Verification that the test configurations extracts the proper network parameters for each internal TVSS protection circuit assumes that each TVSS protection circuit has an approximately equal characteristic impedance. The circuit diagram in Figure 2-3 demonstrates that any alternate current path through the TVSS from port 1 to port 2 is through two protection circuits which equates to approximately twice the impedance. Since current flow is known to travel through the path of least impedance, it is logical to assume that the VNA signal from port 1 travels through the correct circuit to port 2 to extract the proper network parameters. The measurement configuration is shown in Figure 2-14.

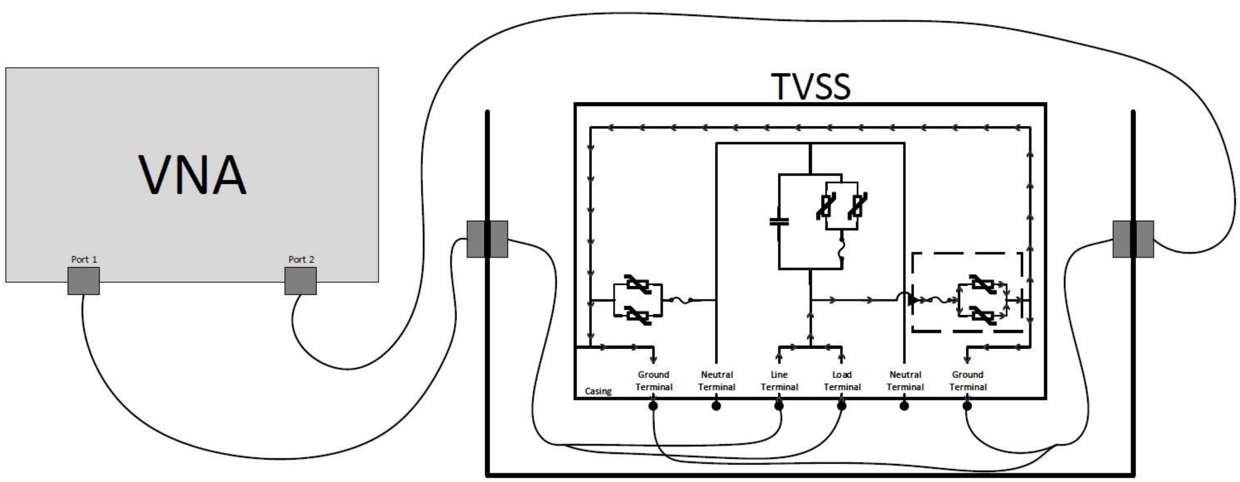

Figure 2-14. VNA Configuration for Line-to-Ground Impedance Sweep

2.3.1.2. Neutral-to-Ground

To extract the network parameters for the circuit in the dashed box shown in Figure 2-15, its through impedance was measured using a VNA. The VNA's port 1 was connected to the TVSS' neutral terminals and port 2 to its ground. The same reasoning provided in Section 2.3.1.1 for current flow through the device can be applied for this configuration. Figure 2-15 contains a diagram of the measurement configuration.

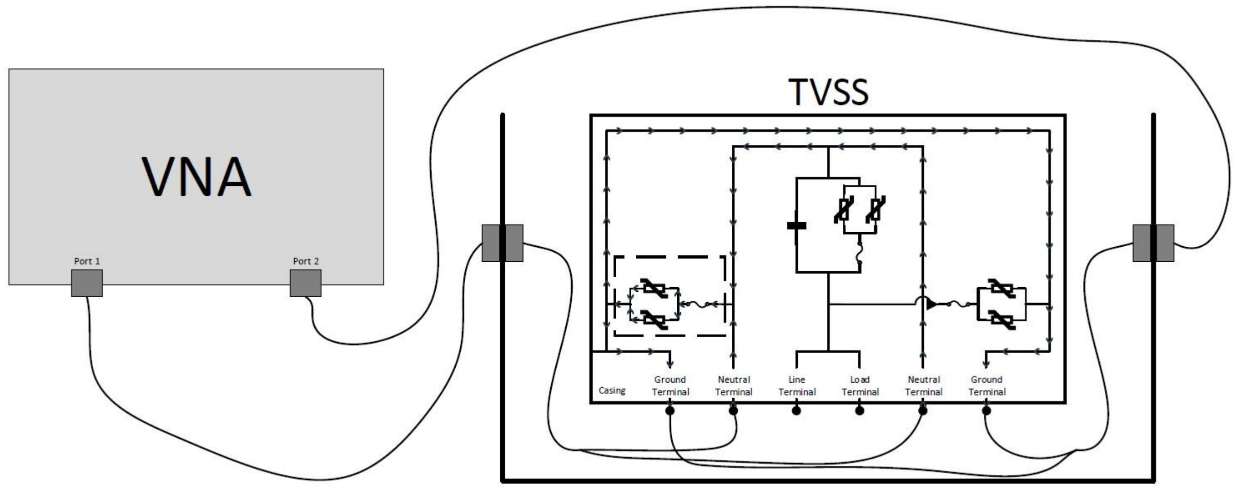

Figure 2-15. VNA Configuration for Neutral-to-Ground Impedance Sweep

2.3.1.3. Line-to-Neutral

To extract the network parameters for the circuit in the dashed box shown in Figure 2-16, its through impedance was measured using a VNA. The VNA's port 1 was connected to the TVSS' line and load terminals and port 2 to its neutral terminals. The same reasoning provided in Section 2.3.1.1 for current flow through the device can be applied for this configuration. Figure 2-16 contains a diagram of the measurement configuration. Table 2-2 is a summary of all VNA measurement configurations.

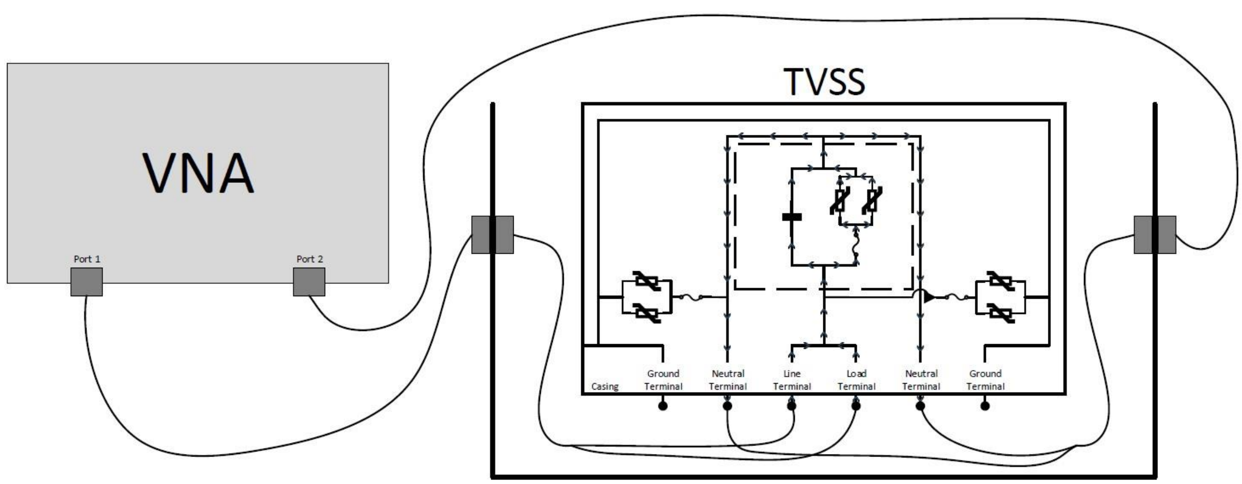

Figure 2-16. VNA Configuration for Line-to-Neutral Impedance Sweep

Table 2-2. Summary of VNA Measurement Configurations

TVSS Terminal	Configuration		
	LTG	NTG	LTN
Line/Load	Port 1	Open	Port 1
Neutral	Open	Port 1	Port 2
Ground	Port 2	Port 2	Open

2.3.2. IV-Curve Characteristics

Evaluating the I-V characteristics of the MOVs in each TVSS protection circuit is another method to determine if the device was damaged. Damaged MOVs can show degradation in their ability to hold off voltage, have a higher leakage current value and will conduct current at a lower voltage. Changes in an I-V curve could denote damage to the MOVs.

I-V curves were generated for each device in every configuration discussed in Section 2.3.1 using a sourcemeter and a multimeter. The sourcemeter supplied a voltage across the TVSS' input and output terminals for the specified configuration and measured the current into the terminals. The multimeter was used to verify that the voltage across the TVSS terminals matched the sourcemeter's voltage output setting. Each curve was generated by selecting predetermined voltage levels on the source meter and documenting the corresponding current. The current from the sourcemeter is expected to travel through the correct TVSS protection circuit for each configuration by the same justification given in Section 2.3.1.1.

Baseline measurements were collected for each device and configuration prior to every test. The curves were collected by incrementing the voltage output by 10 V per step until 250 V was reached, then by 5 V per step until 350 V was reached, and then by 2 V per step until the sourcemeter was current limited. Subsequent curves for each conducted test iteration were conducted with larger voltage increments of 50 V per step until 300 V and 10 V per step until the current output limit of the source meter was reached. The new points were then plotted on top of the baseline curves to compare their correlation and determine if any damage had been incurred. Figure 2-17 shows a representative photo of the measurement configuration. The following sections outline each test configuration used in generating I-V curve characteristics.

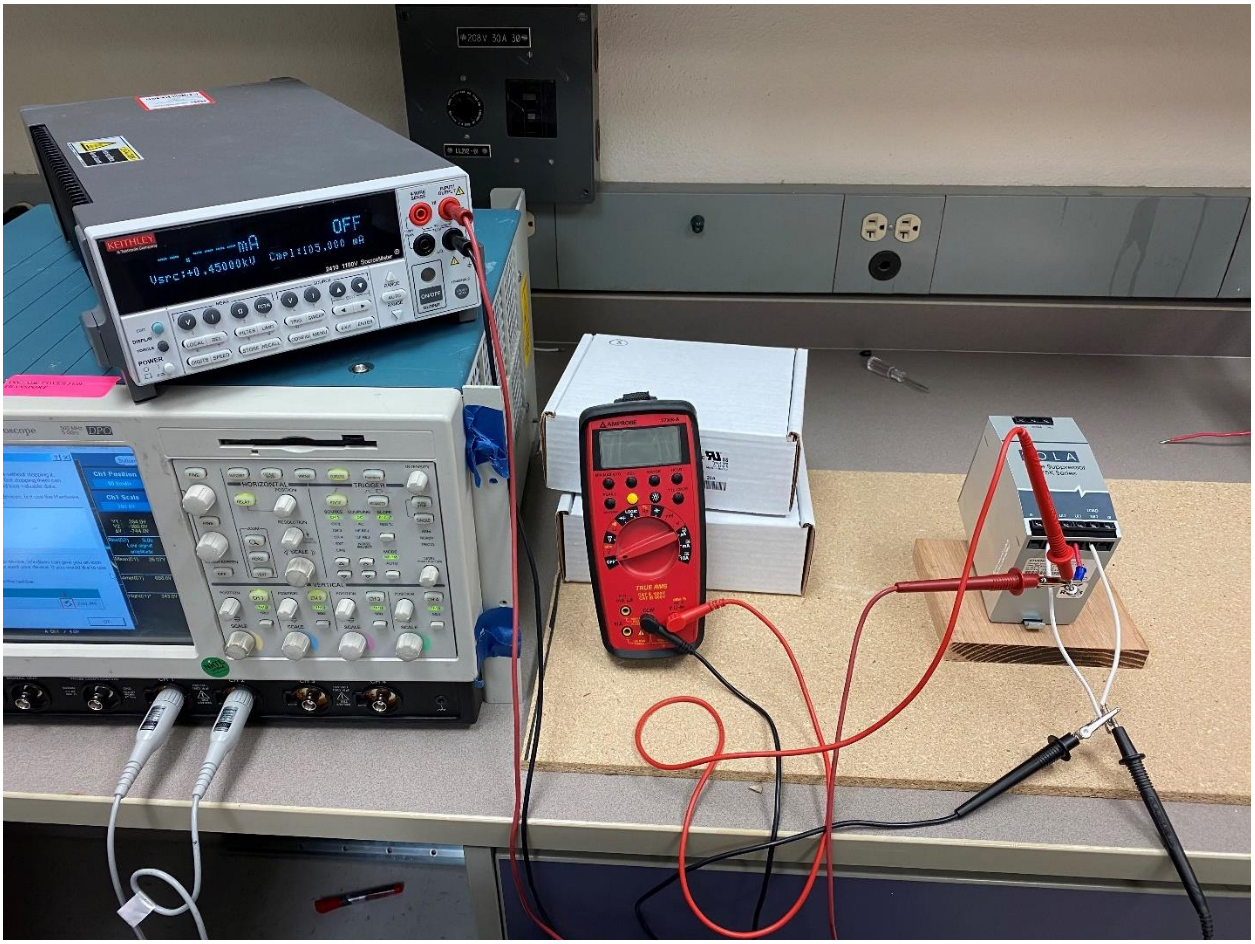

Figure 2-17. Photo of Representative I-V Curve Measurement

2.3.2.1. Line-to-Ground (LTG)

The LTG configuration extracted the I-V characteristics of the circuit boxed in Figure 2-18. The TVSS line and load terminals were connected to the energized terminal of the source meter and the ground terminals to its return terminal. A multimeter verified voltage across TVSS line and ground terminals. The test configuration diagram is in Figure 2-18.

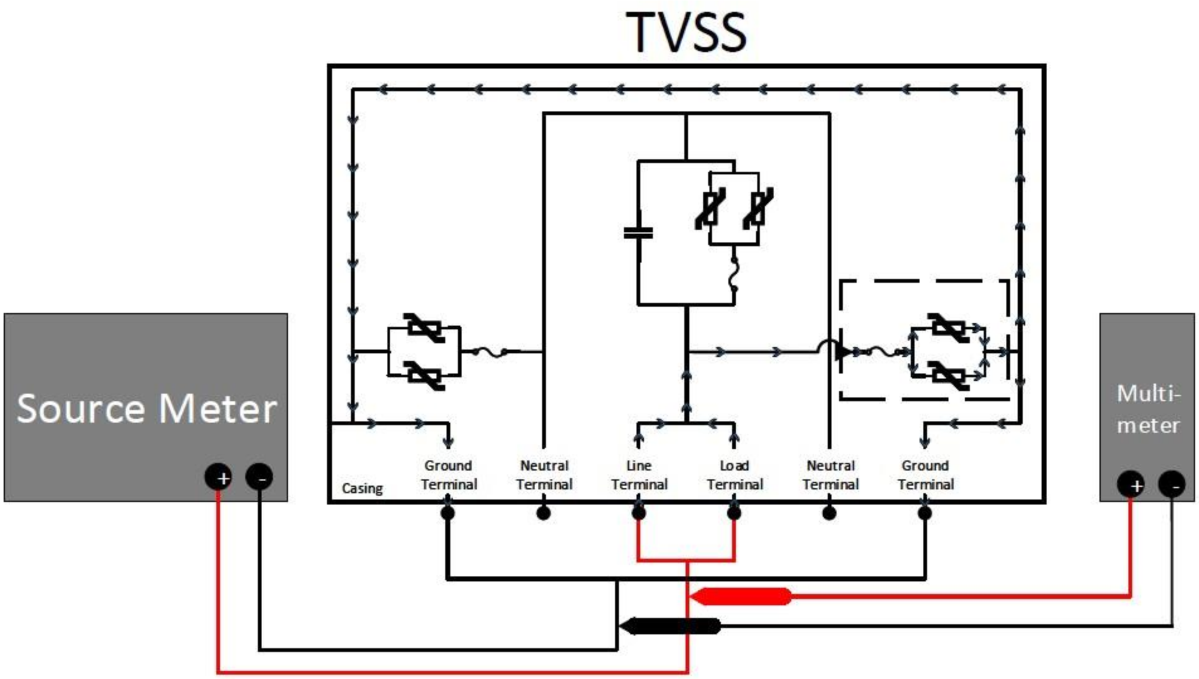

Figure 2-18. Diagram of Line-to-Ground I-V Curve Trace Measurement Configuration

2.3.2.2. Neutral-to-Ground (NTG)

The NTG configuration extracted the I-V characteristics of the circuit boxed in Figure 2-19. The TVSS neutral terminals were connected to the energized terminal of the source meter and the ground terminals to its return terminal. A multimeter verified voltage across neutral and ground TVSS terminals. The test configuration diagram is in Figure 2-19.

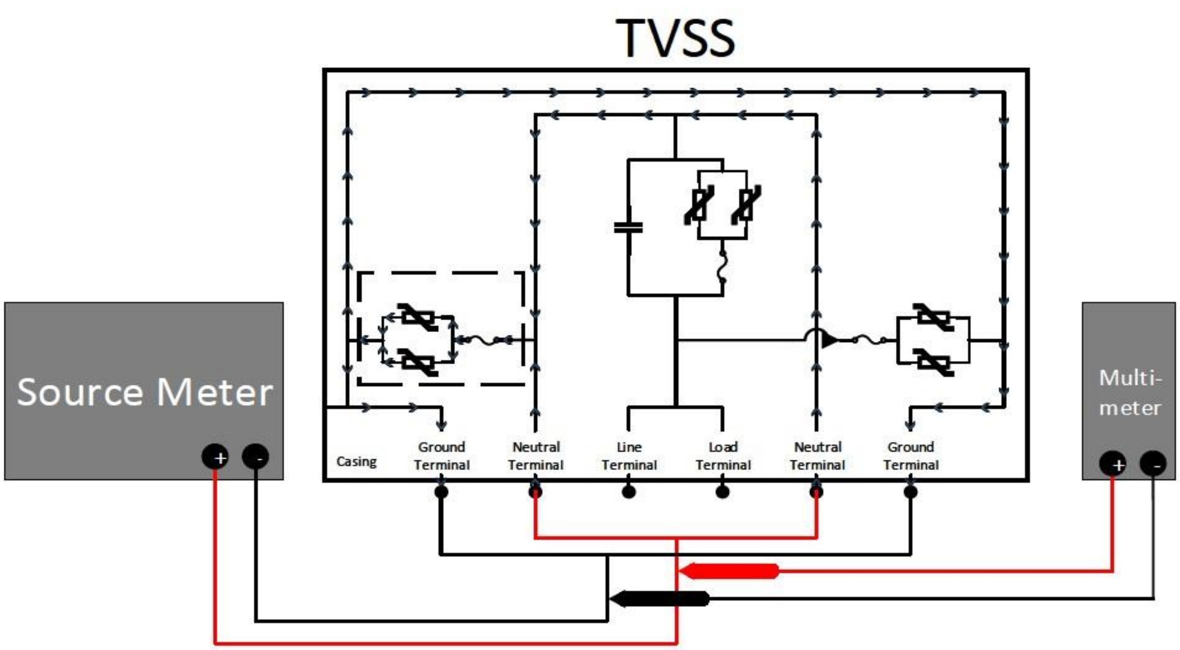

Figure 2-19. Diagram of Neutral-to-Ground I-V Curve Trace Measurement Configuration

2.3.2.3. Line-to-Neutral

The NTG configuration extracted the I-V characteristics of the circuit boxed in Figure 2-20. The TVSS line and load terminals were connected to the energized terminal of the source meter and the neutral terminals to its return terminal. The multimeter verified voltage across TVSS line and neutral terminals. The test configuration diagram is in Figure 2-20. Table 2-3 is a summary of all I-V curve trace configurations.

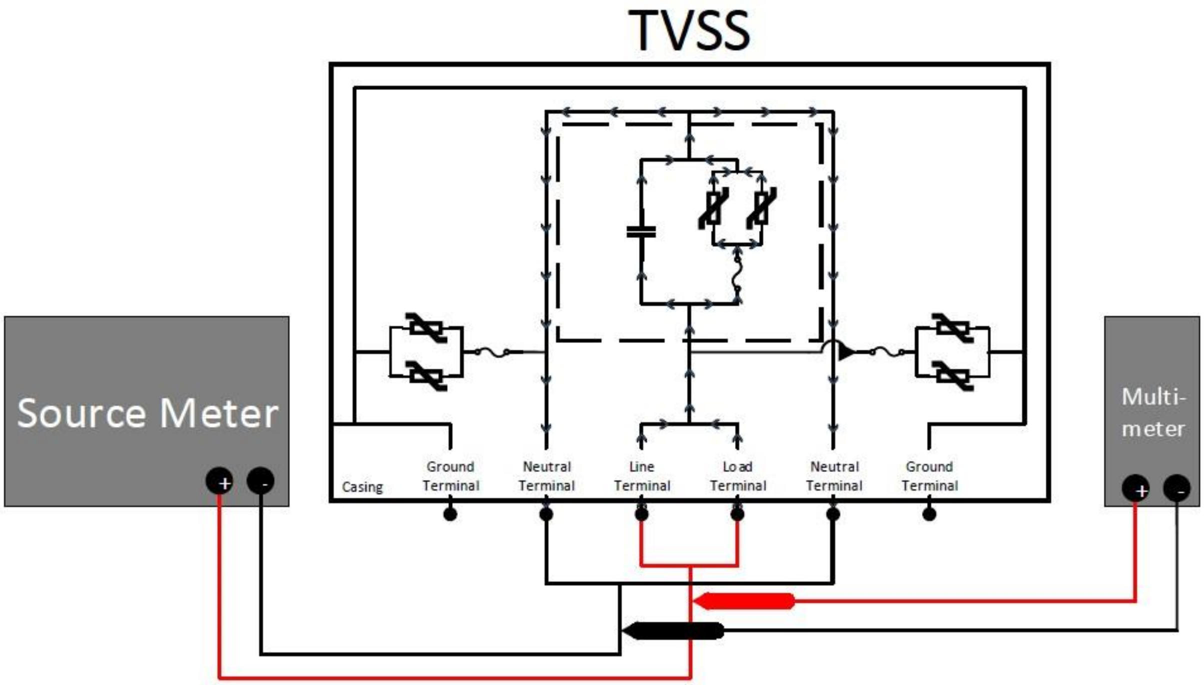

Figure 2-20. Diagram of Line-to-Neutral I-V Curve Trace Measurement Configuration

Table 2-3. Summary of VNA Measurement Configurations

TVSS Terminal	Configuration		
	LTG	NTG	LTN
Line/Load	Sourcemeter Output	Open	Sourcemeter Output
Neutral	Open	Sourcemeter Output	Sourcemeter Return
Ground	Sourcemeter Return	Sourcemeter Return	Open

2.3.3. Signal Distortion

The final SOH measurement determined any signal distortion caused by the TVSS to the normally operating AC circuit. TVSS' often protect sensitive equipment that may not respond correctly to a distorted signal. Any distortion caused by the TVSS would render the device unsuitable to protect certain substation circuits.

The TVSS was placed in the 240 V AC circuit during the measurement. The step-up transformer was connected to the TVSS by connecting the energized, neutral, and ground conductors to the TVSS line, neutral, and ground terminals, respectively. The 150 Ω resistor was connected between the TVSS load and neutral terminals. An oscilloscope was connected to the line terminal of the

TVSS to monitor the input signal into the device. A secondary oscilloscope probe was connected to the load terminal of the TVSS to monitor the output signal leaving the device. The oscilloscope return conductors were connected to ground. Figure 2-21 shows the test setup. Figure 2-22 shows a photo of the measurement setup.

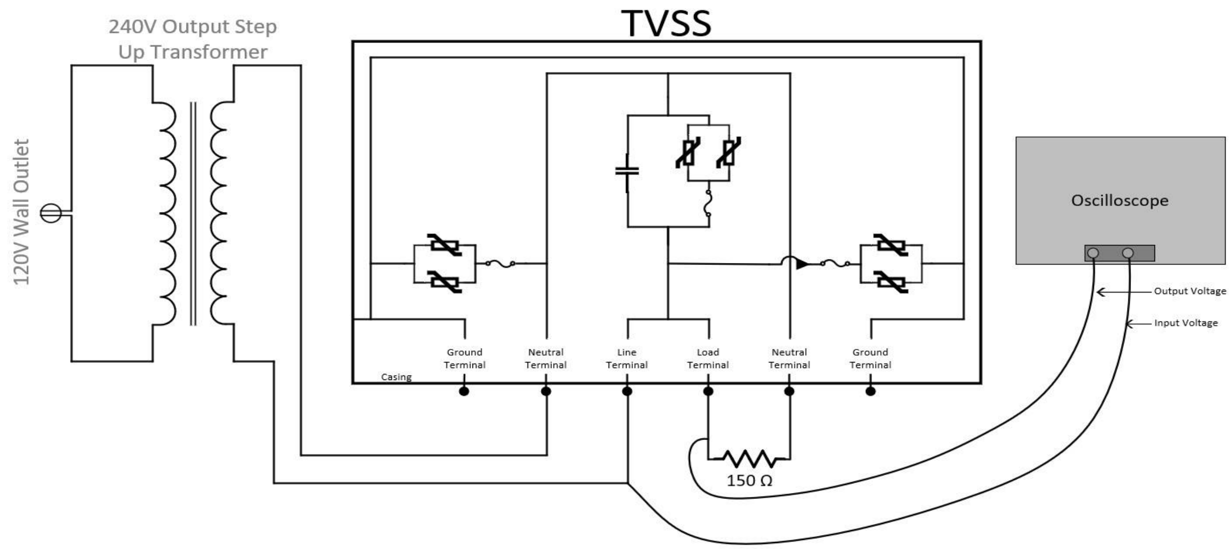

Figure 2-21. Test Setup for Signal Distortion Determination

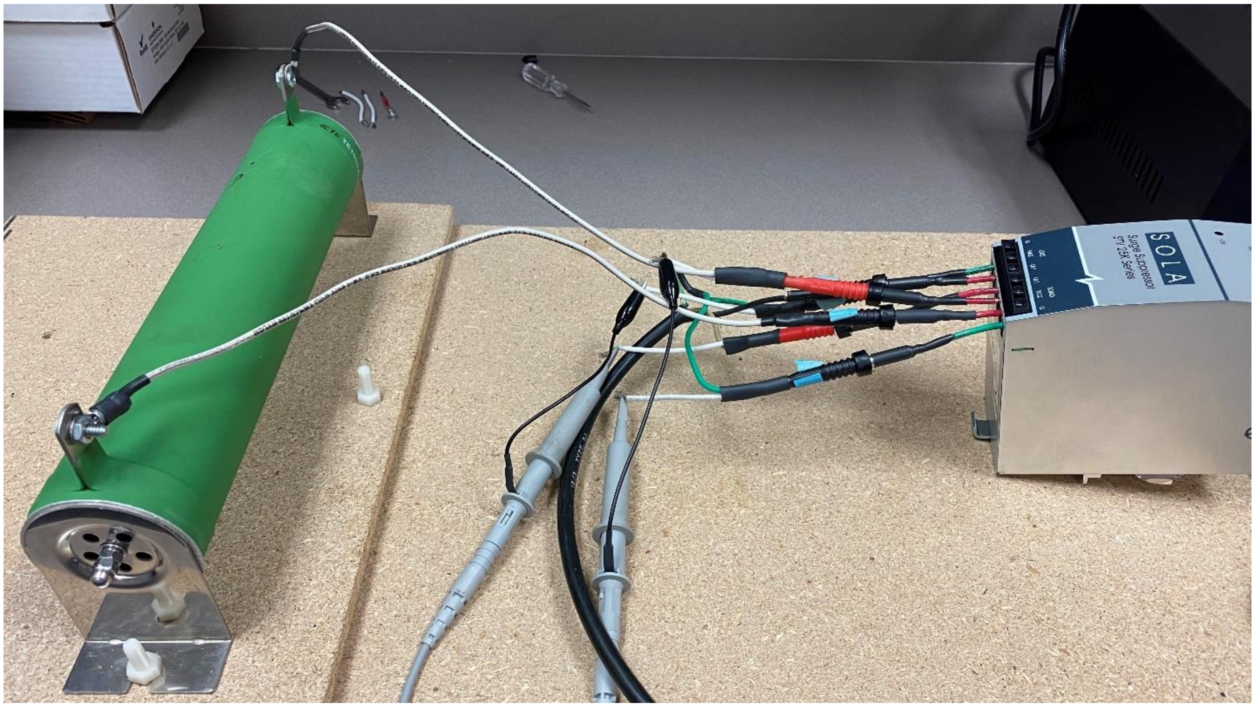

Figure 2-22. Photo of Signal Distortion Measurement Configuration

The time-domain output from the oscilloscope was converted to the frequency domain using a Fast Fourier Transform (FFT) in Matlab to determine their power spectral densities. The power spectral density of the difference between the two signals was also calculated to determine if there was any frequency distortion present in the signal. Any significant changes to the spectral content of the output waveform compared to the input waveform signified damage incurred to the TVSS.

3. RESULTS

Each TVSS was tested in accordance with Section 2.2 and their SOH was evaluated in accordance with Section 2.3. Tests were conducted at 20 kV, 50 kV, and 80 kV pulser open circuit voltage increments. The following sections detail the results of both test configurations and SOH measurements.

3.1. Common Mode Testing

3.1.1. Pulsed Test Response

Eight TVSS' were tested in common mode configuration as described in Section 2.2.1. The voltage response of a single device is shown below in Figure 3-1 – Figure 3.3. Refer to Figure 2-6 for probe placement for each graph below.

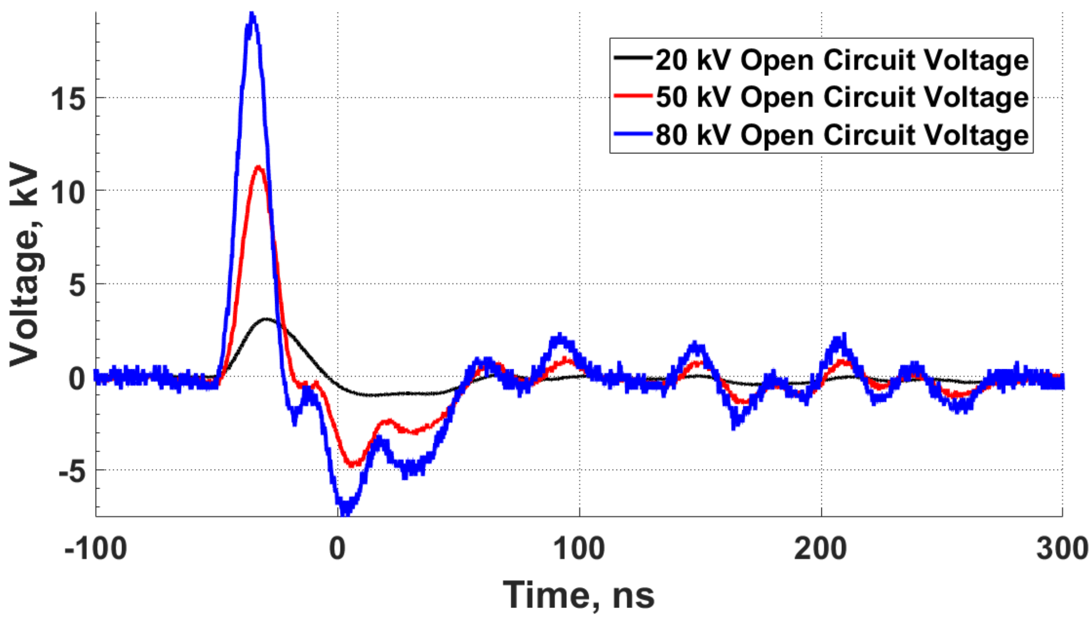

Figure 3-1. Pulser Voltage Output for Common Mode Configuration of TVSS Test (V1)

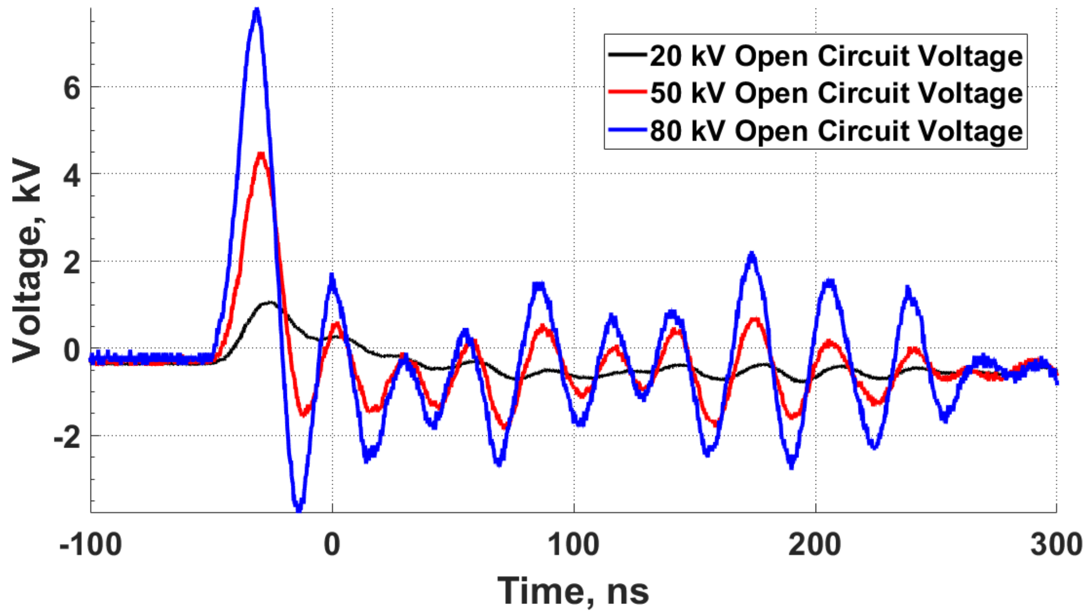

Figure 3-2. Measured Line-to-Ground Voltage for Common Mode Configuration of TVSS Test (V2)

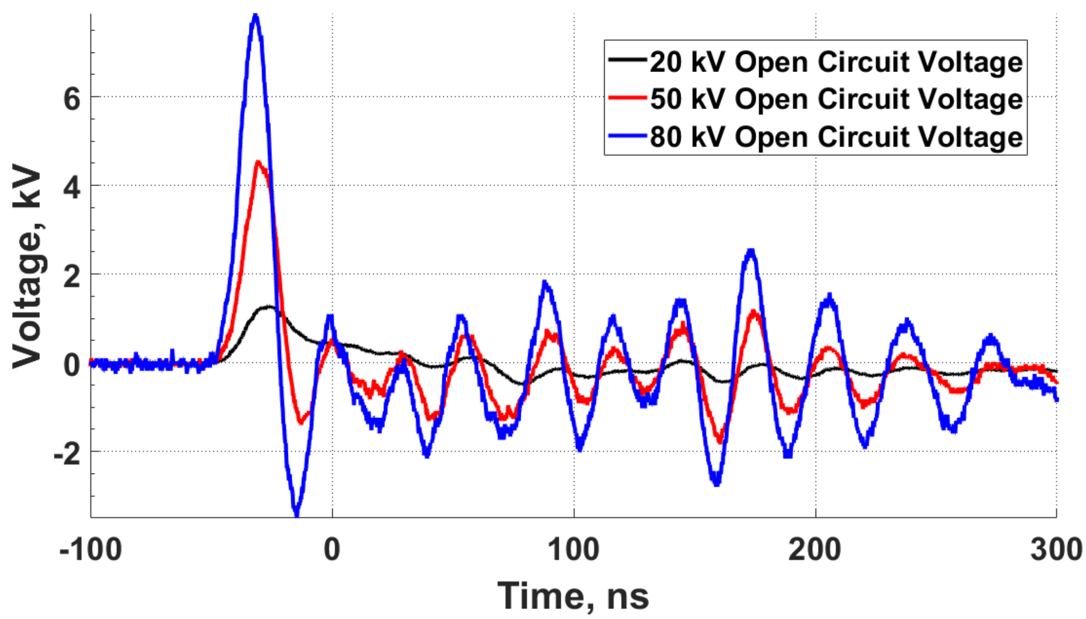

Figure 3-3. Measured Neutral-to-Ground Voltage for Common Mode Configuration of TVSS Test (V3)

The voltage measured throughout the circuit demonstrated a proportional increase as the pulser charge voltage increased. No observable clamping effects were noted which indicates a failure of the TVSS to respond to the insulted pulse. Figure 3-4 – Figure 3-6 demonstrates the response consistency across all devices.

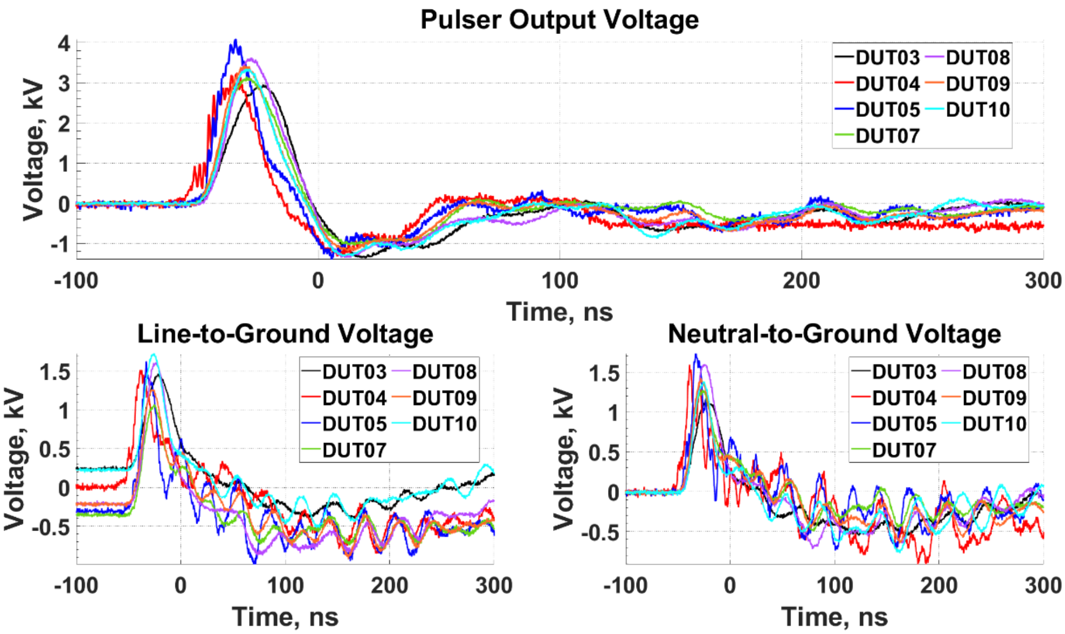

Figure 3-4. 20 kV Pulser Open Circuit Voltage, Common Mode Configuration Voltage Comparison across all Devices

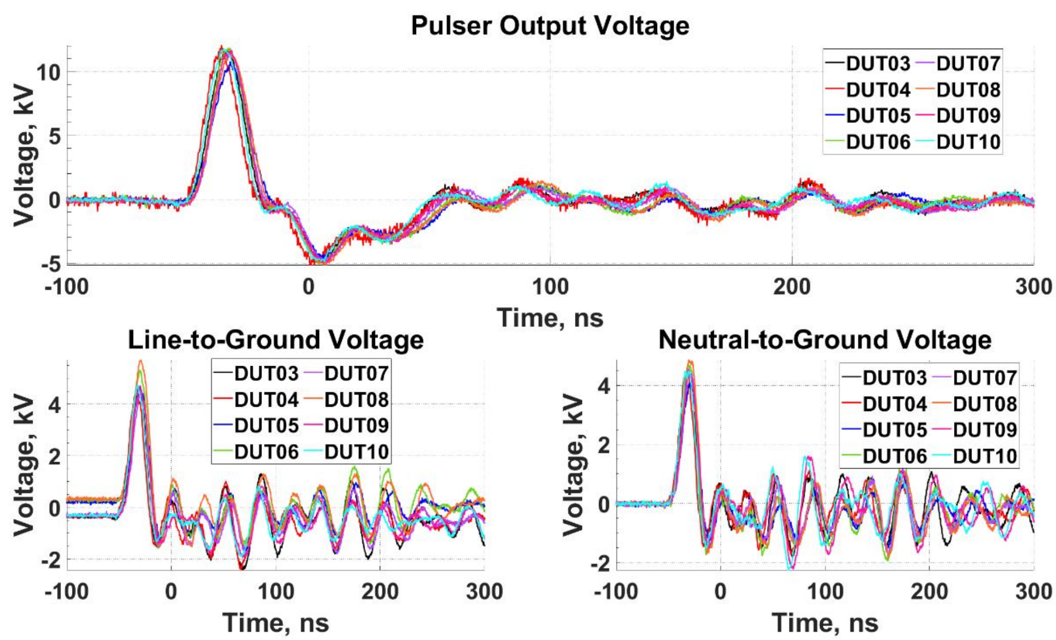

Figure 3-5. 50 kV Pulser Open Circuit Voltage, Common Mode Configuration Voltage Comparison across all Devices

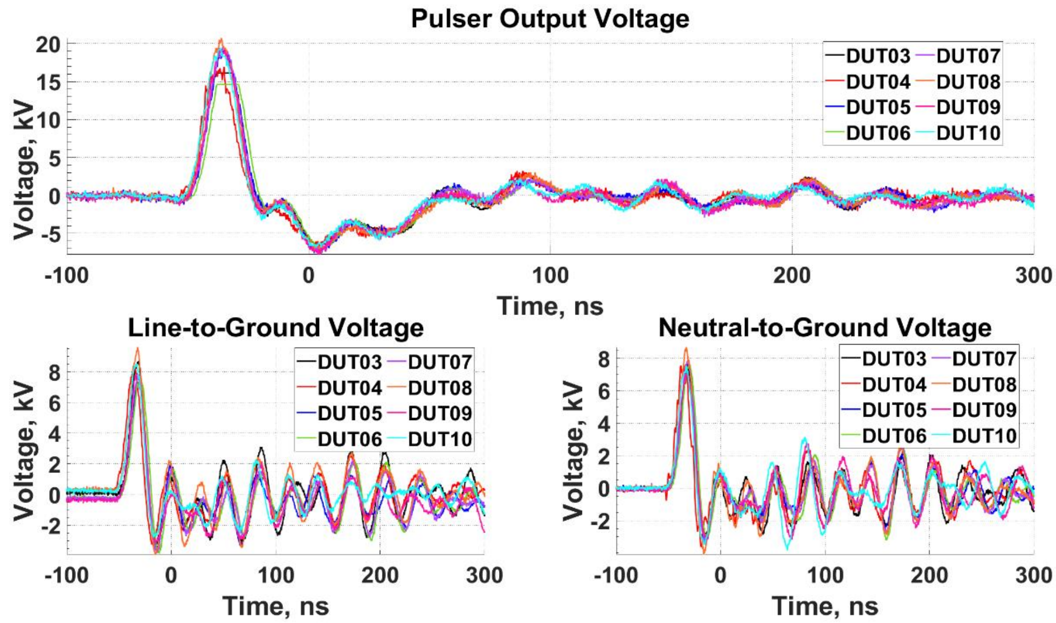

Figure 3-6. 80 kV Pulser Open Circuit Voltage, Common Mode Configuration Voltage Comparison across all Devices

Measured circuit voltage magnitudes for the early time (-100 ns – 0 ns) for each test were significantly lower than the open circuit voltage output of the pulser. However, this does not indicate a clamping response from the TVSS. Instead, this is a result of the impedance of the MOVs inside of the TVSS. Under low bias conditions, MOV impedance is described primarily by its inductance and capacitance [2]. A simple LTSPICE simulation of the test configuration using a simple series LC circuit as the representative TVSS circuit model verified this observation. Comprehensive details of the simulation are in Appendix A.

Since the TVSSs did not respond to the fast pulse, one TVSS device was tested using an insult with a FWHM of approximately 2 μs which is similar to the types of voltage peaks the devices are designed to protect against. Their response to a slower pulse confirmed that the lack of response to the fast pulse was not due to a device defect. Figure 3-7 shows a set of results from the test.

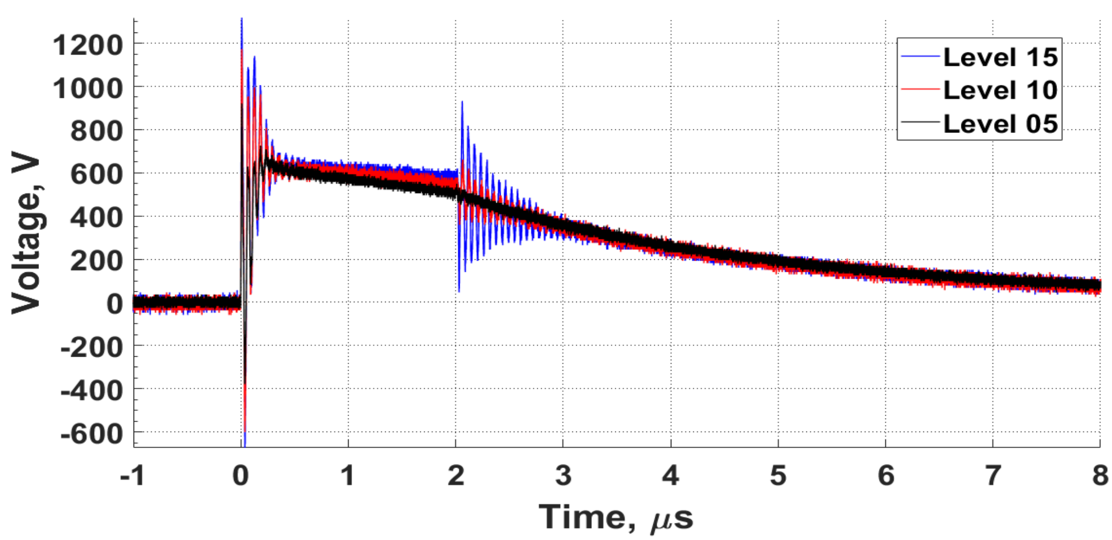

Figure 3-7. Response of TVSS to 2 μs FWHM Pulse

The TVSS devices demonstrated a clamped response at approximately 600 V for multiple pulser open circuit voltage levels. A ringing response was noted for each test that had a duration of approximately 500 ns prior to clamping, as evident in Figure 3-8. This was determined to be the time required for the MOVs inside of the TVSS to fully clamp the voltage across it. Appendix B details the complete test configuration and results.

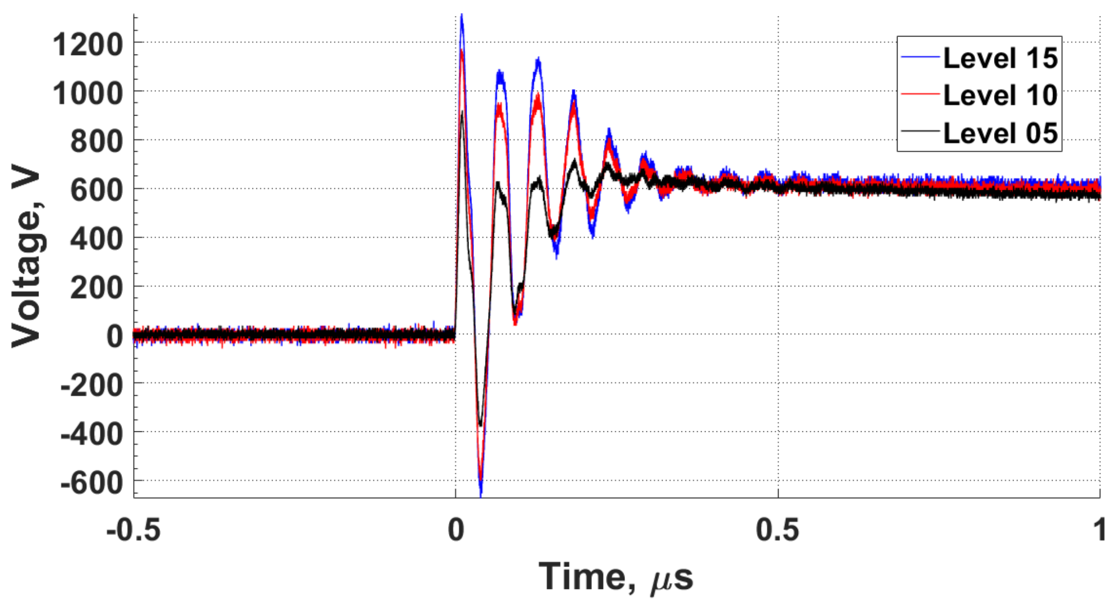

Figure 3-8. Zoomed-In View of Ringing Seen in Clamping Response of TVSS

This clamping time is longer than the duration of the E1 pulse which demonstrates that the TVSSs do not activate quickly enough to respond to it. The response observed in the test is dominated by the capacitance and inductance of the TVSSs.

3.1.2. State-of-Health Response

SOH measurements were conducted on each TVSS as described in Section 2.3. One TVSS was damaged due to testing. A thermal fuse was blown at a 20 kV open circuit voltage test and the cause was unknown. However, no additional damage was incurred and no additional fuses in the TVSS were blown at higher open circuit voltage increments. No fuses on the other TVSSs were damaged. . The subsequent sections detail the SOH measurement results from the common mode configuration. Appendix C contains all SOH data for each device.

3.1.2.1. Impedance Characterization

TVSS impedance characteristics were extracted as detailed in Section 2.3.1. Table 3-1 contains the capacitance and inductance values for each TVSS at each charge voltage increment.

Table 3-1. Capacitance and Inductance Values for TVSS State of Health Measurements for Common Mode Test Configuration

Device	Voltage (kV)	LTG		LTN		NTG	
		C (nF)	L (nH)	C (nF)	L (nH)	C (nF)	L (nH)
DUT03	Baseline	3.38	238.71	491.46	251.43	3.38	236.08
	20	3.12	240.48	498.21	251.59	3.13	233.72
	50	3.13	236.04	496.69	246.55	3.13	232.55
	80	3.11	233.91	494.93	243.49	3.11	230.08
DUT04	Baseline	3.42	240.68	489.41	252.79	3.42	236.24
	20	3.23	243.21	494.62	250.02	3.23	236.19
	50	3.21	232.77	494.96	242.81	3.22	229.05
	80	3.22	235.75	499.37	248.78	3.24	230.06
DUT05	Baseline	3.38	246.8	487.36	259.95	3.4	239.52
	20	3.23	239.62	494.02	253.81	3.23	231.73
	50	3.15	242.63	493.27	252.07	3.16	235.78
	80	3.23	242.56	487.39	248.53	3.24	233.8
DUT06	Baseline	3.43	244.22	485.01	254.81	3.43	234.8
	20	3.17	244.76	487.46	250.2	3.18	238.33
	50	3.19	238.38	490.36	248.56	3.2	229.73
	80	3.16	243.18	491.42	253.72	3.17	233.47
DUT07	Baseline	3.46	244.58	485.53	256.12	3.46	231.28
	20	3.23	237.68	493.87	251.67	3.25	231.7
	50	3.23	241.92	492.35	249.73	3.24	232.86
	80	3.18	240.79	494.76	248.78	3.21	232.83
DUT08	Baseline	3.39	241.08	495.46	249.02	3.39	234.42
	20	1.64	273.4	504.13	252.25	1.65	247.64
	50	1.6	266.76	501.24	246.82	1.6	246.98
	80	1.59	261.73	500.34	248.51	1.6	249.53
DUT09	Baseline	3.4	238.67	471.6	253.73	3.39	235.93
	20	3.24	245.38	477.03	246.17	3.25	236.75
	50	3.12	234.43	471.54	244.35	3.13	230.9
	80	3.12	239.01	471.56	245.38	3.12	233.92

Device	Voltage (kV)	LTG		LTN		NTG	
		C (nF)	L (nH)	C (nF)	L (nH)	C (nF)	L (nH)
DUT10	Baseline	3.47	243.54	484.77	253.92	3.47	233.56
	20	3.27	239.7	490.57	251.5	3.28	234.84
	50	3.19	238.81	489.26	248.27	3.19	234.64
	80	3.17	237.76	489.65	247.88	3.19	323.99

Only DUT08, with a blown thermal fuse displayed a noticeably different measured impedance. No other significant difference in capacitance and inductance was noted which indicates no damage was incurred to the TVSSs.

3.1.2.2. IV-Curve Characteristics

The I-V characteristics of each TVSS were collected as described in Section 2.3.2. Figure 3-9 – Figure 3-11 details the results of a single device. Refer to Appendix C for results from each common mode test.

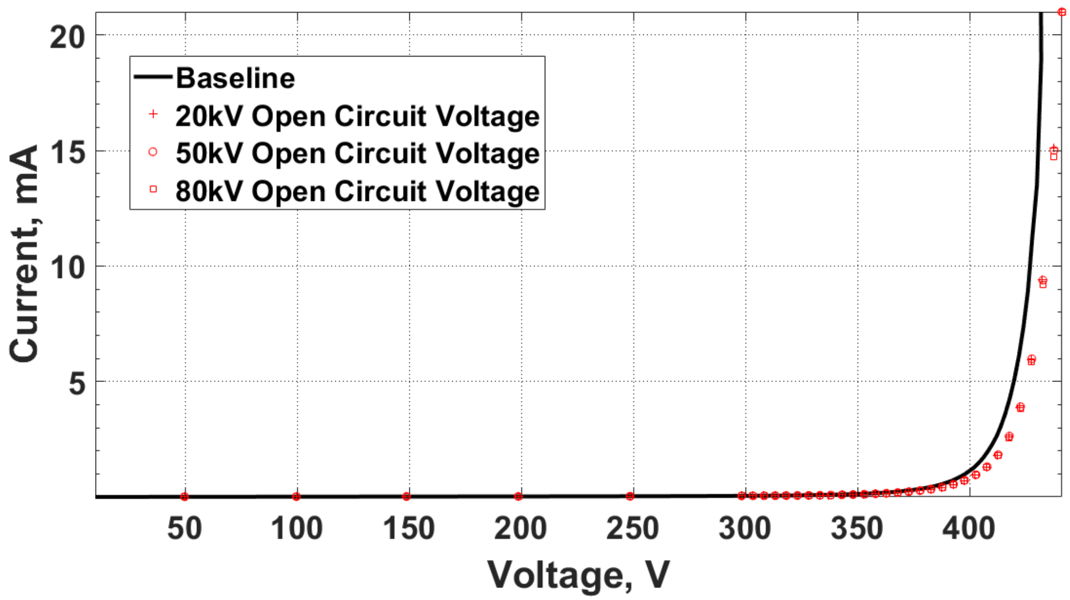

Figure 3-9. Line-to-Ground IV-Curve Comparison for Common Mode Test Configuration

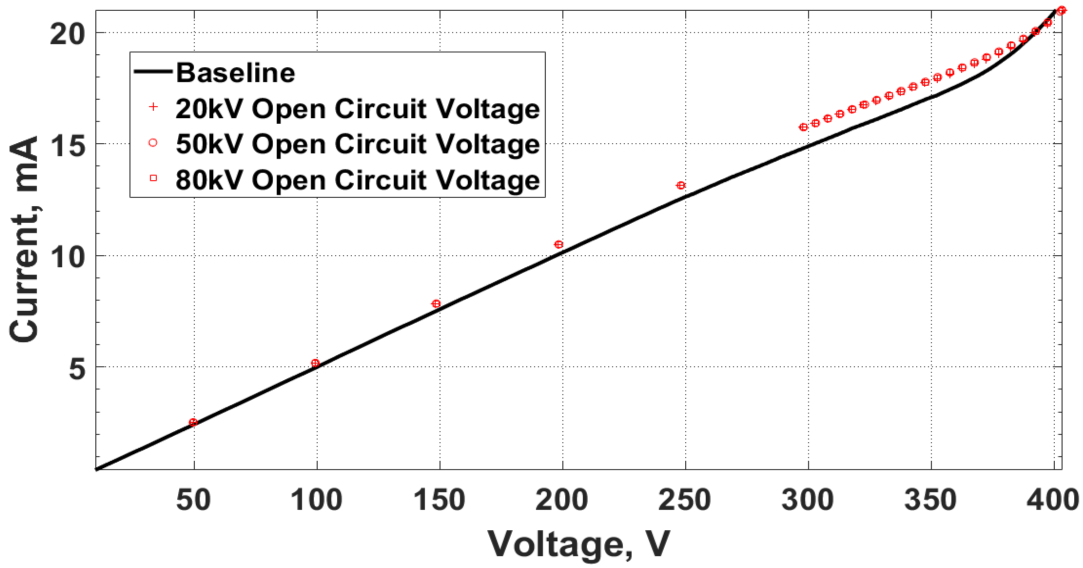

Figure 3-10. Line-to-Neutral IV-Curve Comparison for Common Mode Test Configuration

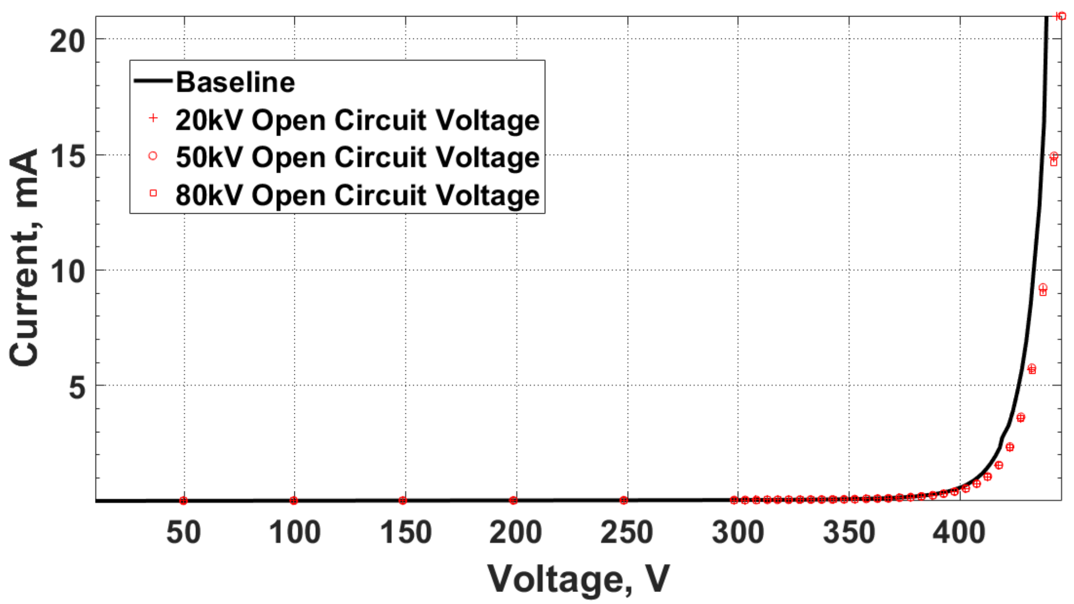

Figure 3-11. Neutral-to-Ground IV-Curve Comparison for Common Mode Test Configuration

Each figure shows a noticeable shift in I-V characteristics which was observed for each device. Multiple factors could have introduced error into the measurement. Firstly, each measurement was conducted by hand which may have introduced error based on which lab worker performed the measurement. Additionally, as mentioned in Section 2.3.2, post-test curves were comprised of fewer points due to an increased voltage step between each point. Figure 3-12 shows six different LTN I-V curves extracted prior to testing from the same device in five different ways: the original IV-curve, a repeated IV-curve taken using the same procedure for a baseline measurement, a curve taken using 10 V increment steps, a curve using 10 V increments and waiting a few seconds between each measurement, a curve using 10 V increments while turning off the source meter output between each shot, and a curve using 5 V increments.

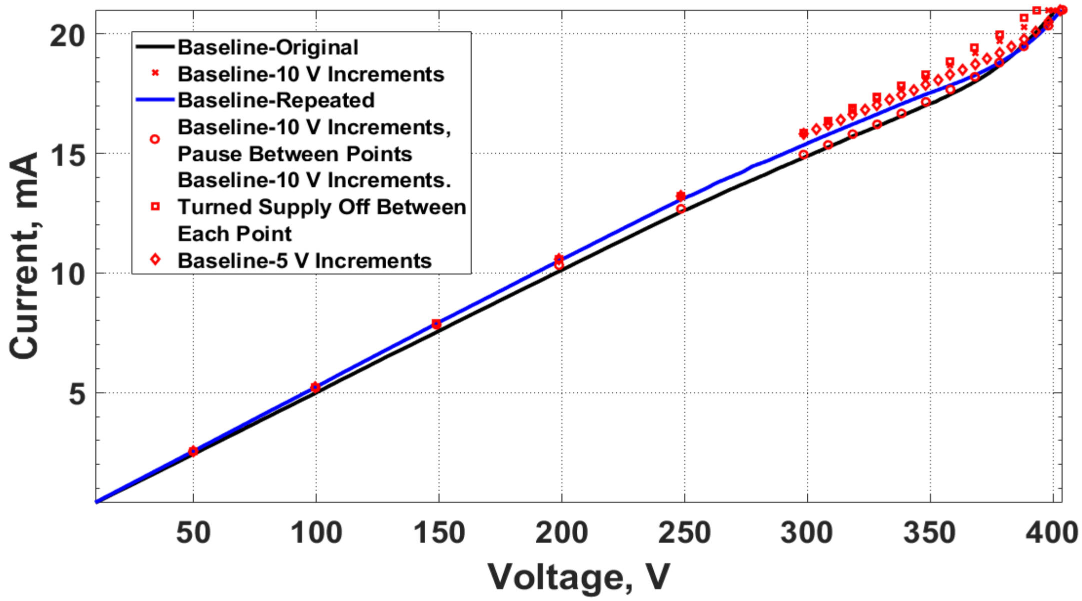

Figure 3-12. Line-to-Neutral IV-Curve Trace Comparisons

Each method returned a different result which demonstrates the potential for error between the baseline measurements and the post-test measurements. These factors were difficult to quantify without significant effort and as such, could not be eliminated from the measurements.

The point consistency between each post-test measurement, however, indicates that the TVSS' incurred no damage during testing. A steady curve degradation after each test would be noted if damage had been incurred. The rightward shift of the LTG and LTN curve also suggest that the shift is related to the method and repeatability of the measurement. If damage had been incurred, the MOVs inside of the device would have conducted current at a lower voltage, not a higher one. Damage would also have caused an increase in leakage current. The I-V characteristic curves indicate that the TVSS' incurred no damage.

3.1.2.3. Signal Distortion

The signal distortion test was conducted as described in Section 2.3.3. Figure 3-13 – Figure 3-15 detail the results of a single device. Refer to Appendix C for results from each common mode test.

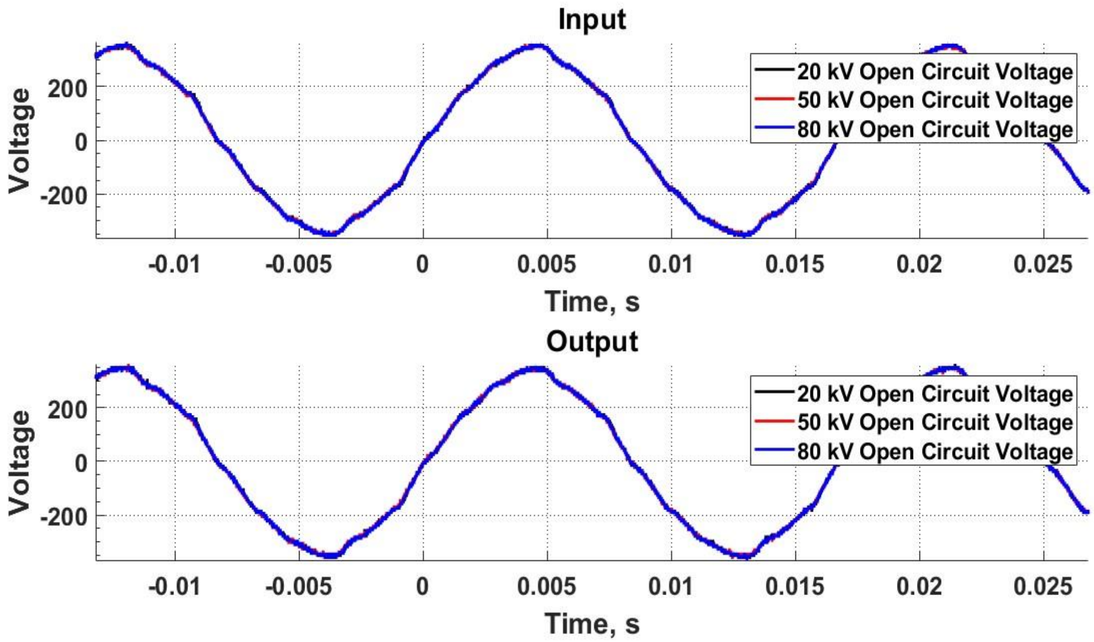

Figure 3-13. Time-Domain Signal from Signal Distortion Test, Common Mode

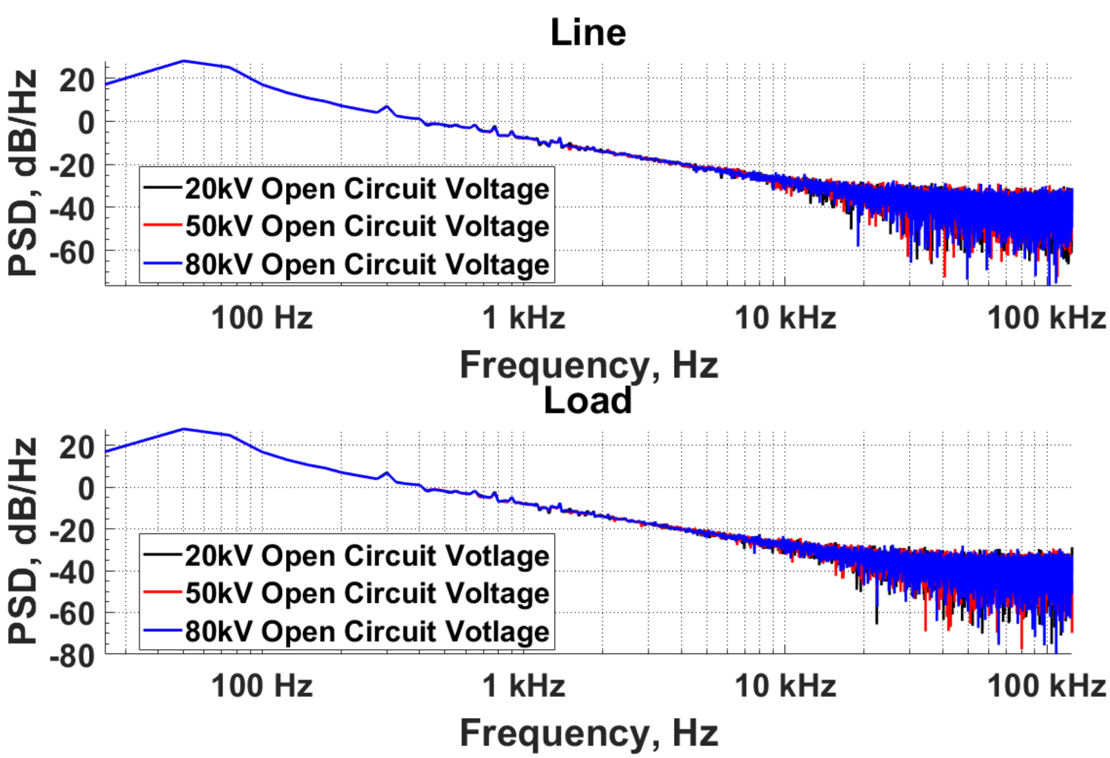

Figure 3-14. Power Spectral Density Comparison of Input and Output Signals for Common Mode Test Configuration

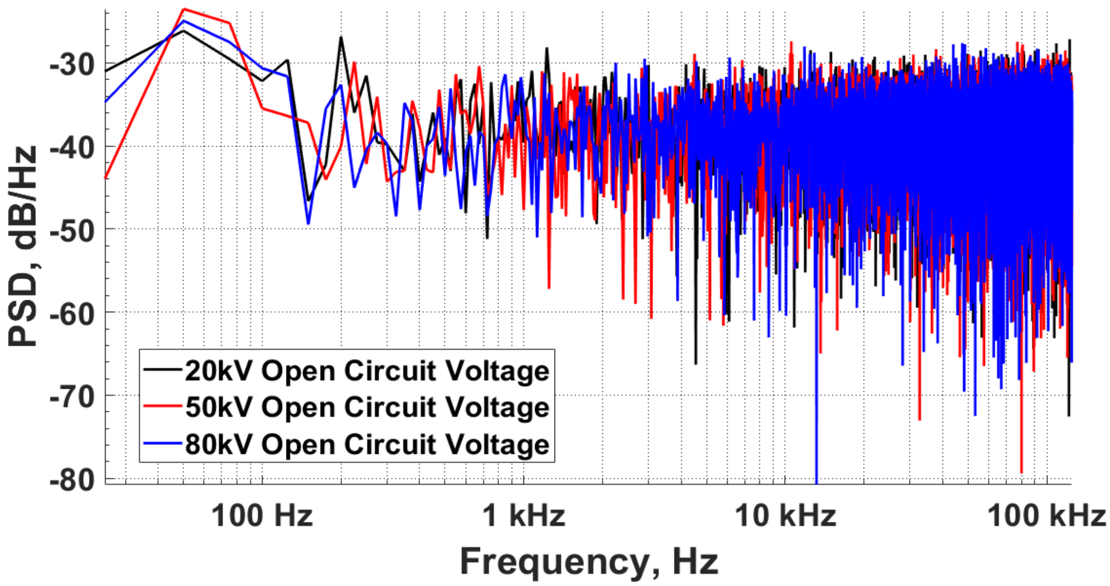

Figure 3-15. Power Spectral Density Comparison of Input and Output Signal Difference for Common Mode Test Configuration

The input and output signal spectral content did not exhibit any observable differences. Signal degradation was not detected in any measurement. The magnitude of the signals in Figure 3-13 indicates that the difference in peak frequencies is due to noise and does not demonstrate any observable signal distortion.

3.2. Single-Ended Testing

3.2.1. Pulsed Test Response

Seven TVSS' were tested in the single-ended configuration as described in Section 2.2.2. The blown fuse of DUT08 rendered it unable to be tested in this configuration. The voltage response of a single device is shown below in Figure 3-16 – Figure 3.17. Refer to Figure 2-11 for probe placement for each graph below.

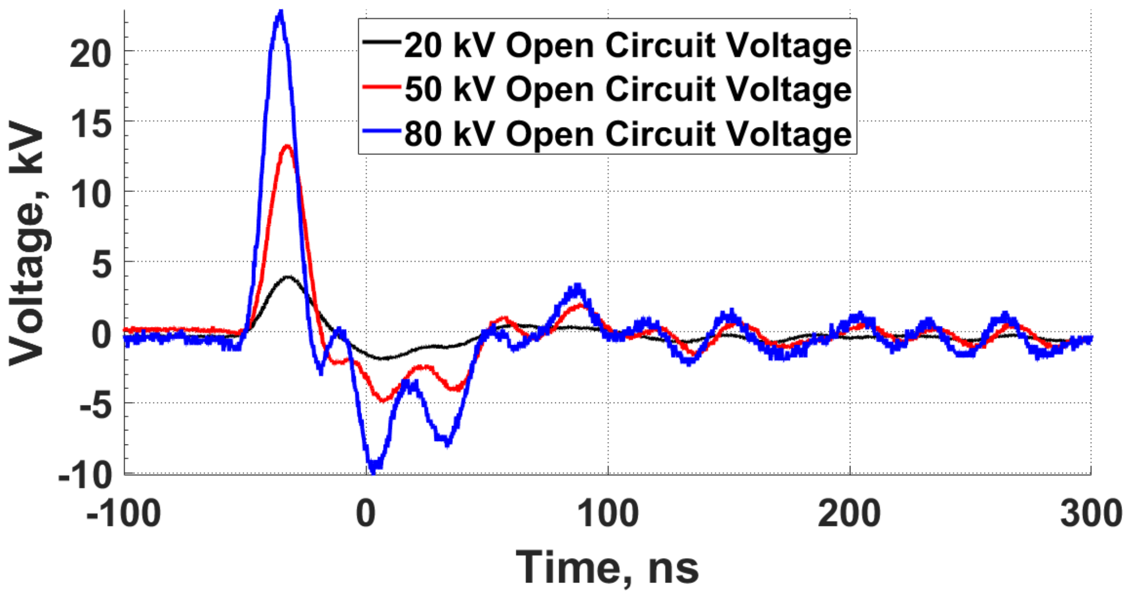

Figure 3-16. Pulser Voltage Output for Single-Ended Configuration Comparison

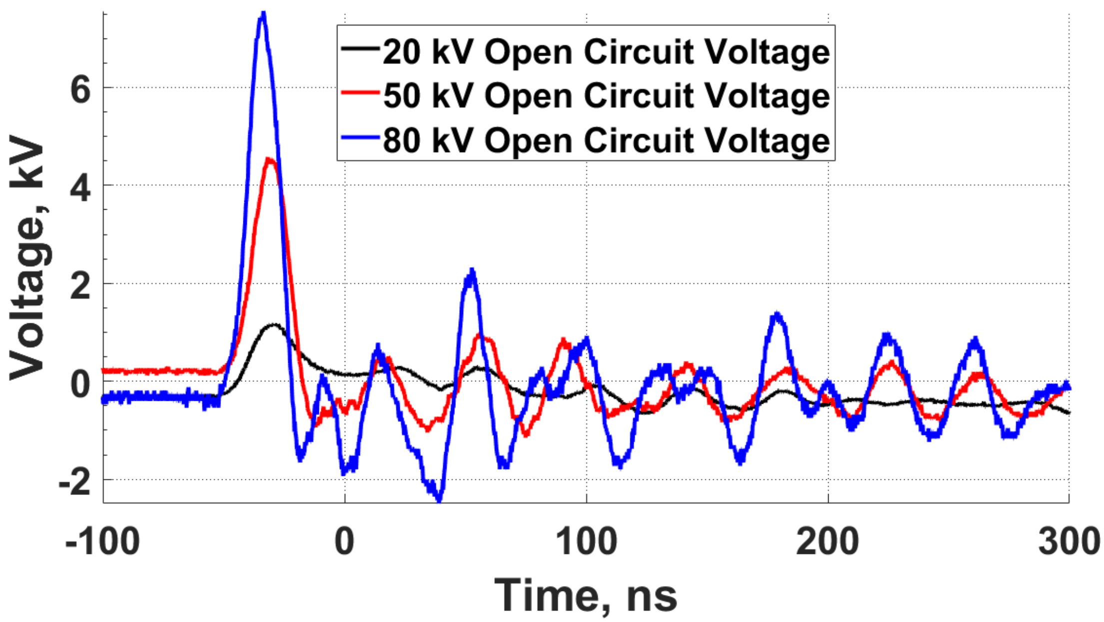

Figure 3-17. Measured Line-to-Ground Voltage for Single-Ended Configuration Comparison

The TVSS' responded similarly in the single-ended configuration as common mode. Measured voltage throughout the circuit increase proportionately with increased charge voltage and no clamping effects were noted. The voltage response in early time (-100 ns – 0 ns) was primarily dominated by the TVSSs internal MOV capacitance and inductance. The results did not demonstrate any non-linear characteristics due to the clamping time of approximately 500 ns being longer than the conducted pulse duration. The result consistency was verified across all devices in Figure 3-18 – Figure 3-20.

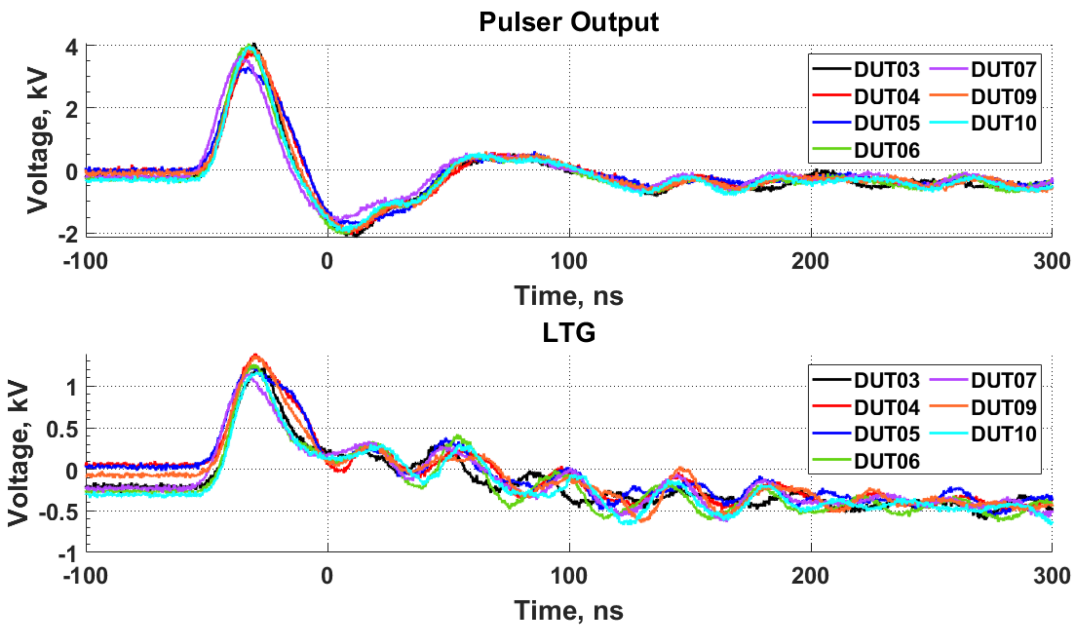

Figure 3-18. 20 kV Pulser Open Circuit Voltage, Single-Ended Configuration Voltage Comparison across all Devices

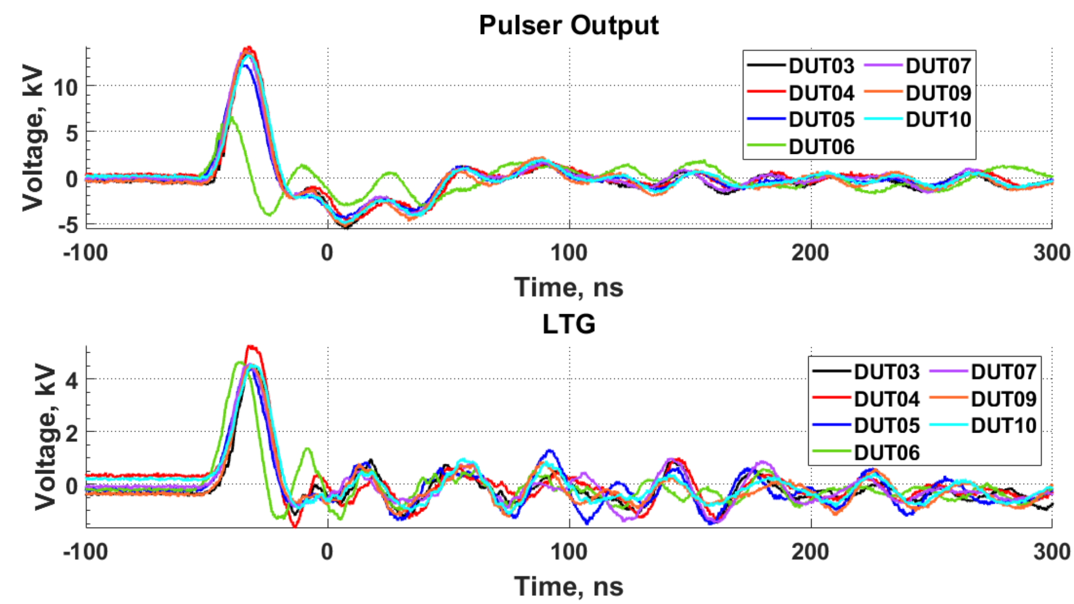

Figure 3-19. 50 kV Pulser Open Circuit Voltage, Single-Ended Configuration Voltage Comparison across all Devices

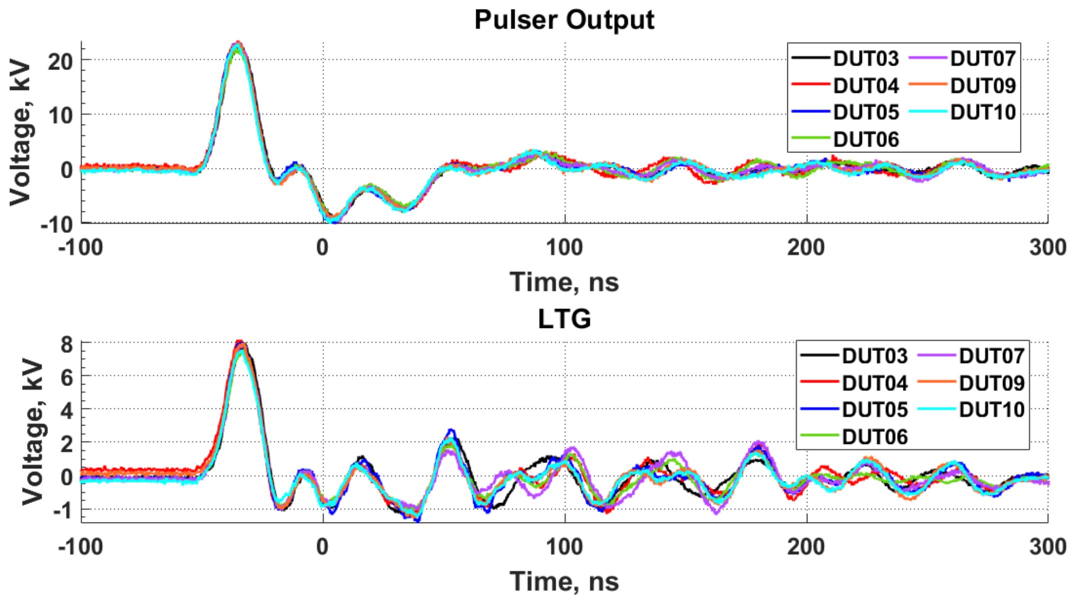

Figure 3-20. 80 kV Pulser Open Circuit Voltage, Single-Ended Configuration Voltage Comparison across all Devices

3.2.2. State-of-Health Response

SOH measurements were conducted on each TVSS as described in Section 2.3. The subsequent section detail the SOH measurement results from the single-ended configuration. Appendix D contains all SOH data from each device.

3.2.2.1. Impedance Characterization

TVSS impedance characteristics were extracted as detailed in Section 2.3.1. Table 3-2 contains the capacitance and inductance values for each TVSS at each charge voltage increment.

Table 3-2. Capacitance and Inductance Values for TVSS State of Health Measurements for Single-Ended Test Configuration

Device	Voltage (kV)	LTG		LTN		NTG	
		C (nF)	L (nH)	C (nF)	L (nH)	C (nF)	L (nH)
DUT03	Baseline	3.38	238.71	491.46	251.43	3.38	236.08
	20	3.11	240.59	497.9	248.42	3.12	232.21
	50	3.1	236.51	495.92	243.42	3.1	230.75
	80	3.07	239.27	498.7	246.2	3.08	231.85
DUT04	Baseline	3.42	240.68	489.41	252.79	3.42	236.24
	20	3.13	234.36	495.03	245.82	3.14	232.06
	50	3.13	235.86	492.45	241.73	3.14	232.08
	80	3.13	239.88	494.42	247.55	3.14	232.09
DUT05	Baseline	3.38	246.8	487.36	259.95	3.4	239.52

Device	Voltage (kV)	LTG		LTN		NTG	
		C (nF)	L (nH)	C (nF)	L (nH)	C (nF)	L (nH)
	20	3.14	240	488.88	245.65	3.14	234.95
	50	3.16	300	488.08	246.34	3.16	234.27
	80	3.14	241.88	491.35	249.31	3.14	233.59
DUT06	Baseline	3.43	244.22	485.01	254.81	3.43	234.8
	20	3.17	239.45	490.83	246.89	3.18	232.79
	50	3.14	237.59	491.58	247.41	3.15	231.73
	80	3.13	237.5	488.55	246.28	3.14	232.35
DUT07	Baseline	3.46	244.58	485.53	256.12	3.46	231.28
	20	3.18	270.52	487.55	247.34	3.2	228.33
	50	3.19	239.26	488.11	246.9	3.19	234.62
	80	3.18	238.56	487.79	245	3.19	233.31
DUT09	Baseline	3.4	238.67	471.6	253.73	3.39	235.93
	20	3.13	242.63	472.95	249.1	3.14	231.75
	50	3.15	241.29	473.9	250.77	3.16	234.06
	80	3.13	237.3	475.75	246.71	3.14	233.69
DUT10	Baseline	3.47	243.54	484.77	253.92	3.47	233.56
	20	3.18	240.38	489.94	250.45	3.18	235.29
	50	3.18	236.67	490.58	248.56	3.2	232
	80	3.16	239.4	492.28	249.85	3.18	234.44

The table shows no significant difference in capacitance and inductance throughout testing. This indicates that the single-ended testing did not cause any TVSS damage.

3.2.2.2. IV-Curve Tracer

The I-V characteristics of each TVSS were collected as described in Section 2.3.2. Figure 3-21 – Figure 3-23 details the results of a single device. Refer to Appendix D for results from each single-ended test.

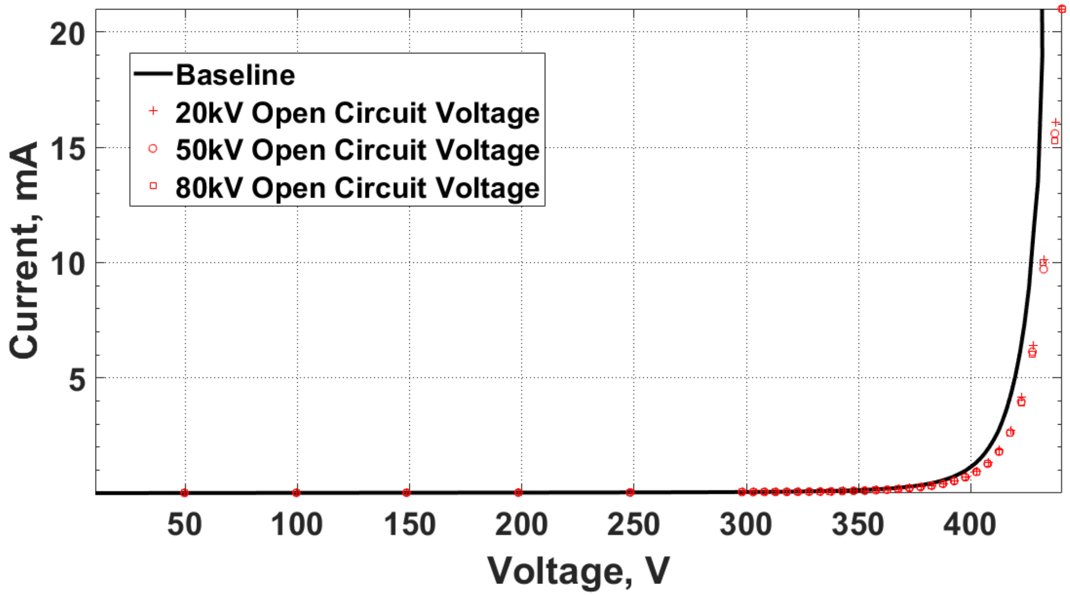

Figure 3-21. Line-to-Ground IV-Curve Comparison for Single-Ended Test Configuration

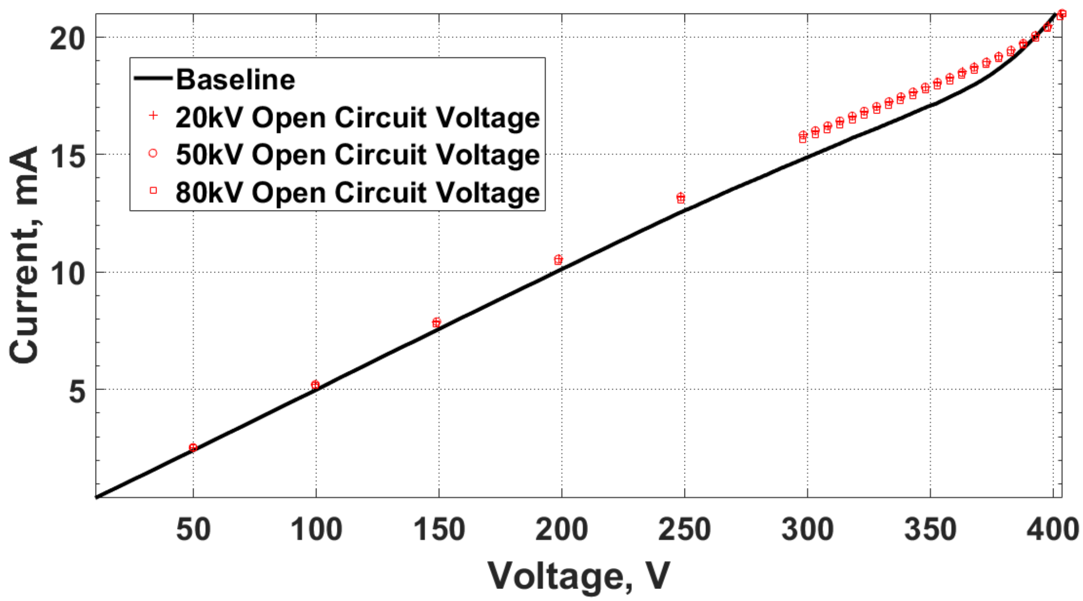

Figure 3-22. Line-to-Neutral IV-Curve Comparison for Single-Ended Test Configuration

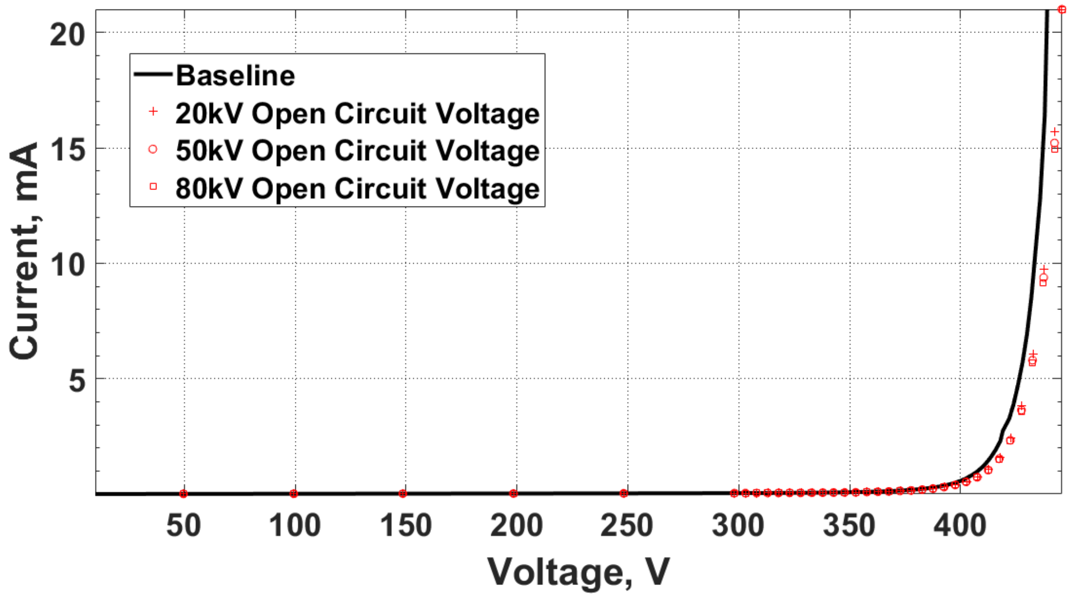

Figure 3-23. Neutral-to-Ground IV-Curve Comparison for Single-Ended Test Configuration

Noticeable curve shifts are evident from the baseline state of health. The same conclusions from Section 3.1.2.2 can be applied to the single-ended configuration data. No noticeable damage was observed to the TVSS'.

3.2.2.3. Signal Distortion

The signal distortion test was conducted as described in Section 2.3.3. Figure 3-24 – Figure 3-25 detail the results of a single device. Refer to Appendix D for results from each single-ended test.

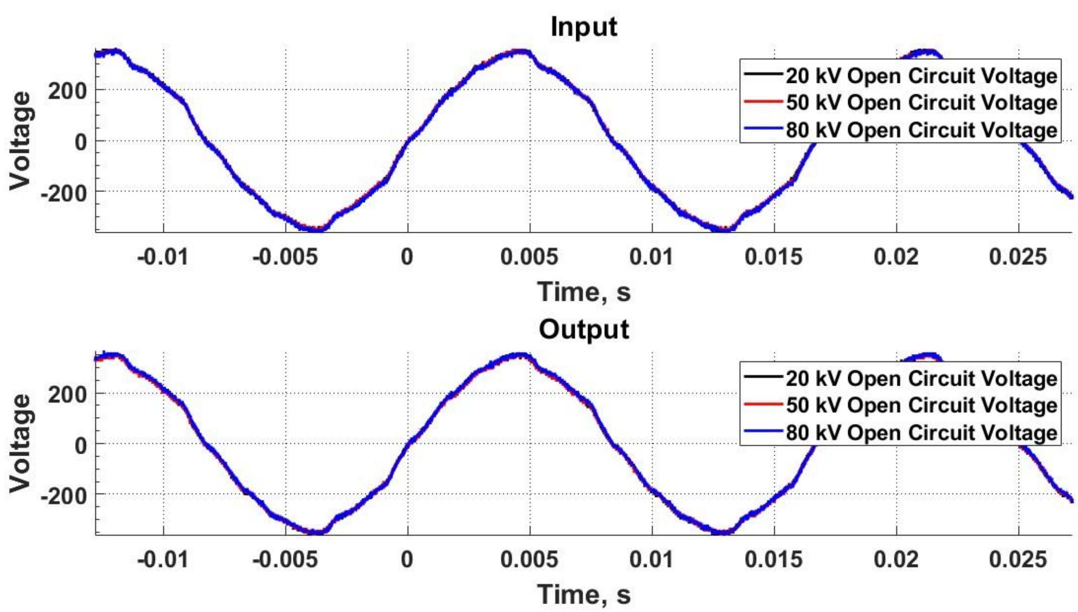

Figure 3-24. Time-Domain Signals for Signal Distortion Test, Single-Ended Configuration

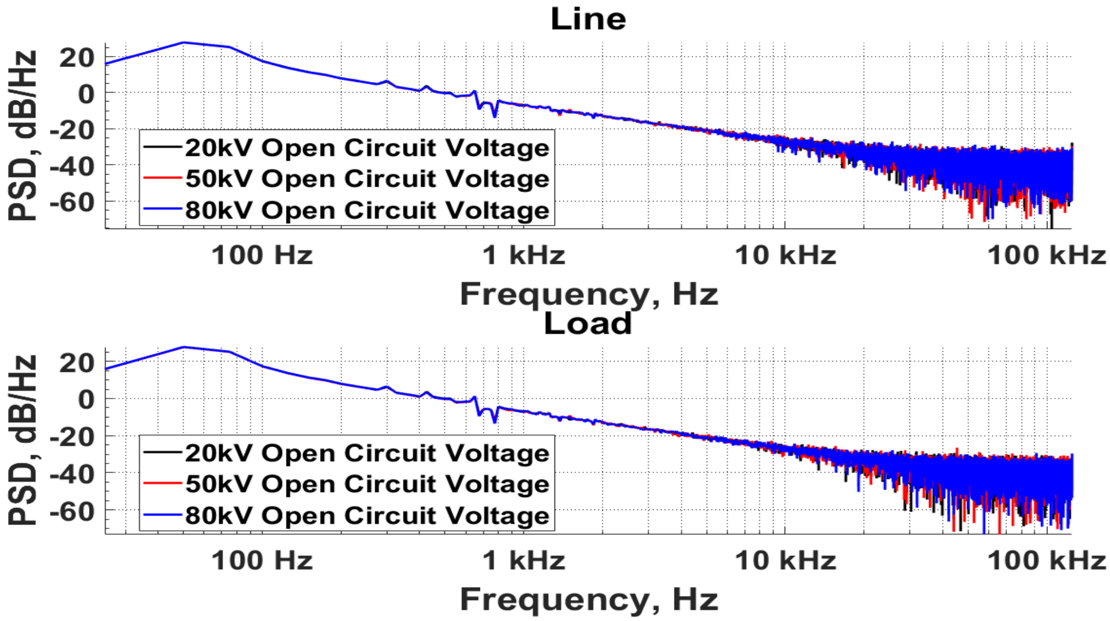

Figure 3-25. Power Spectral Density Comparison of Input and Output Signals for Single-Ended Test Configuration

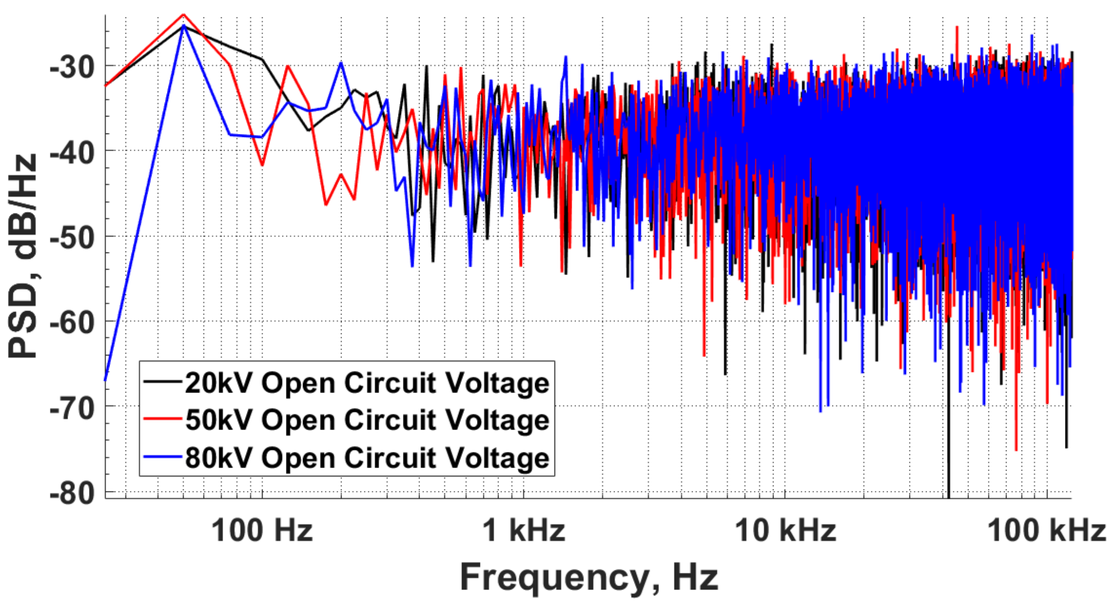

Figure 3-26. Power Spectral Density Comparison of Input and Output Signal Difference for Single-Ended Test Configuration

The input and output signal spectral content did not exhibit any noticeable differences. Signal degradation was not detected in any measurement.

4. CONCLUSION

Both common mode and single-ended test configurations demonstrated the TVSS' failure to protect against the E1 pulse. The TVSS' internal MOVs did not respond to the fast pulse due to their activation time. The voltages measured throughout the circuits were significantly lower than the pulser output in an open circuit configuration, but this was due to the impedance of the TVSSs. No non-linear clamping effects of the MOVs were noted during the conducted test. The devices were verified to clamp a voltage insult with a time scale of several μs which ensures that the lack of clamping in each test is not due to faulty devices.

The TVSSs proved to be resilient, however. They withstood all tests with no detectable damage except a single blown fuse resulting from a 20 kV charge voltage test. The cause of the blown fuse is unknown. However, the MOVs in the TVSS circuit were not damaged and the device withstood testing up to 80 kV open circuit voltage with no observable damage or degradation. No other fuses in the remaining TVSSs were blown throughout the duration of testing.

Conclusions regarding the conducted pulse testing of TVSS devices are that while they respond to voltage pulses with FWHM of at least several μs in duration , they do not respond to an E1 HEMP pulse. The devices themselves, however, are resilient and can withstand significant overvoltages from an EMP with minimal to no damage or degradation.

To fully determine the implications of the test results described in this report, further testing on equipment vulnerability must be conducted. Understanding substation equipment response to the conducted pulses observed in this test due to the failed response of the TVSSs will help determine the level of concern for grid resilience.

Future work for TVSS testing could be conducting tests with a higher voltage output pulser to determine the damage threshold of the devices. The maximum voltage output in an open circuit configuration for the UNM pulser was reached at 80 kV and the devices showed no indication of damage. Understanding the damage threshold of the TVSSs would establish margins for their ability to withstand an E1 conducted pulse.

REFERENCES

[1] Pfeiffer, R., Llanes, R. Warne, L., Halligan, M. "Substation Cable Layouts for EMP Coupling Analysis," Sandia Report, 2020.

[2] T.K. Gupta, "Application of zinc oxide varistors," J. Amer. Ceram. Soc., vol. 73, no. 7, pp. 1817-1840, July 1990.

[3] D. Sanabria, "Early Time (E1) Electromagnetic Pulse Effects on Lightning Surge Arresters and Trip Coils," University of New Mexico, 2020.

[4] Bowman, T., Halligan, M, Llanes, R, "High-Frequency Metal-Oxide Varistor Modeling Response to Early-time Electromagnetic Pulses." Sandia Report SAND2020-5243C, 2020

[5] Pozar, D. M., "Microwave Engineering, 4th Edition," 2012

APPENDIX A. LTSPICE SIMULATION VARIFICATION OF COMMON MODE CONFIGURATION RESPONSE

A simple simulation was conducted to verify the output results from the common mode test configuration. The TVSS devices were modeled using a simple series LC circuit using values obtained from SOH impedance characterization measurements. The values were adjusted slightly until an acceptable agreement between the simulation and test results was reached. Figure A-1 contains the circuit simulated in LTSPICE and Figure A-2 – Figure A-4 display the results of the simulation. Table A-1 shows some approximate value comparisons between the test and the simulation.

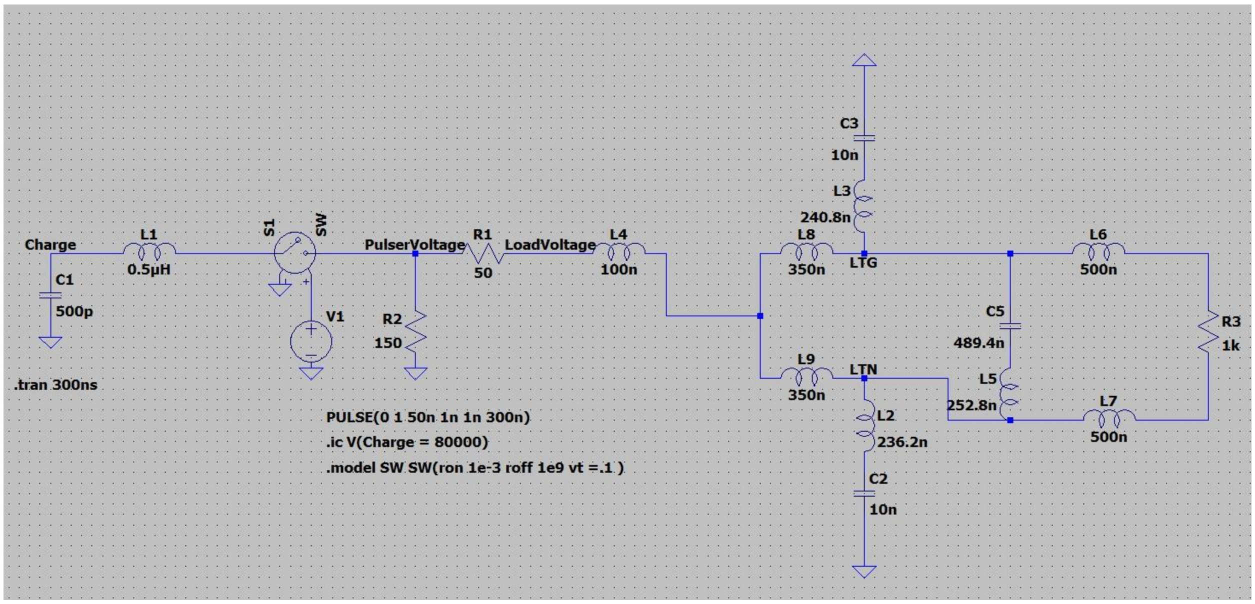

Figure A-1. LTSPICE Simulation Circuit of Common Mode Test Configuration

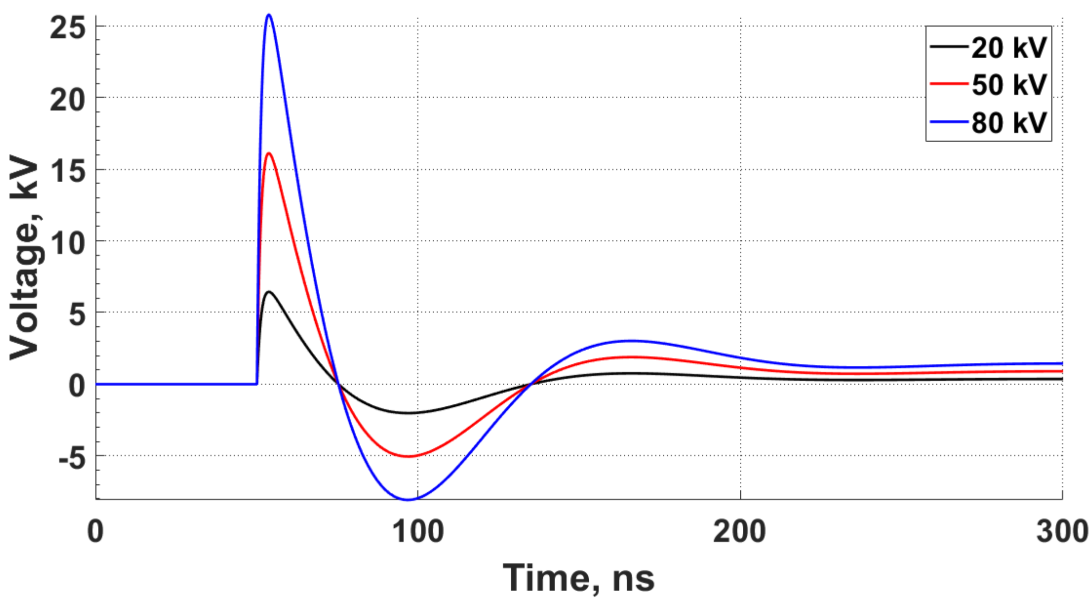

Figure A-2. LTSPICE Simulation Pulser Voltage Output for Common Mode Configuration

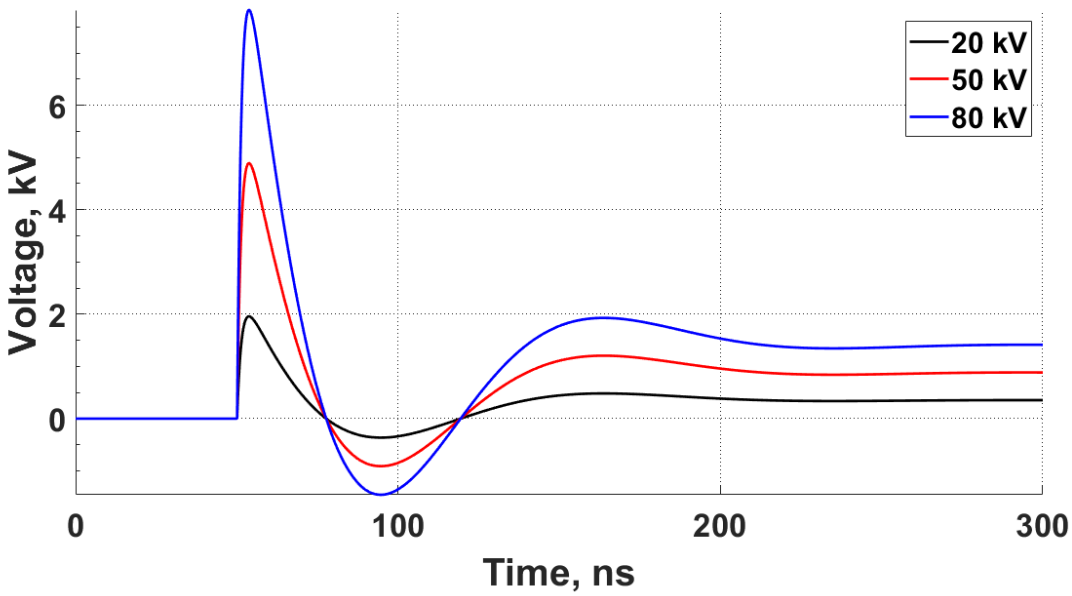

Figure A-3. LTSPICE Simulation Line-to-Ground Voltage for Common Mode Configuration

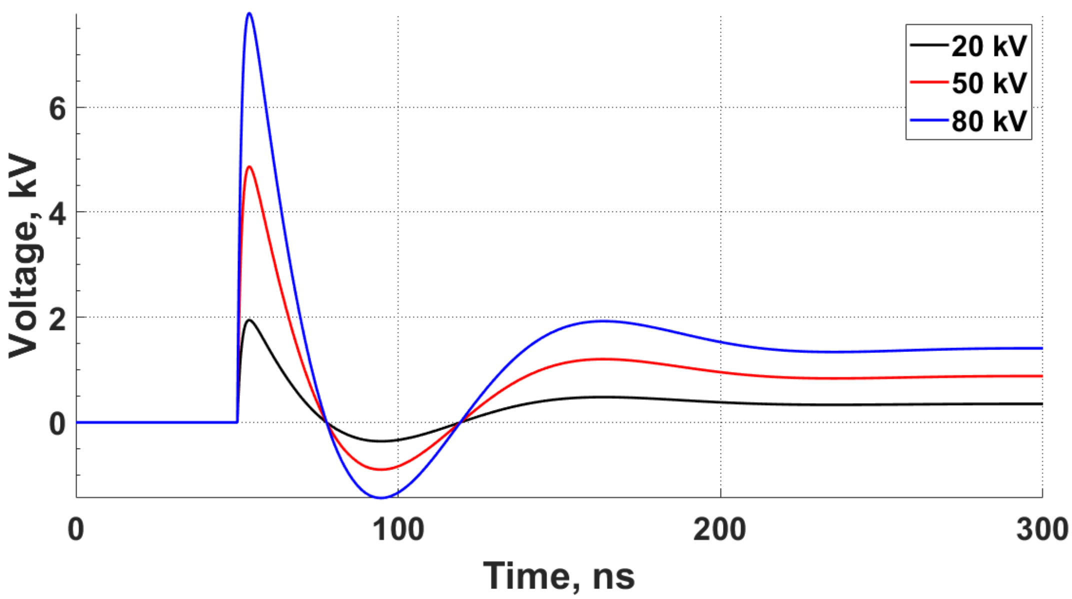

Figure A-4. LTSPICE Simulation Neutral-to-Ground Voltage for Common Mode Configuration

Table A-1. Comparisons Between Simulation and Test

Configuration	Voltage	Amplitude (kV)		Risetime (ns)		Pulsewidth (Start-1st Valley) (ns)	
		Test	Simulation	Test	Simulation	Test	Simulation
Pulser Output	20 kV	~3.5	~6	~10-15	~2	~50	~50
	50 kV	~12	~16	~10-15	~2	~50	~50
	80 kV	~18	~25	~10-15	~2	~50	~50

Configuration	Voltage	Amplitude (kV)		Risetime (ns)		Pulsewidth (Start-1st Valley) (ns)	
		Test	Simulation	Test	Simulation	Test	Simulation
LTG	20 kV	~1.5	~2	~10-15	~2	~40	~50
	50 kV	~5	~5	~10-15	~2	~40	~50
	80 kV	~8	~7.8	~10-15	~2	~40	~50
NTG	20 kV	~1.5	~2	~10-15	~2	~40	~50
	50 kV	~5	~5	~10-15	~2	~40	~50
	80 kV	~8	~7.8	~10-15	~2	~40	~50

The simulation demonstrated a similar response as the common mode testing response detailed in Section 3.1. The amplitude of the pulse is slightly higher in the simulation than testing. The risetime of the simulation is significantly faster than in testing due to the usage of an ideal switch and not an accurate representation of the spark gap switch present in testing. The pulsewidth measured form the beginning of the pulse to the first valley demonstrates a similar time correlation. Certain deviating results exist due to specifics in the testing configuration that are not present in the simulation such as parasitic capacitance, test configuration inductance, non-ideal switch characteristics, the output MOV characteristics, and the specific characteristics of the MOVs. However, developing an accurate circuit model for the TVSS devices was not in the scope of this project and the accuracy of the discussed simulation is sufficient for demonstrating the expected response of the TVSS device and verify the testing results.

APPENDIX B. VERIFYING TVSS AND MOV FUNCTIONALITY WITH SLOW PULSER

B.1. MOV in Parallel with 1 kΩ Resistor using Slow Pulser

A single MOV and a single TVSS device was used to verify their ability to protect against transient overvoltages with durations of several microseconds (μs). Verifying the functionality of the TVSS devices against transient overvoltage pulses similar to their intended use was essential to confirm that the results from the fast pulse duration conducted pulse testing would be accurate. A slower pulser owned by UNM with a square pulse output with an approximate risetime of 100 ns and a pulsewidth of approximately 2μs was used to replicate this type of transient event.

The response of individual MOVs inside of the TVSS was first evaluated by removing them from a sample device and placing it in parallel with a 1 kΩ resistor. The two devices were then used as a terminating load for the pulser and various pulser voltage output levels were used to test the clamping effects of the device. A circuit model of the test is found in Figure B-1.

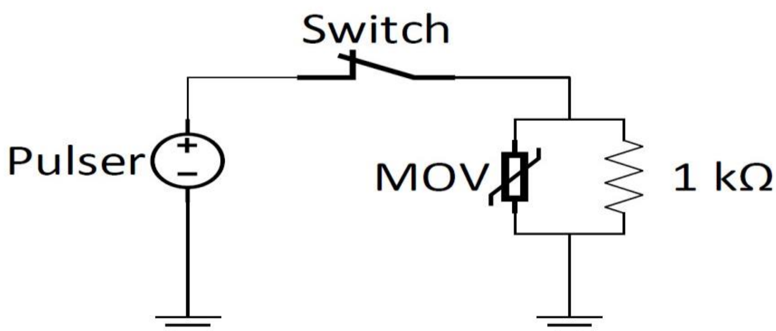

Figure B-1. Circuit Model for Functionality Verification Test with MOV

A 1 kΩ resistor was used as a termination for the slow pulser to collect a reference response for the output from the pulser across the load. Figure B-2 shows the voltage across the resistor at three different voltage output levels of the pulser. The level 05, 10, and 15 correspond to “open circuit” voltages of 3 kV, 6 kV, and 9 kV, respectively.

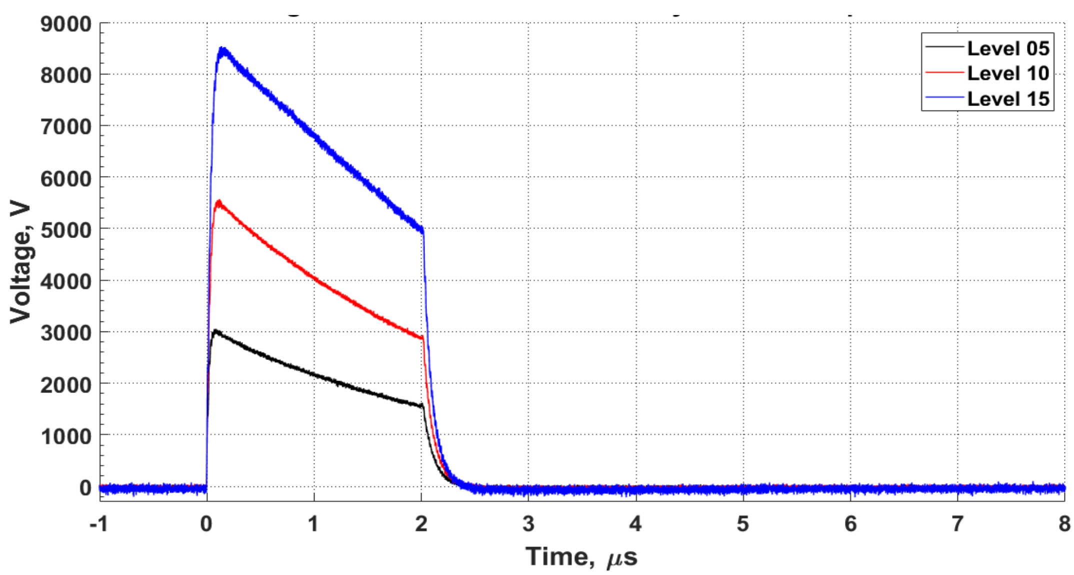

Figure B-2. Voltage Across 1 kΩ Resistor, Slow Pulser

The response was as expected – voltage increased proportionately as the output of the pulser was increased.

A single MOV was then placed in parallel to the 1 kΩ load. The combination load was then used to terminate the pulser and the load was pulsed at the same levels as the baseline reference. The voltage response is in Figure B-3 below.

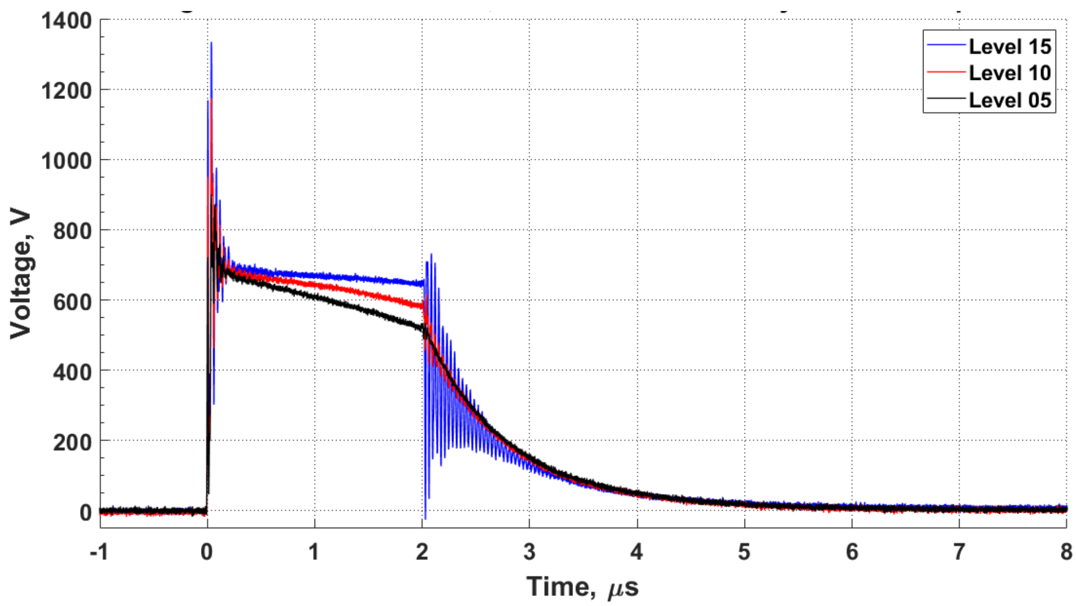

Figure B-3. Voltage Across 1 kΩ Resistor with MOV in Parallel, Slow Pulser

The results of this test demonstrated the clamping characteristics of the MOVs. When one is in parallel with the resistor, the output of the pulser was clamped consistently at approximately 650 V. An increased amplitude of ringing at the beginning and end of the pulse duration was noted with each voltage level. The ringing is assumed to be related to the time the MOV requires to clamp. The ringing response is seen to be on the order of approximately 500 ns.

B.2. TVSS in Parallel with 1 kΩ Resistor using Slow Pulser

A further round of testing was conducted using a complete TVSS assembly in place of a singular MOV in parallel with the 1kΩ resistor to test the clamping response of the TVSS. Each protection mode of the TVSS (LTN, LTG, and NTG) was placed in parallel with the load and its response was evaluated. A circuit model of the test is found in Figure B-4 and Figure B-5 – Figure B-7 display the output response for each TVSS configuration.

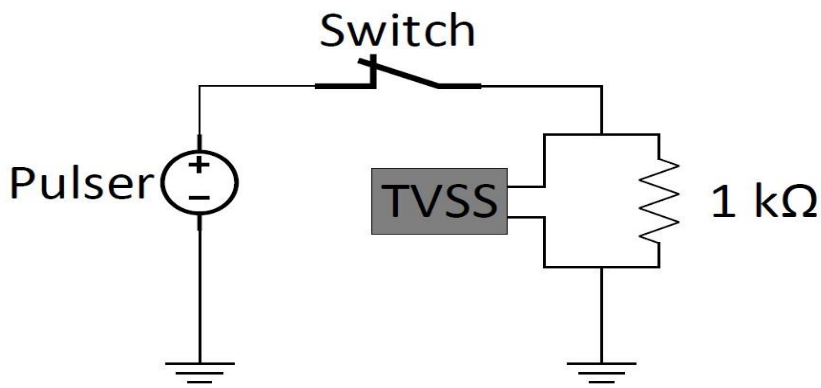

Figure B-4. Circuit Model for Functionality Verification Test with TVSS

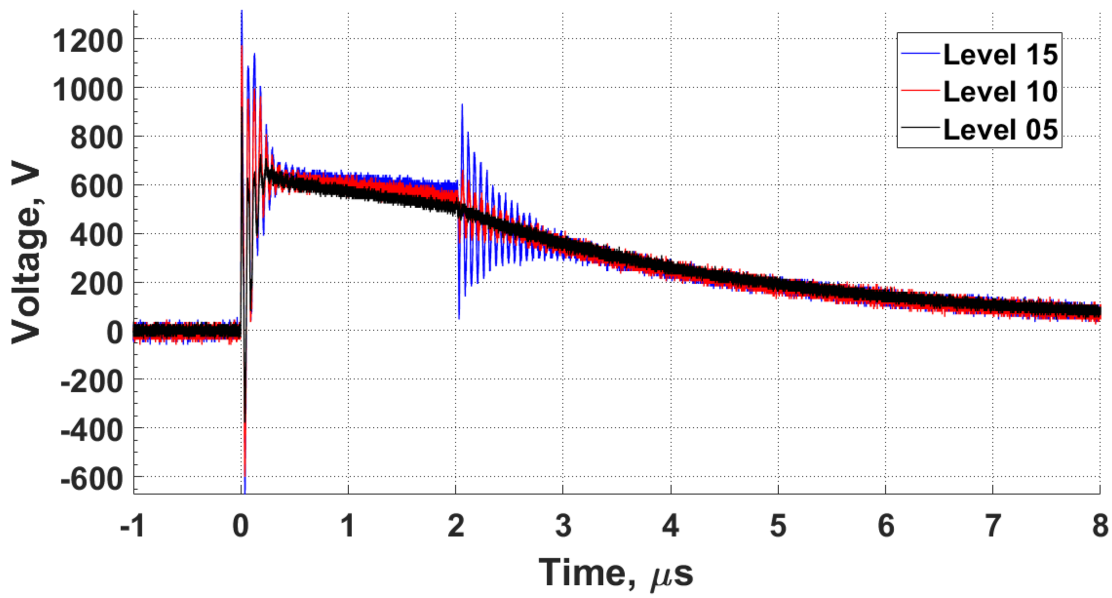

Figure B-5. Voltage Across 1 kΩ Resistor with LTG Protection Circuit in Parallel, Slow Pulser

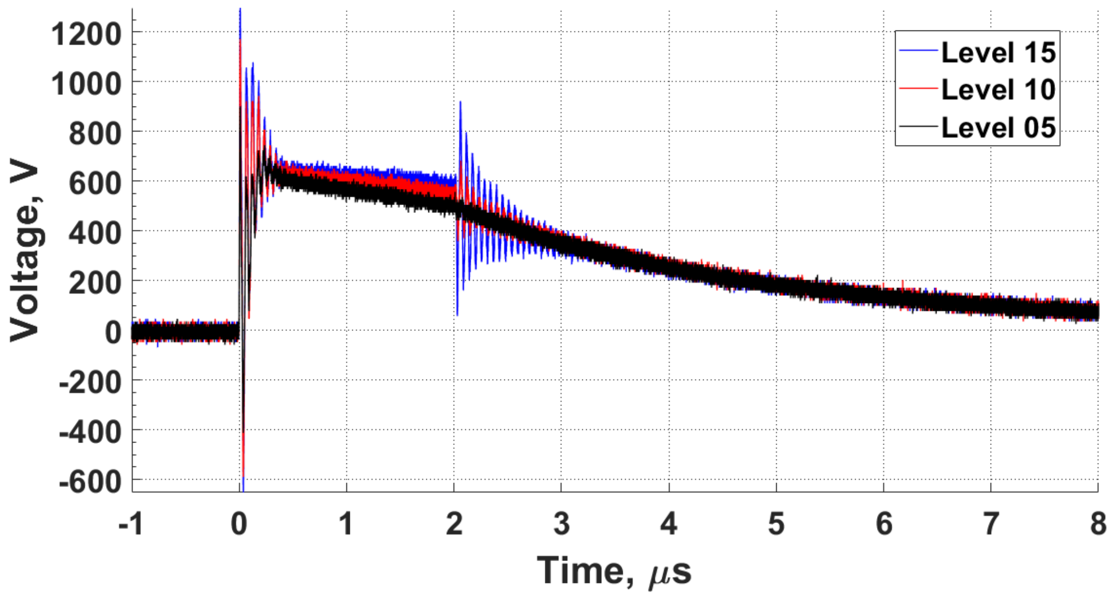

Figure B-6. Voltage Across 1 kΩ Resistor with NTG Protection Circuit in Parallel, Slow Pulser

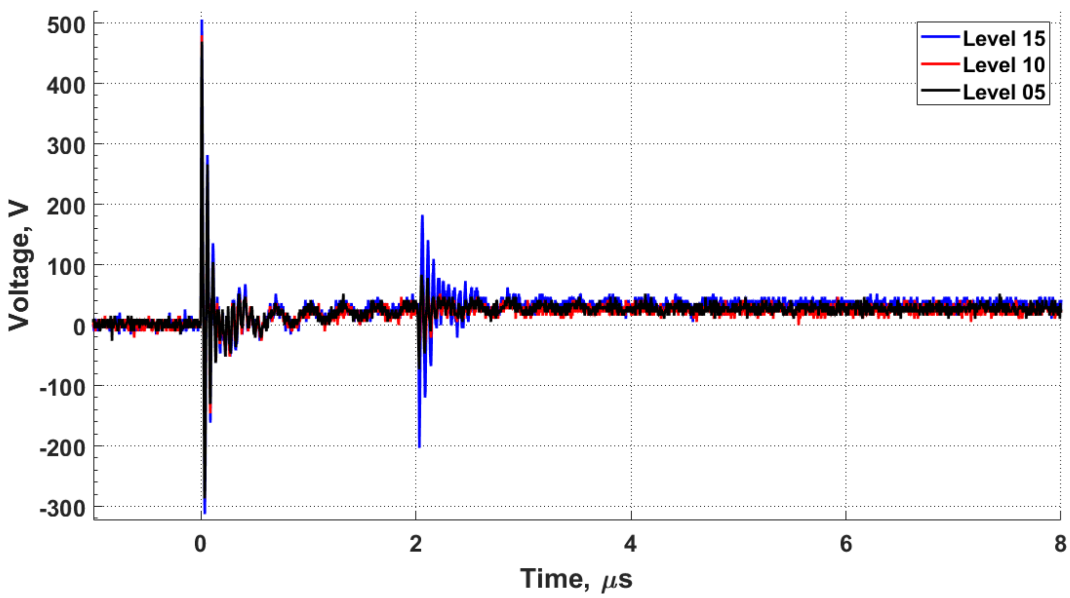

Figure B-7. Voltage Across 1 kΩ Resistor with LTN Protection Circuit in Parallel, Slow Pulser

Similar results to the singular MOV in parallel were observed for the LTG and NTG protection modes. The LTN protection mode had a differing response with ringing at the rising and falling edge of the pulse and a gradual rise in voltage to approximately 20 V. The LTN protection circuit differs from the other two circuits in that it contains a capacitor in parallel of the MOVs in addition to components for operations not relevant to this study. The difference in circuit most likely caused the differing response. The LTN circuit still provided protection to the load as the voltage across it was significantly lower than displayed in Figure B-2. A noticeable difference between the two tests is a significant increase in fall time of the pulse in the complete TVSS assembly, most notably in the line-to-neutral configuration. The increased fall time of the line-to-neutral configuration is a product of the parallel capacitor located uniquely in that specific protection circuit. The capacitor discharges much more slowly than the MOVs and, as a result, the pulse is discharged more slowly than with just an MOV.

Both the singular MOV and the TVSS protection circuits demonstrate the same ringing effects as the MOVs are activated and begin to clamp. The ringing in the MOVs also appears to be consistent with the time duration of approximate 500 ns.

B.3. TVSS in Parallel with 1 kΩ Resistor using Fast Pulser

The test configuration described above was then repeated with the same TVSS device using the fast pulser in place of the slow pulser. Like the slow pulse configuration, each protection mode of the TVSS was placed in parallel with a 1 kΩ resistor. The response of the TVSS was evaluated for incremental pulser open circuit voltages of 20 kV, 40 kV, 60 kV, and 80 kV. Shots at the previously mentioned voltage levels were conducted on the load by itself to determine a baseline response for the voltage across the load with no protection in place. Figure B-8 contain the results of the testing across the load by itself.

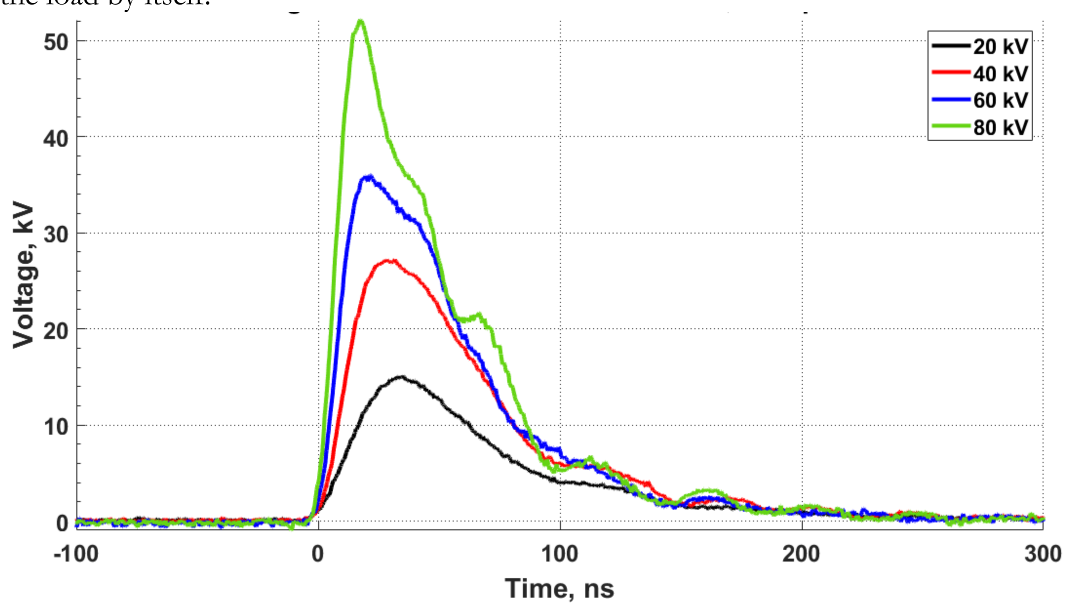

Figure B-8. Voltage Across 1 kΩ Resistor with Fast Pulser

The TVSS device was the placed in parallel with the load and the results are found in Figure B-9 – Figure B-11.

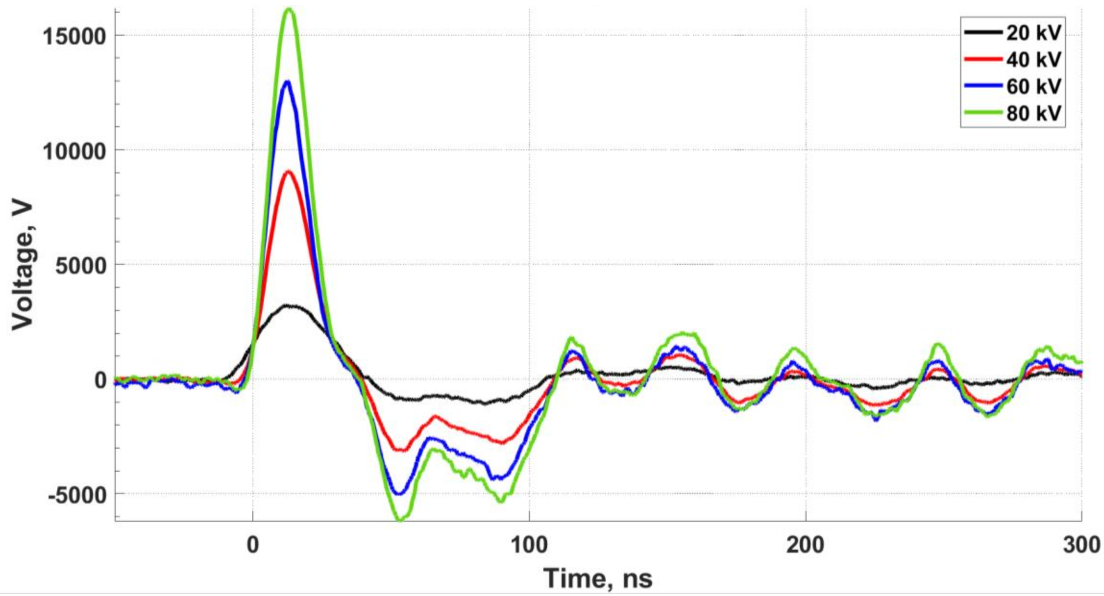

Figure B-9. Voltage Across 1 kΩ Resistor with LTG Protection Circuit in Parallel, Fast Pulser

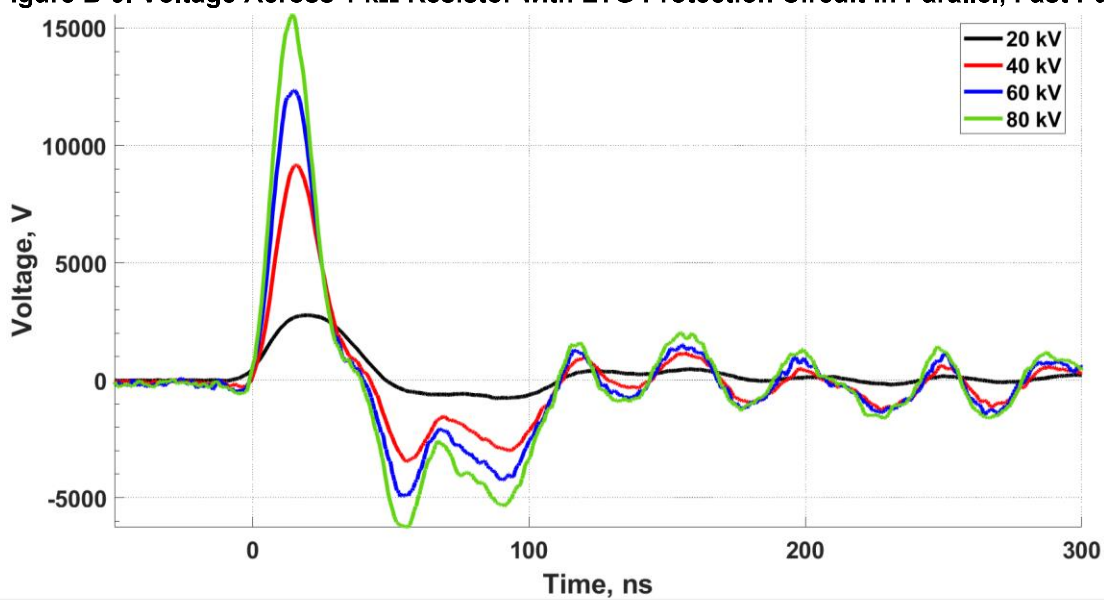

Figure B-10. Voltage Across 1 kΩ Resistor with NTG Protection Circuit in Parallel, Fast Pulser

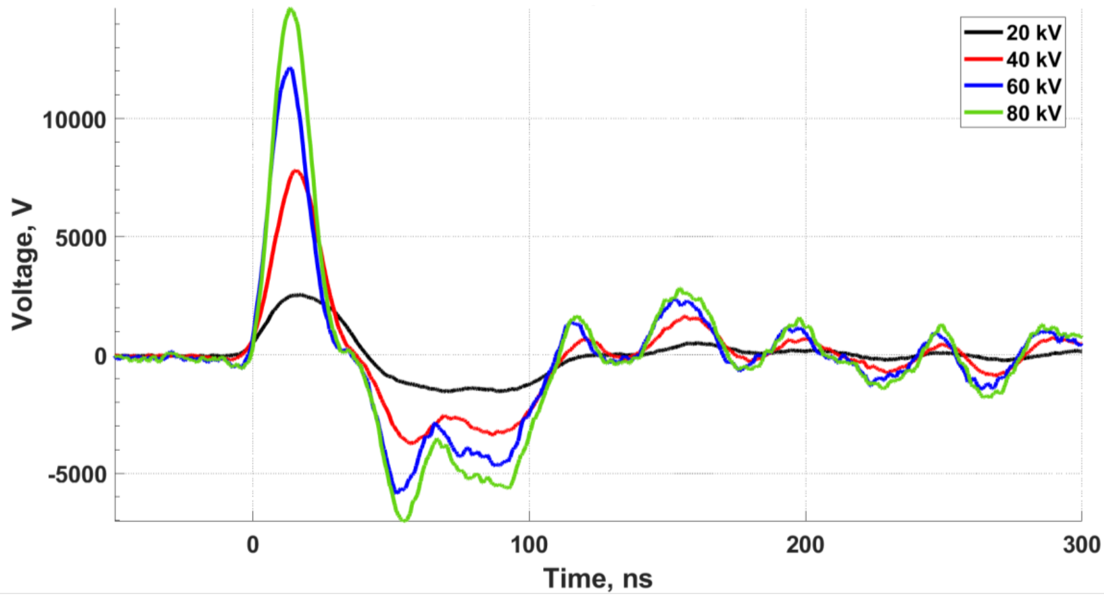

Figure B-11. Voltage Across 1 kΩ Resistor with LTN Protection Circuit in Parallel, Fast Pulser

A comparison with the response of the MOVs with the slow pulser reveals that the devices do not clamp as they did previously. The voltage and current increased proportionately with the output voltage level of the pulser. The output voltage was measured to be significantly lower with the TVSS in parallel than with the resistor by itself. However, this is due to the impedance characteristics of the TVSS circuit and is not related to the non-linear clamping effects of the MOVs.

B.4. LTSPICE Verification of Fast Pulser Response

A simple LTSPICE verified the output response shown in Appendix B.4 was primarily a result of the impedance characteristics of the device. The TVSS devices were modeled as a simple LC circuit using capacitance and inductance values extracted from the VNA state of health measurements on the devices. The results of the simulation are shown in Figure B-12 - Figure B-14. Table B-1 contains the values for capacitance and inductance used for each simulation.

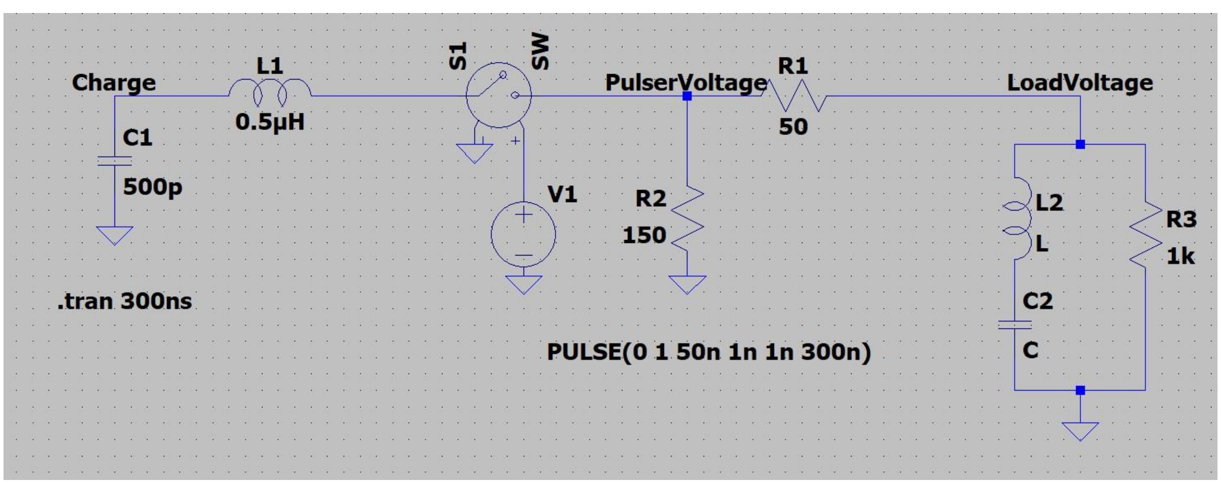

Figure B-12. LTSPICE Simulation Diagram for Verification of Fast Pulser Response

Table B- 1. Capacitance and Inductance Values used in Simulation

Configuration	Capacitance (nF)	Inductance (nH)
LTG	3.21	236
LTN	479	248
NTG	3.21	230

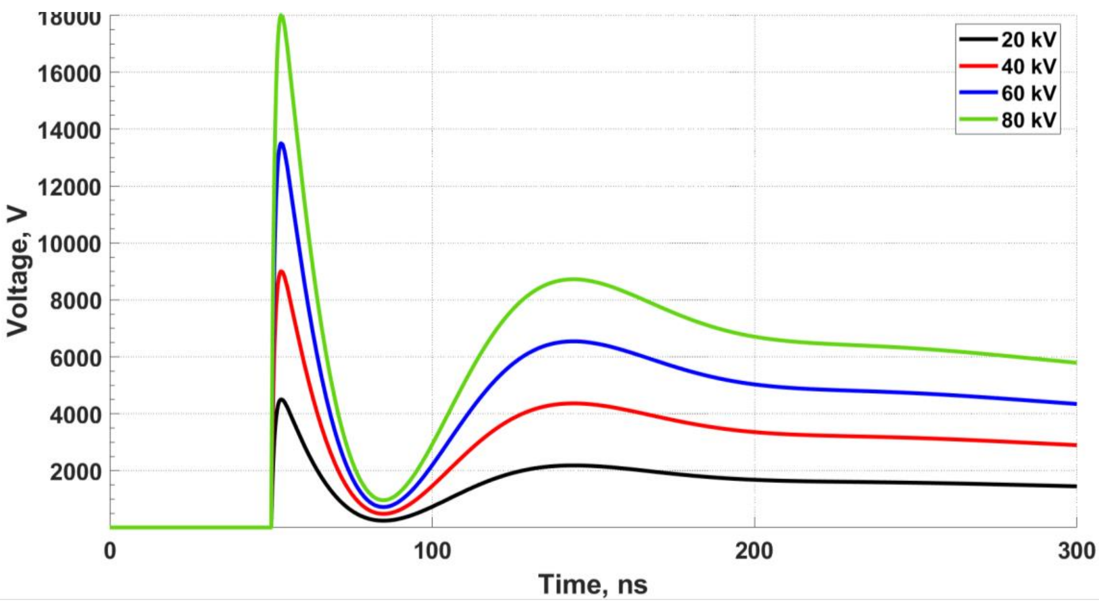

Figure B-13. Simulation Results, LTG in Parallel with 1 kΩ Resistor

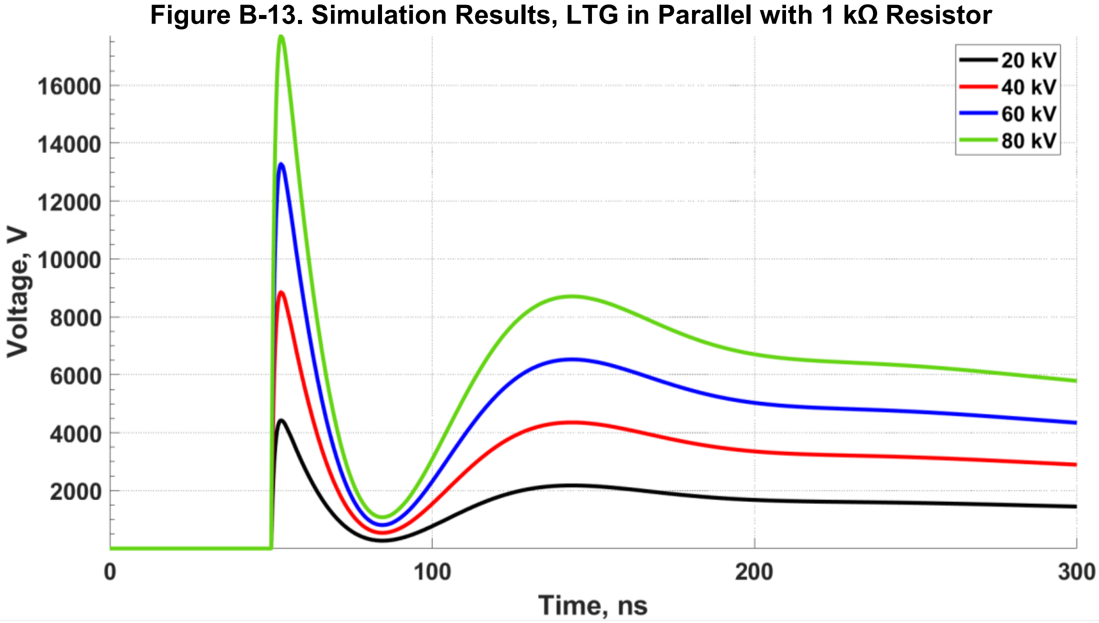

Figure B-14. Simulation Results, NTG in Parallel with 1 kΩ Resistor

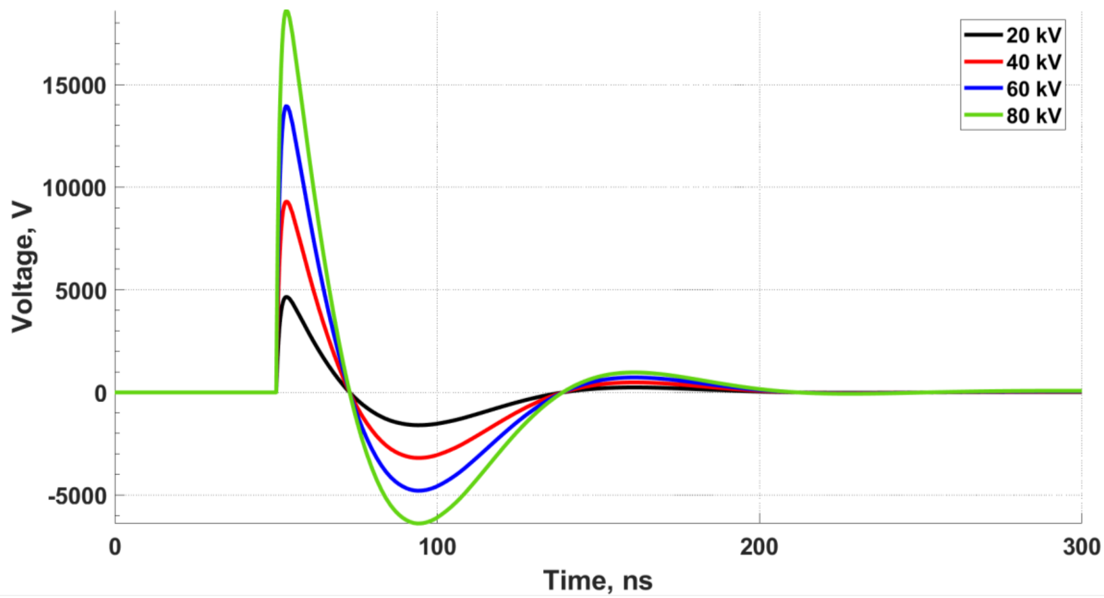

Figure B-15. Simulation Results, LTN in Parallel with 1 kΩ Resistor

Table B-2. Comparisons Between Simulation and Test

Configuration	Voltage	Amplitude (kV)		Risetime (ns)		Pulsewidth (Start – 2nd Peak) (ns)	
		Test	Simulation	Test	Simulation	Test	Simulation
LTG	20 kV	~3	~4.5	10-15	~2	~150	~80
	40 kV	~9	~9	10-15	~2	~150	~80
	60 kV	~13	~13.5	10-15	~2	~150	~80
	80 kV	~16	~18	10-15	~2	~150	~80
NTG	20 kV	~3	~4.5	10-15	~2	~150	~80
	40 kV	~9	~9	10-15	~2	~150	~80
	60 kV	~12	~13.5	10-15	~2	~150	~80
	80 kV	~15.5	~17.5	10-15	~2	~150	~80
LTN	20 kV	~3	~4.5	10-15	~2	~150	~100
	40 kV	~8	~9	10-15	~2	~150	~100
	60 kV	~12	~13.5	10-15	~2	~150	~100
	80 kV	~15	~18.5	10-15	~2	~150	~100

The simulation results demonstrated a similar pulser output to what was observed in the test. Simulation amplitudes are slightly higher than observed in testing. The significantly faster simulation is due to the usage of an ideal switch model instead of a realistic spark gap switch. The time measured from the start of the pulse to the top of the second peak was not identical but still provided a close correlation. Deviations in results are due to specifics in the testing configuration not accounted for in the simulation. However, the correlation observed with just a simple model adequately verifies the assertion made about the test results.

APPENDIX C. COMMON MODE STATE OF HEALTH DATA

C.1. DUT03

C.1.1. IV-Curve Trace

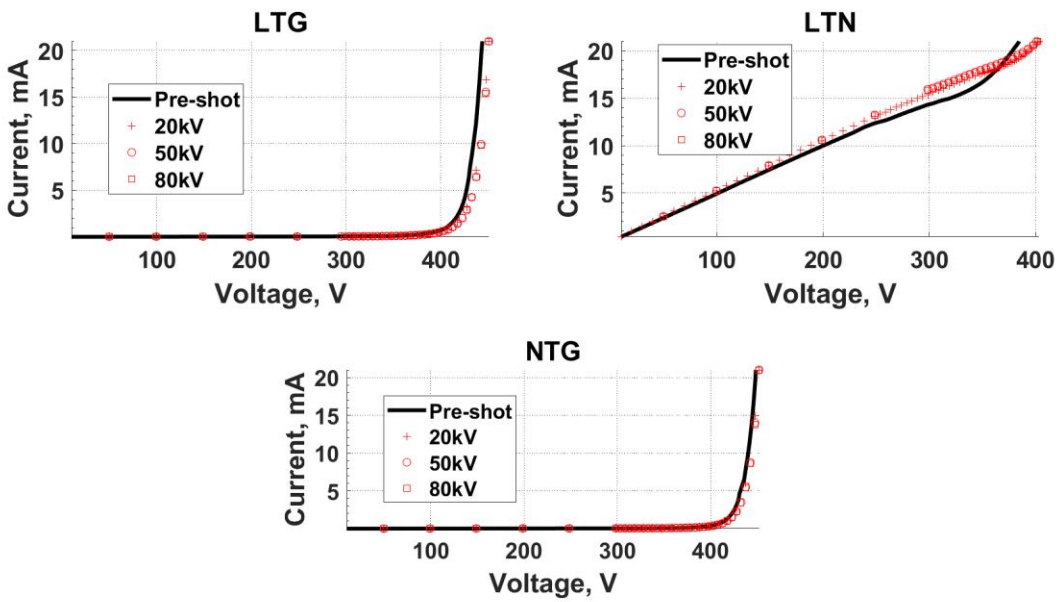

Figure C-1. DUT03 IV-Curves, Common Mode

C.1.2. Signal Distortion

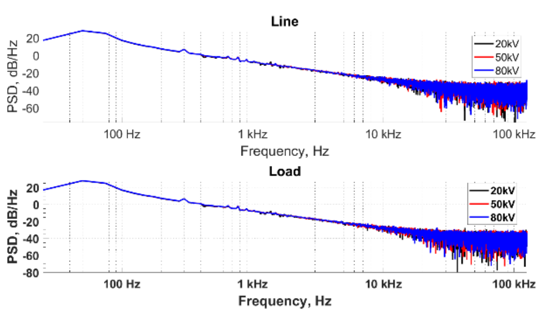

Figure C-2. DUT03 Power Spectral Density, Common Mode

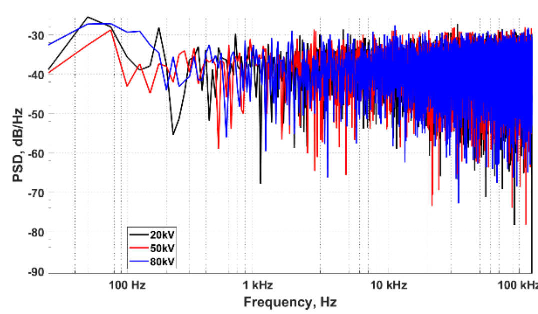

Figure C-3. DUT03 Power Spectral Density Difference, Common Mode

C.1.3. VNA Sweep

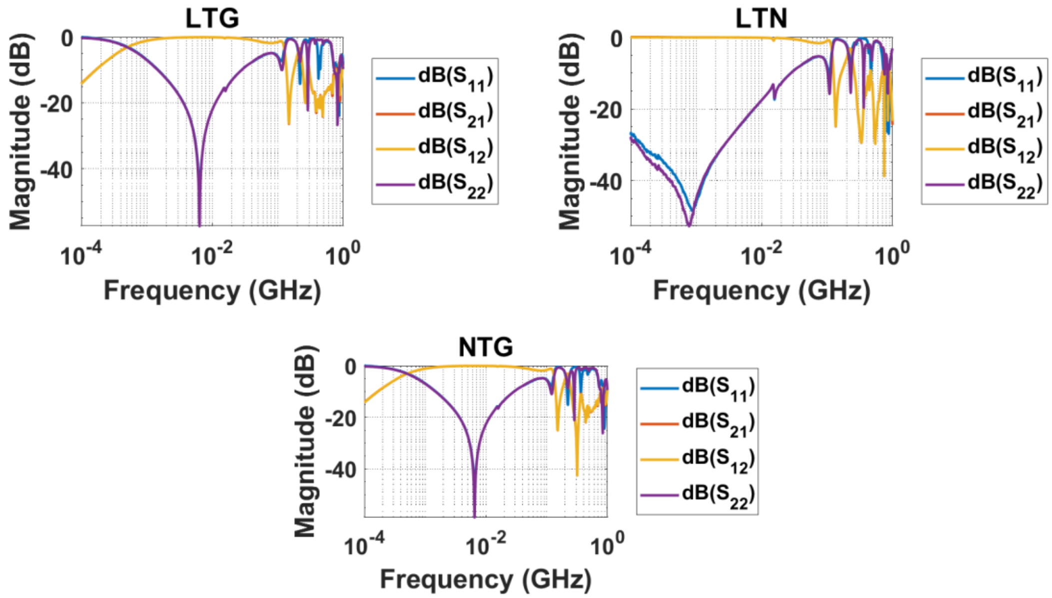

Figure C-4. DUT03 20 kV Network Parameters, Common Mode

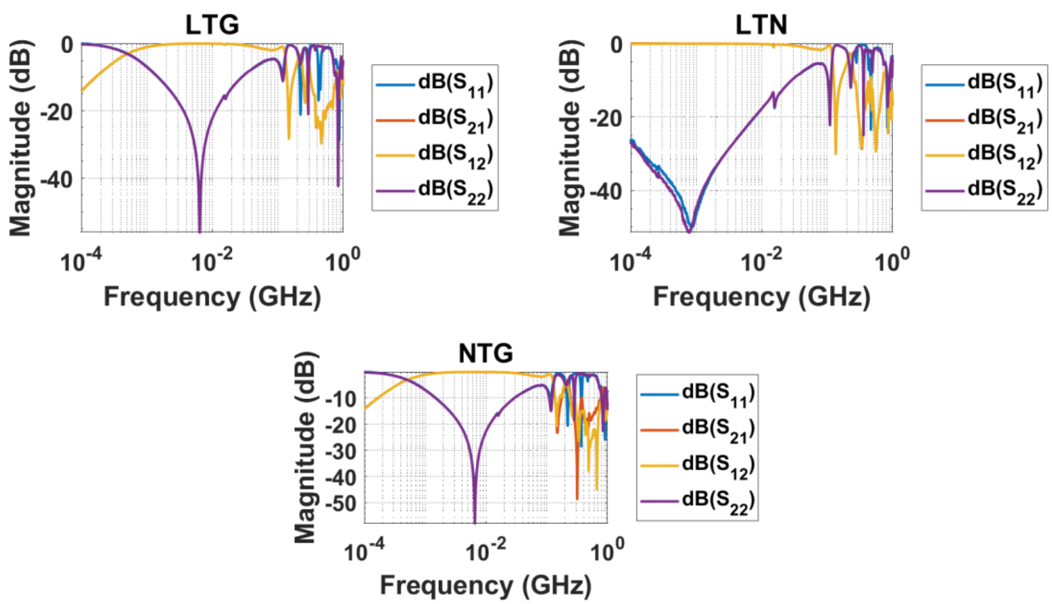

Figure C-5. DUT03 50 kV Network Parameters, Common Mode

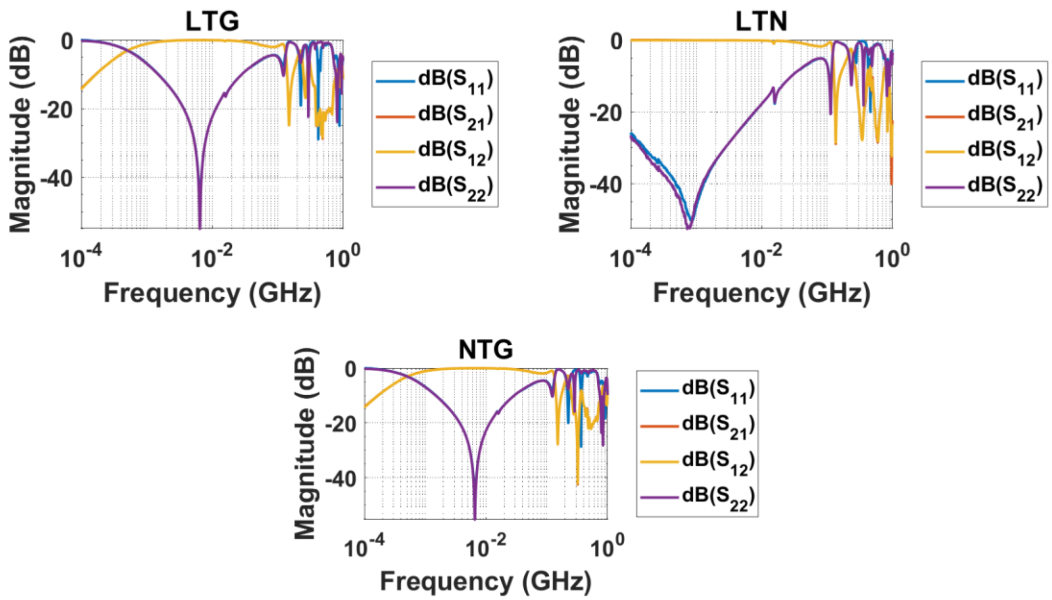

Figure C-6. DUT03 80 kV Network Parameters, Common Mode

C.2. DUT04

C.2.1. IV-Curve Trace

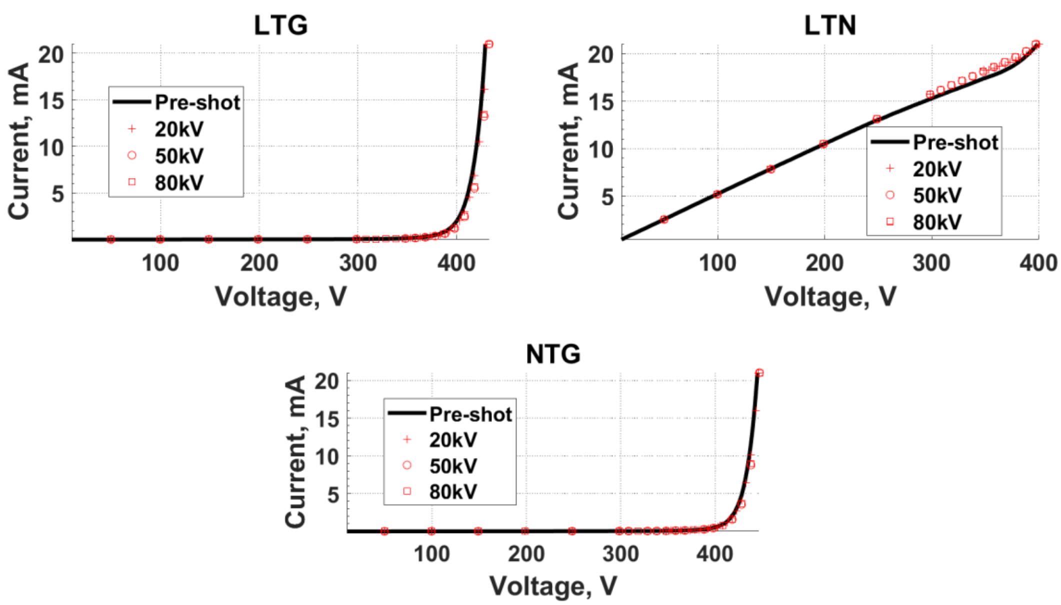

Figure C-7. DUT04 IV-Curves, Common Mode

C.2.2. Signal Distortion

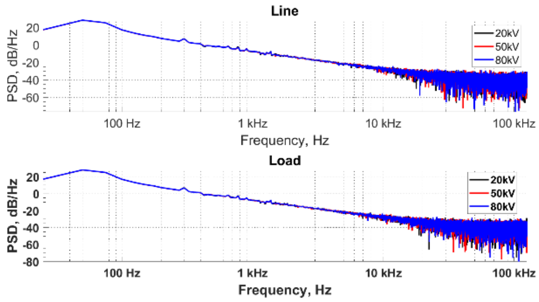

Figure C-8. DUT04 Power Spectral Density, Common Mode

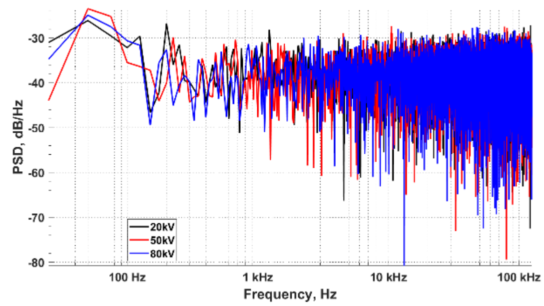

Figure C-9. DUT04 Power Spectral Density Difference, Common Mode

C.2.3. VNA Sweep

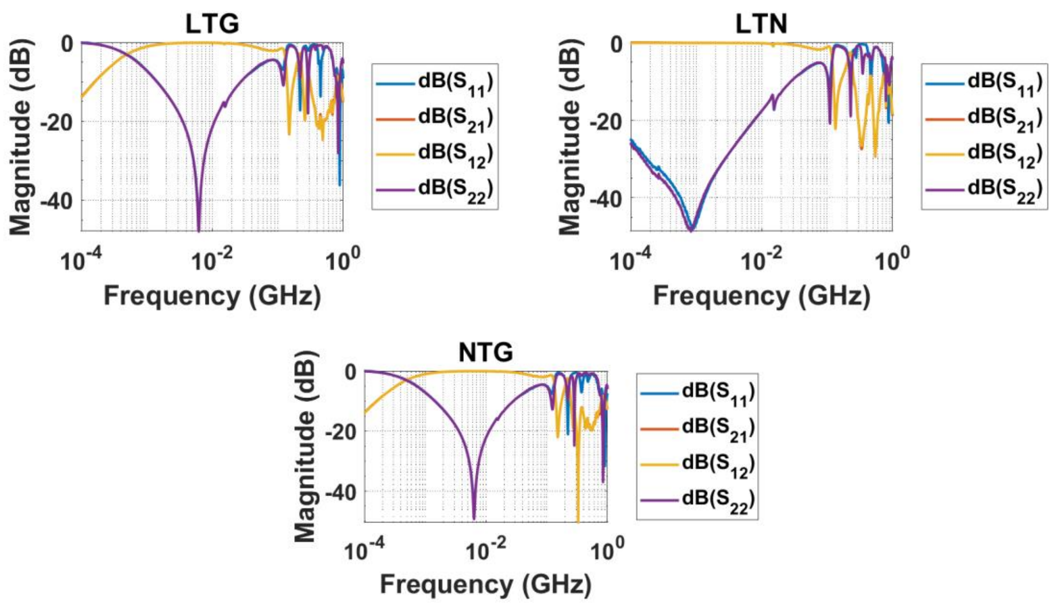

Figure C-10. DUT04 20 kV Network Parameters, Common Mode

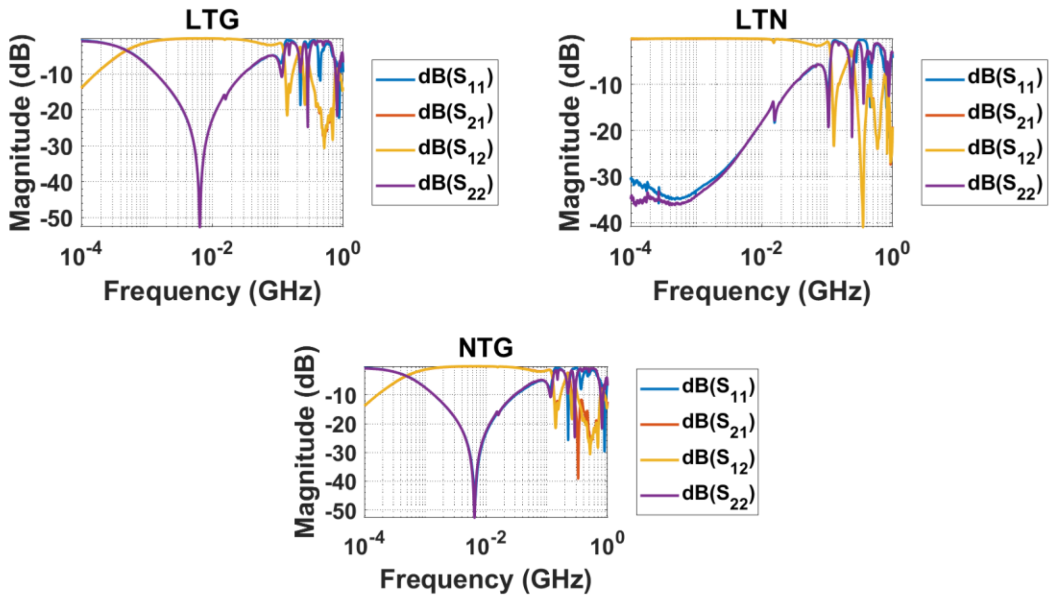

Figure C-11. DUT04 50 kV Network Parameters, Common Mode

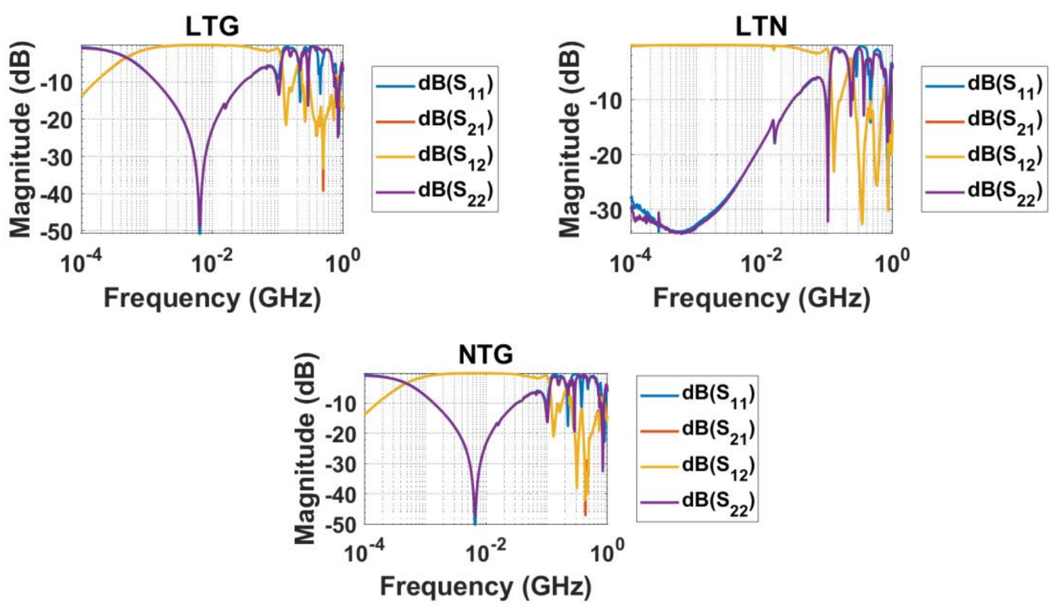

Figure C-12. DUT04 80 kV Network Parameters, Common Mode

C.3. DUT05

C.3.1. IV-Curve Trace

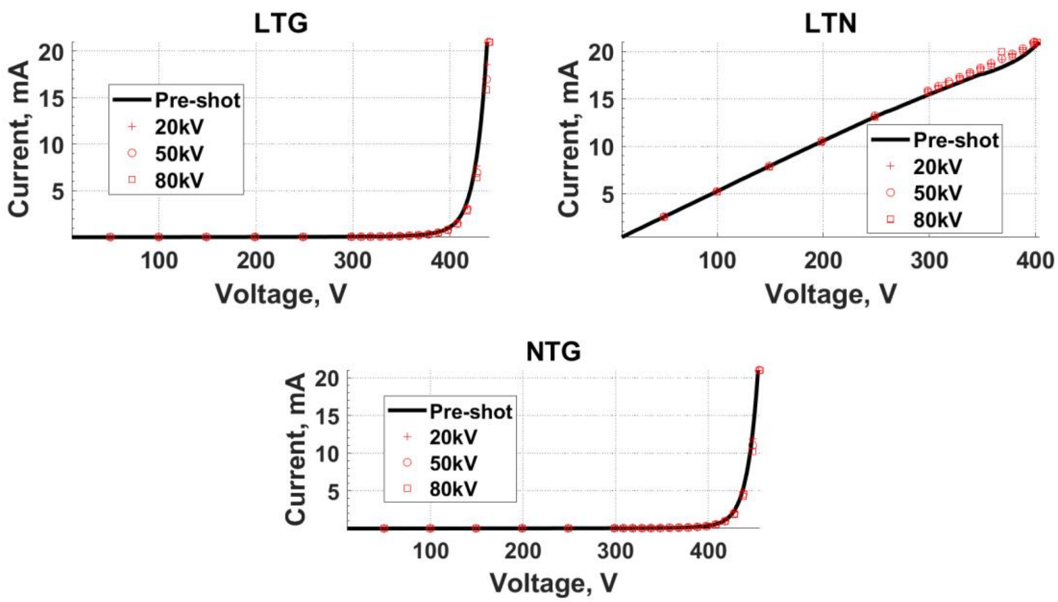

Figure C-13. DUT05 IV-Curves, Common Mode

C.3.2. Signal Distortion

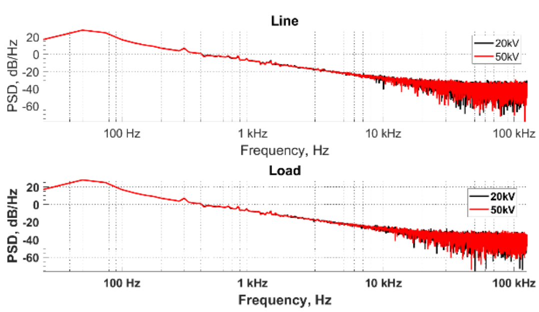

Figure C-14. DUT05 Power Spectral Density, Common Mode

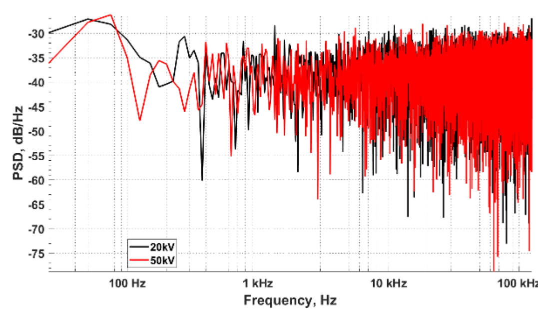

Figure C-15. DUT05 Power Spectral Density Difference, Common Mode

Note: Due to oscilloscope error, signal distortion data is not available for DUT05, 80kV common mode configuration. However, results from other state of health measurements and future testing conducted in single-ended configuration ensures that no damage was incurred to the device.

C.3.3. VNA Sweep

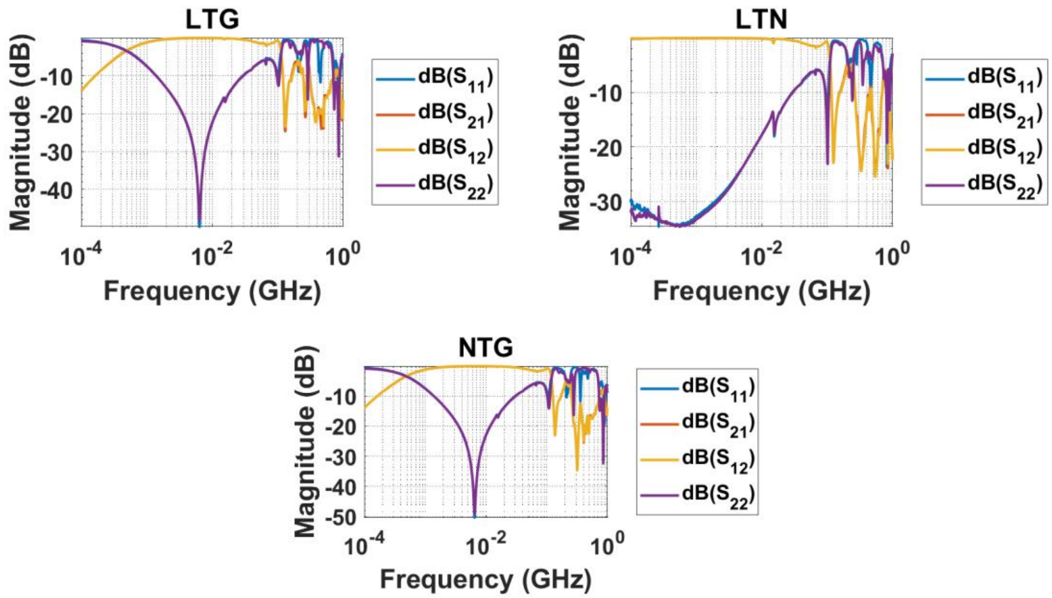

Figure C-16. DUT05 20 kV Network Parameters, Common Mode

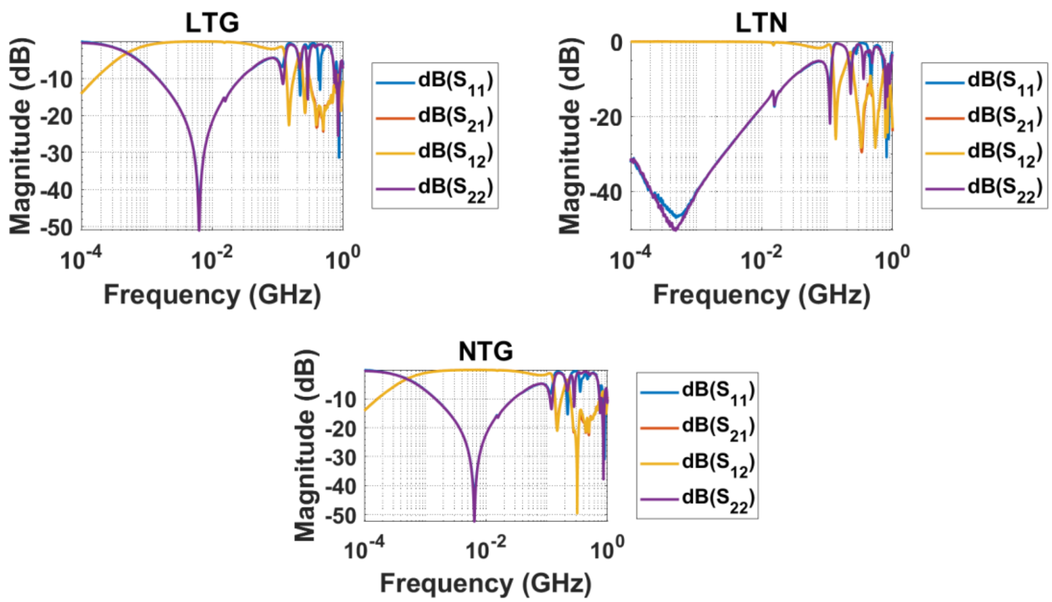

Figure C-17. DUT05 50 kV Network Parameters, Common Mode

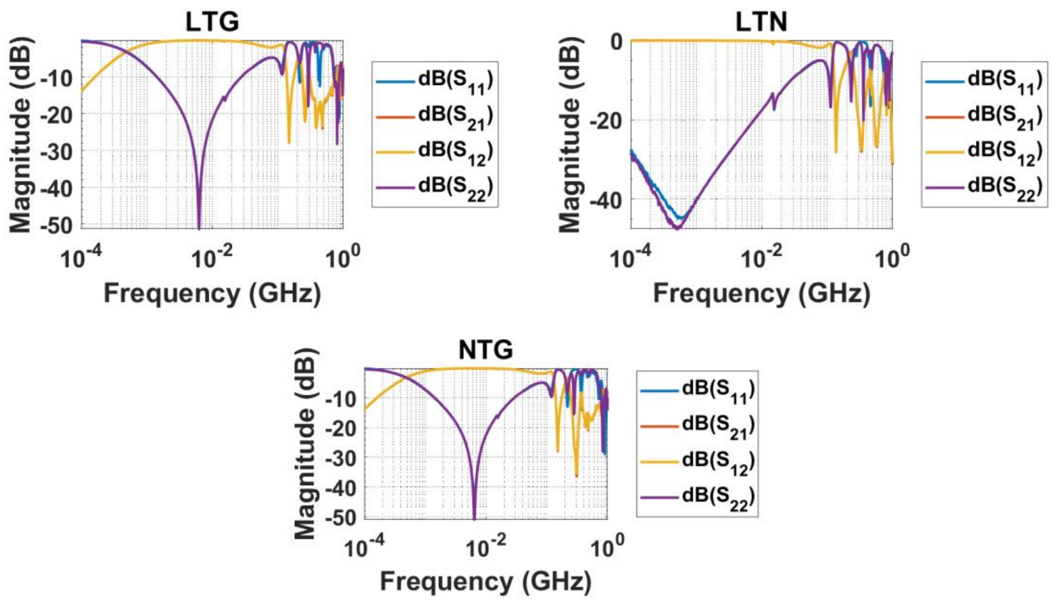

Figure C-18. DUT05 80 kV Network Parameters, Common Mode

C.4. DUT06

C.4.1. IV-Curve Trace

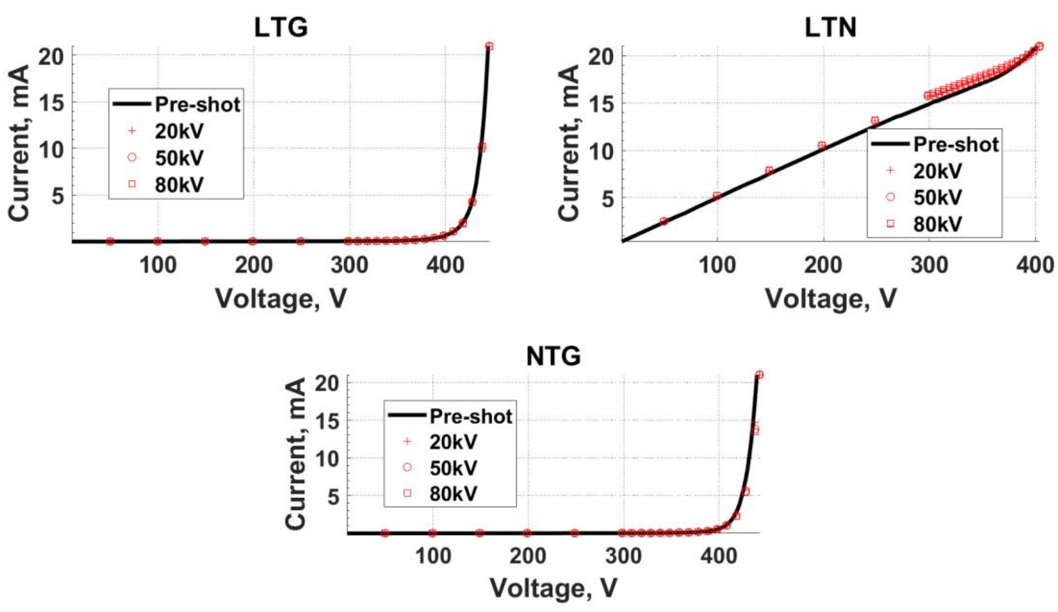

Figure C-19. DUT06 IV-Curves, Common Mode

C.4.2. Signal Distortion

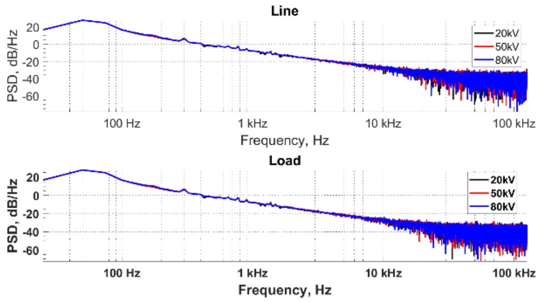

Figure C-20. DUT06 Power Spectral Density, Common Mode

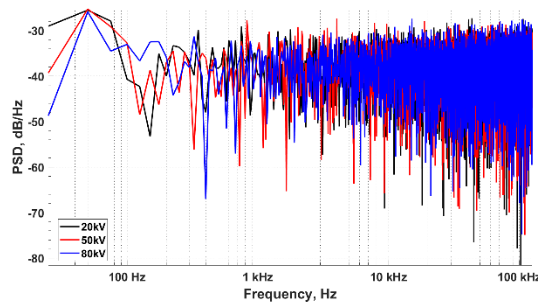

Figure C-21. DUT06 Power Spectral Density Difference, Common Mode

C.4.3. VNA Sweep

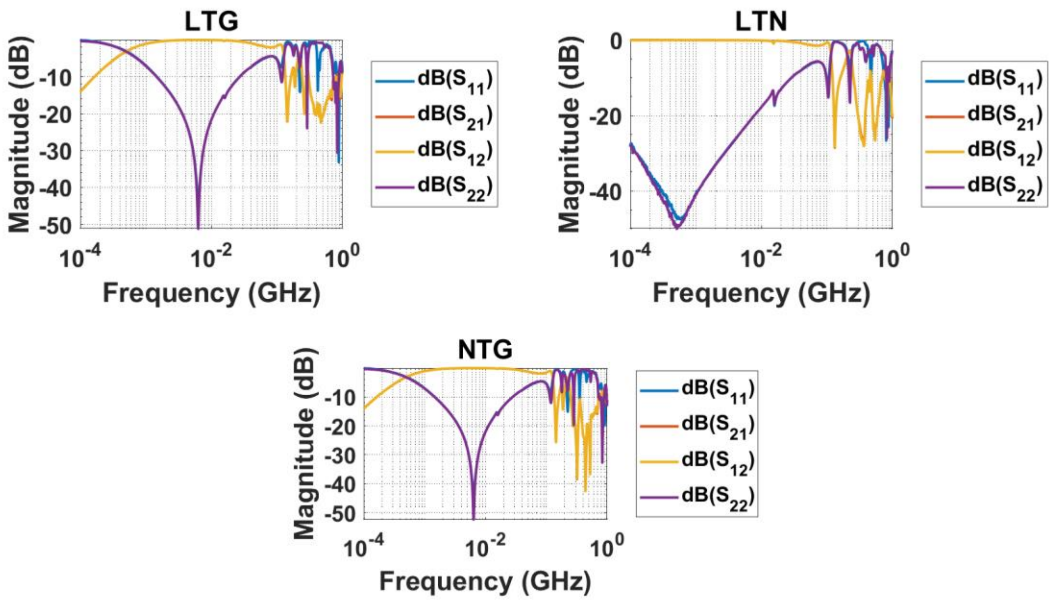

Figure C-22. DUT06 20 kV Network Parameters, Common Mode

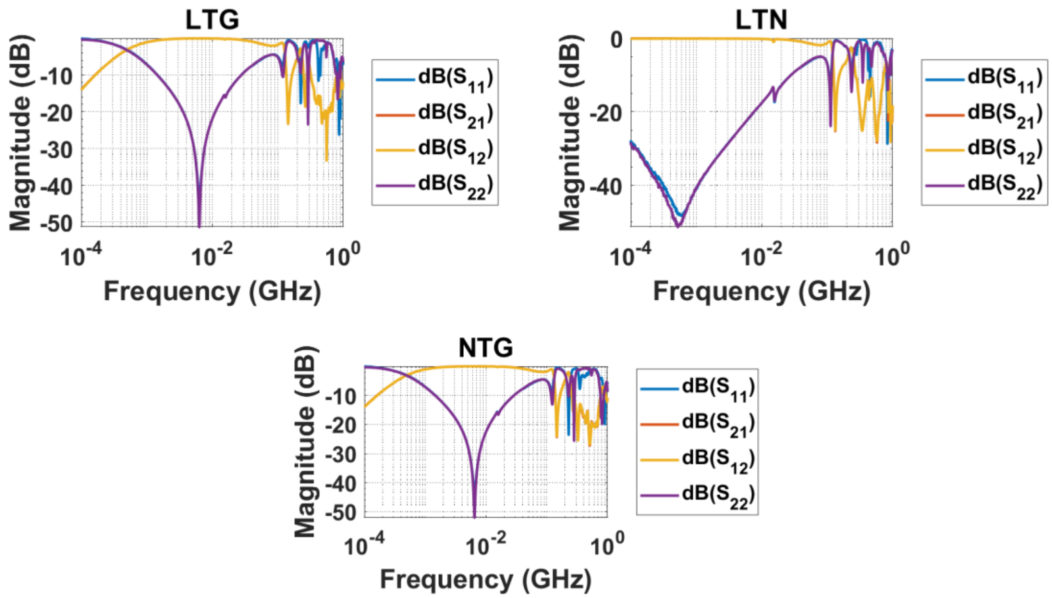

Figure C-23. DUT06 50 kV Network Parameters, Common Mode

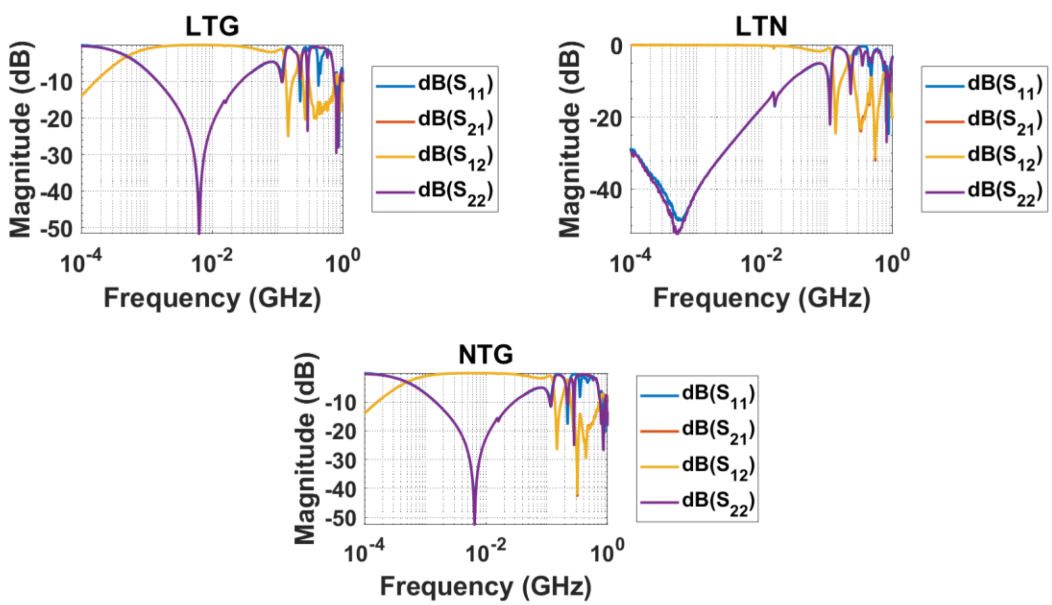

Figure C-24. DUT06 80 kV Network Parameters, Common Mode

C.5. DUT07

C.5.1. IV-Curve Trace

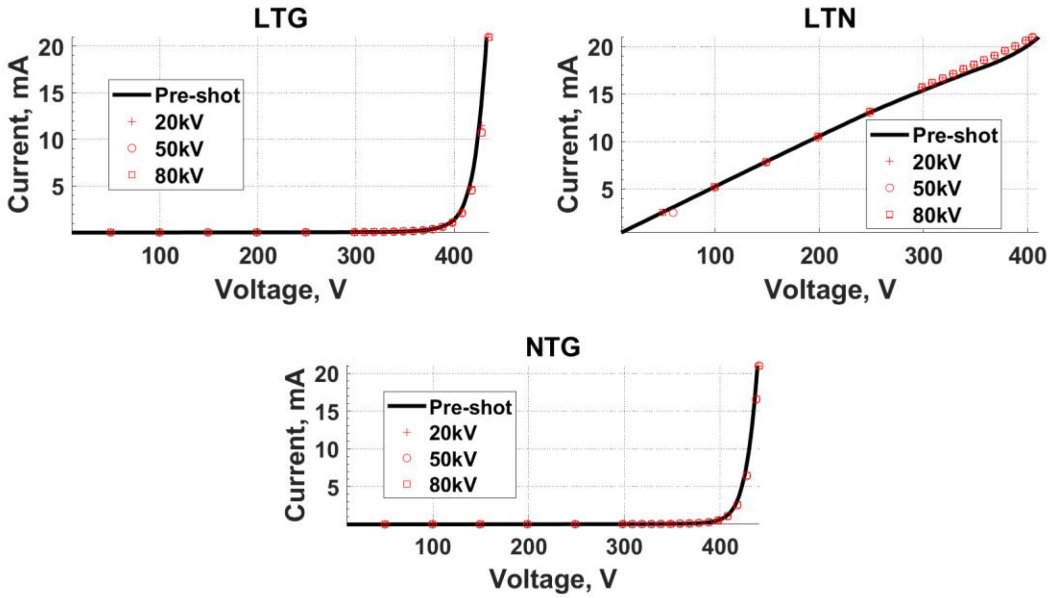

Figure C-25. DUT07 IV-Curves, Common Mode

C.5.2. Signal Distortion

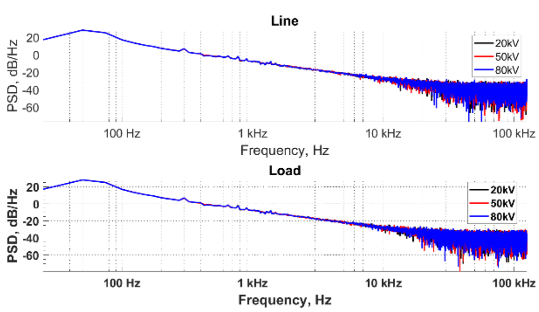

Figure C-26. DUT07 Power Spectral Density, Common Mode

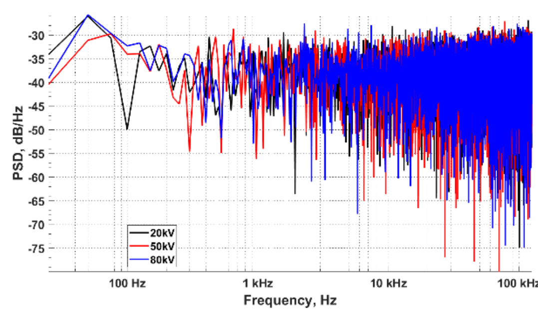

Figure C-27. DUT07 Power Spectral Density Difference, Common Mode

C.5.3. VNA Sweeps

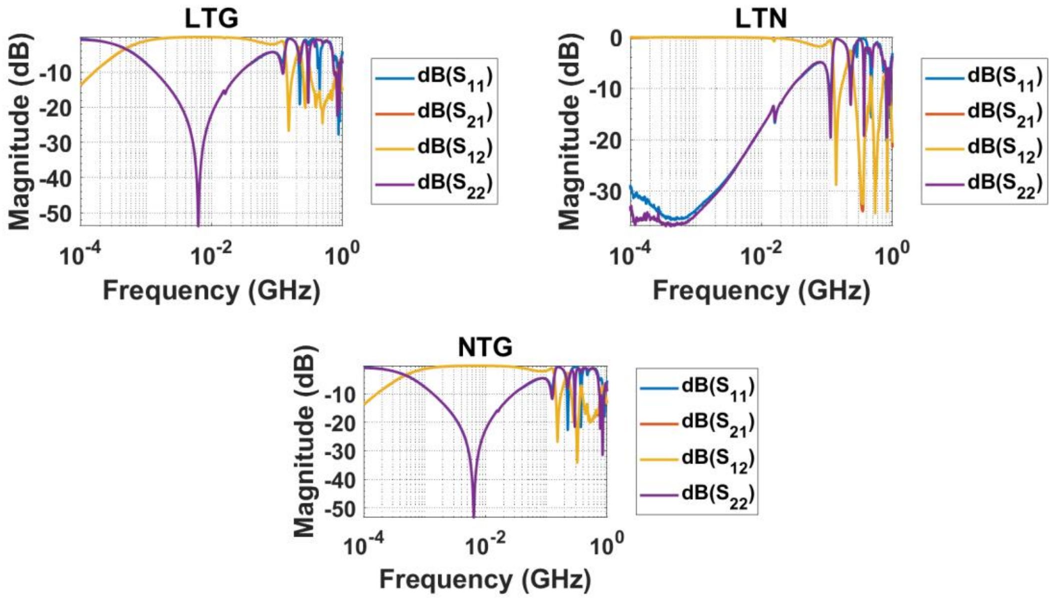

Figure C-28. DUT07 20 kV Network Parameters, Common Mode

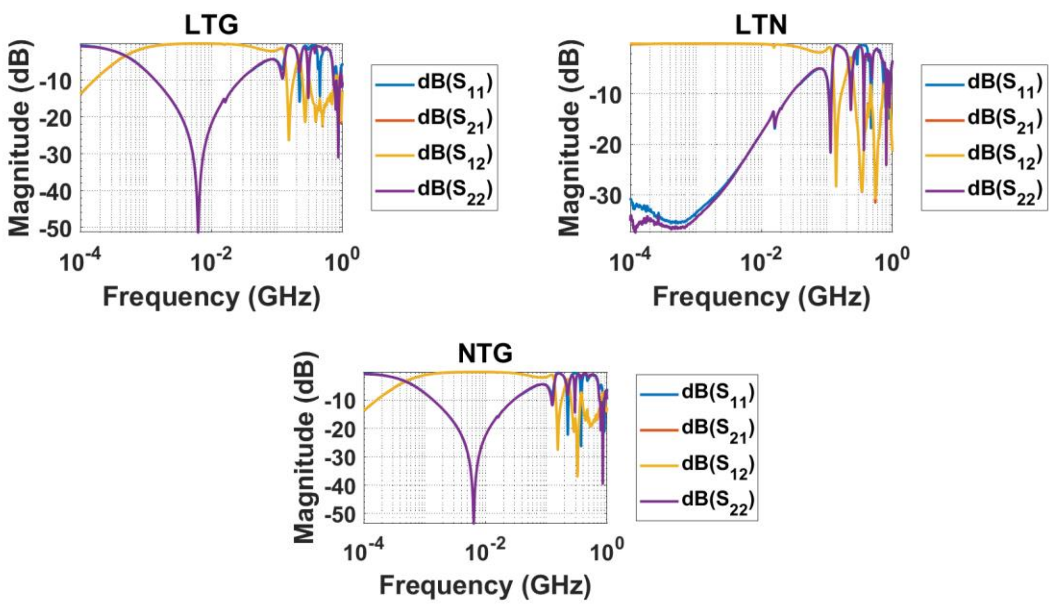

Figure C-29. DUT07 50 kV Network Parameters, Common Mode

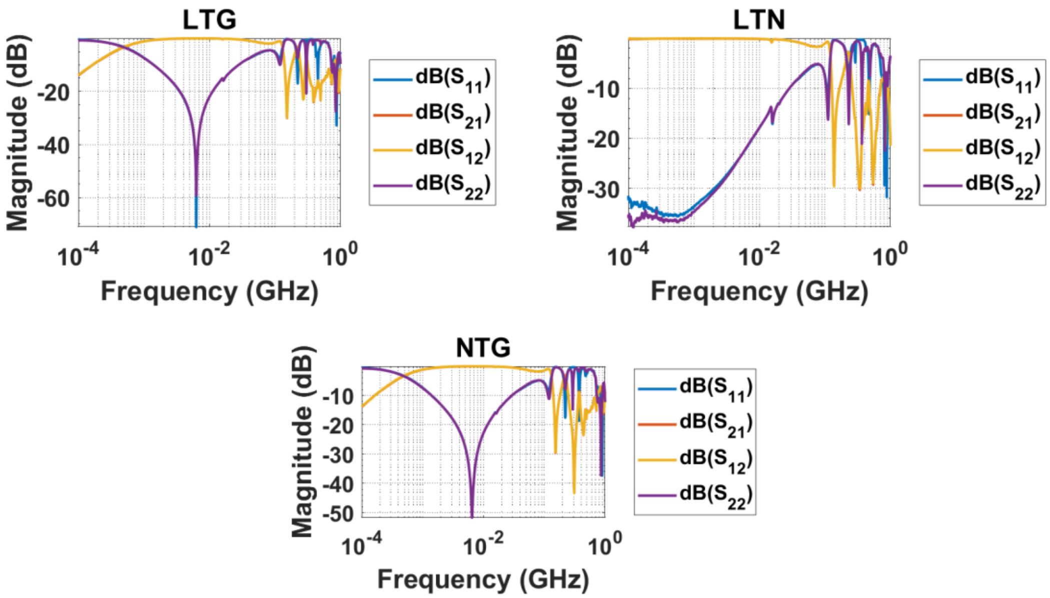

Figure C-30. DUT07 80 kV Network Parameters, Common Mode

C.6. DUT08

C.6.1. IV-Curve Trace

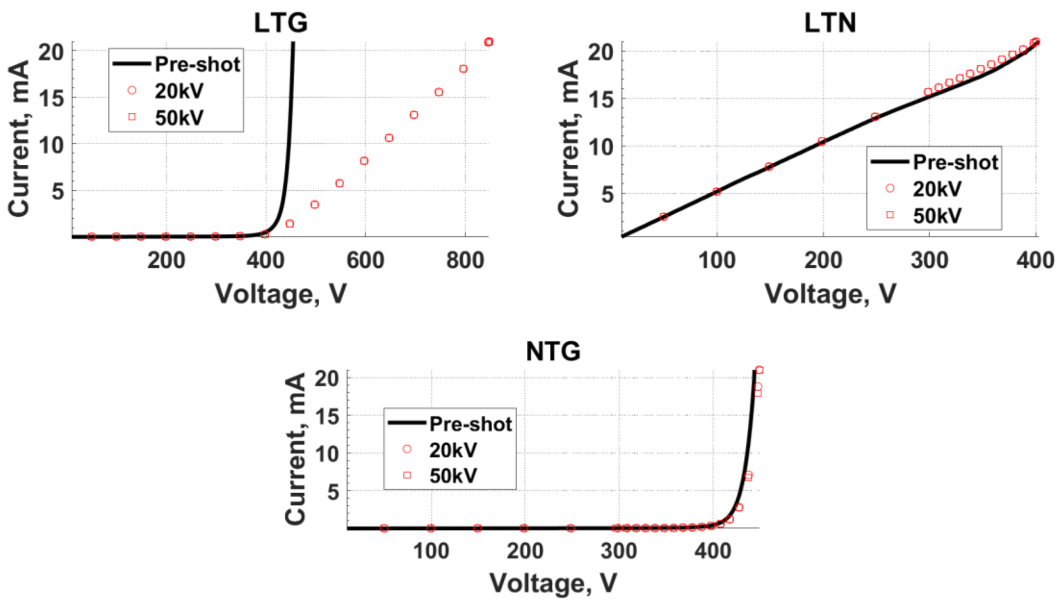

Figure C-31. DUT08 IV-Curves, Common Mode

Note the significant difference in LTG curve is due to the blown fuse due to testing. This does not signify that damage to the MOVs inside of the device was incurred.

C.6.2. Signal Distortion

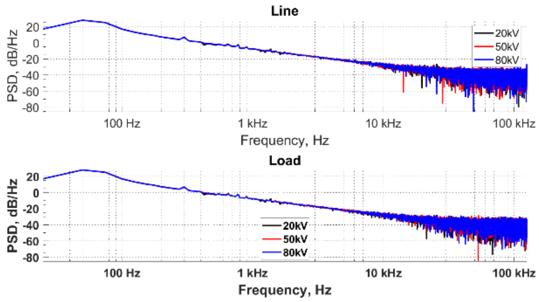

Figure C-32. DUT08 Power Spectral Density, Common Mode

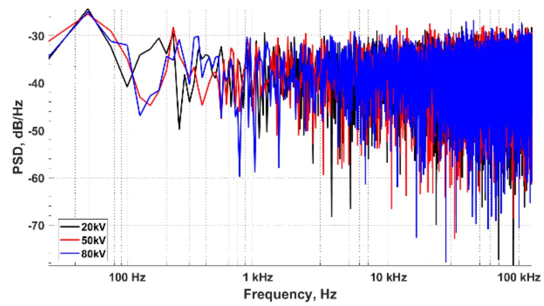

Figure C-33. DUT08 Power Spectral Density Difference, Common Mode

C.6.3. VNA Sweep

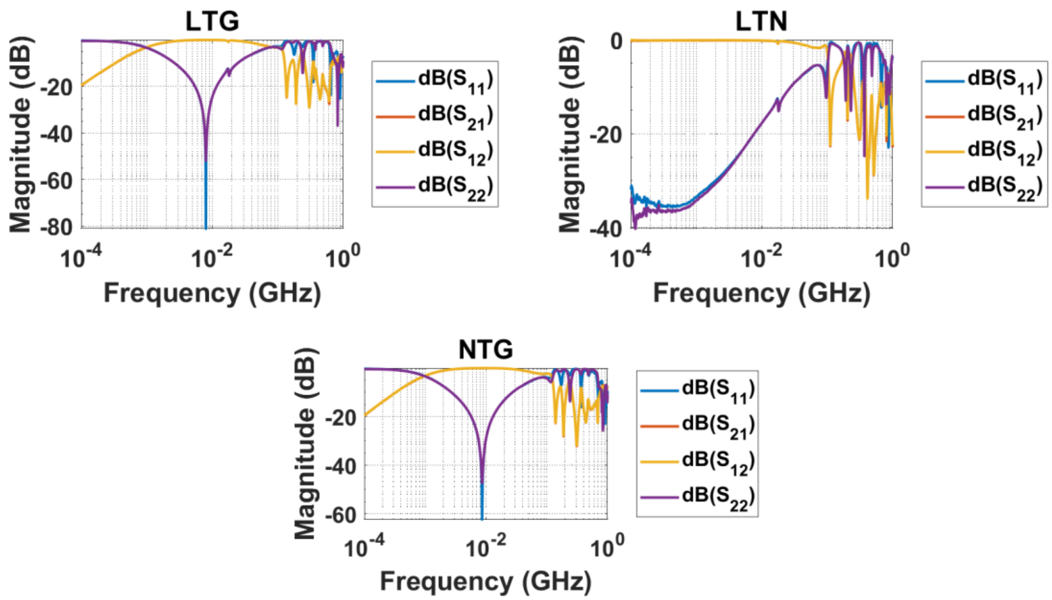

Figure C-34. DUT08 20 kV Network Parameters, Common Mode

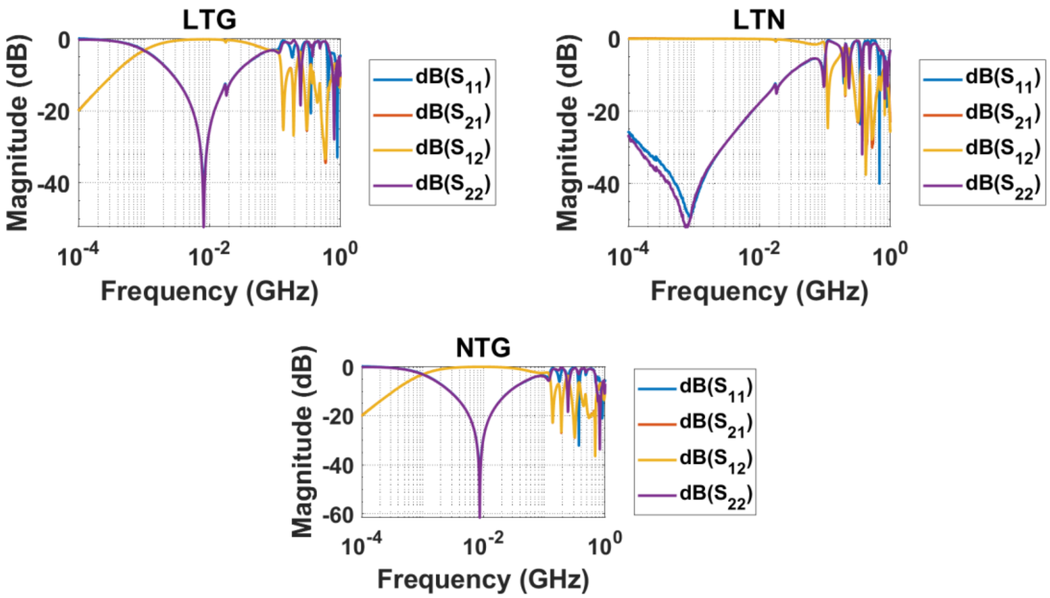

Figure C-35. DUT08 50 kV Network Parameters, Common Mode

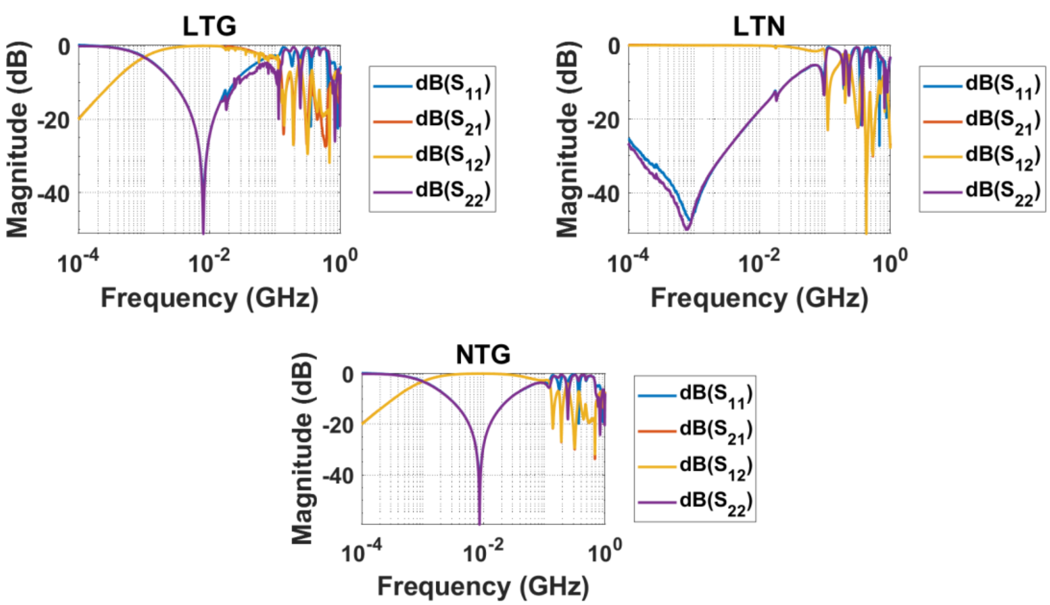

Figure C-36. DUT08 80 kV Network Parameters, Common Mode

C.7. DUT09

C.7.1. IV-Curve Trace

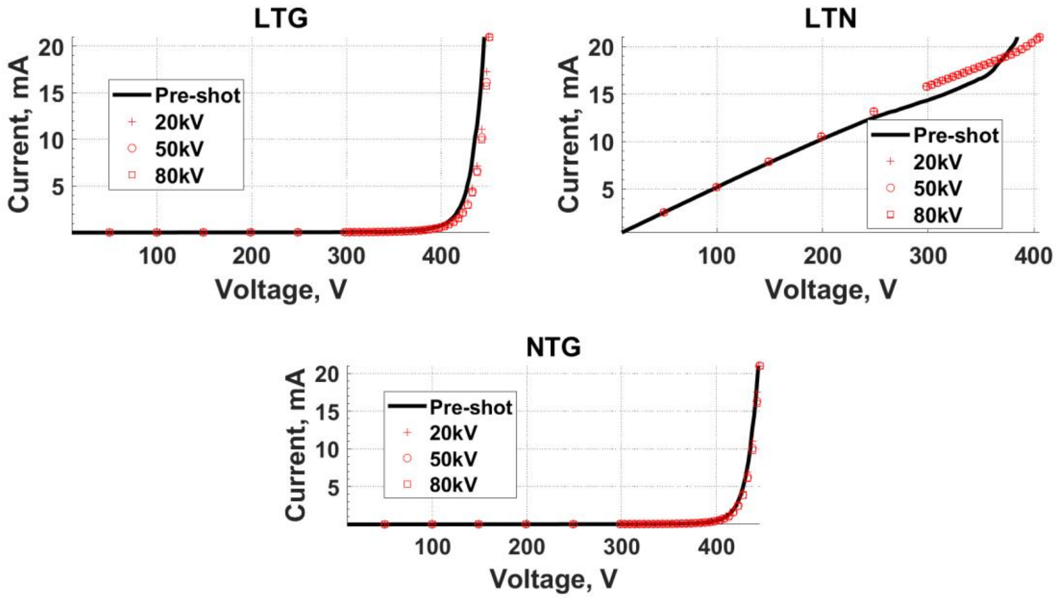

Figure C-37. DUT09 IV-Curves, Common Mode

C.7.2. Signal Distortion

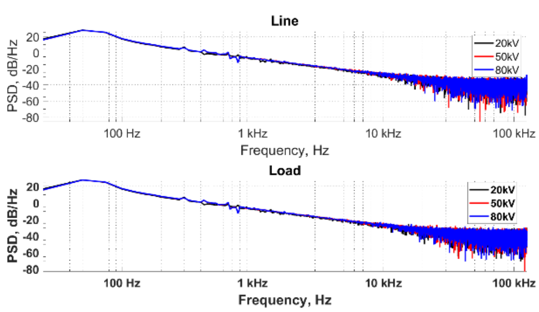

Figure C-38. DUT09 Power Spectral Density, Common Mode

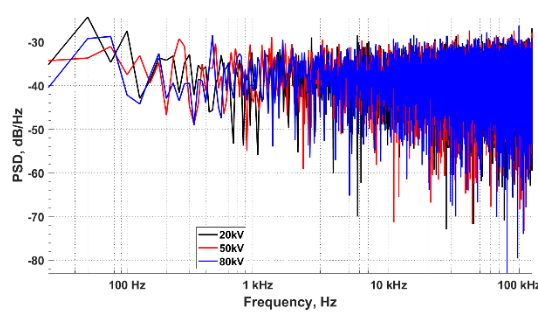

Figure C-39. DUT09 Power Spectral Density Difference, Common Mode

C.7.3. VNA Sweep

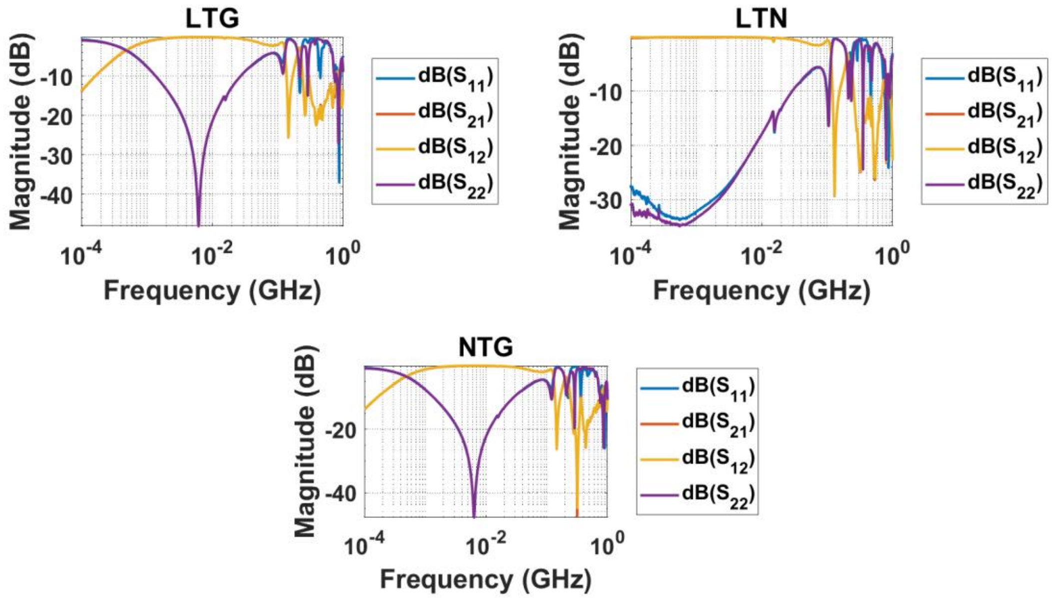

Figure C-40. DUT09 20 kV Network Parameters, Common Mode

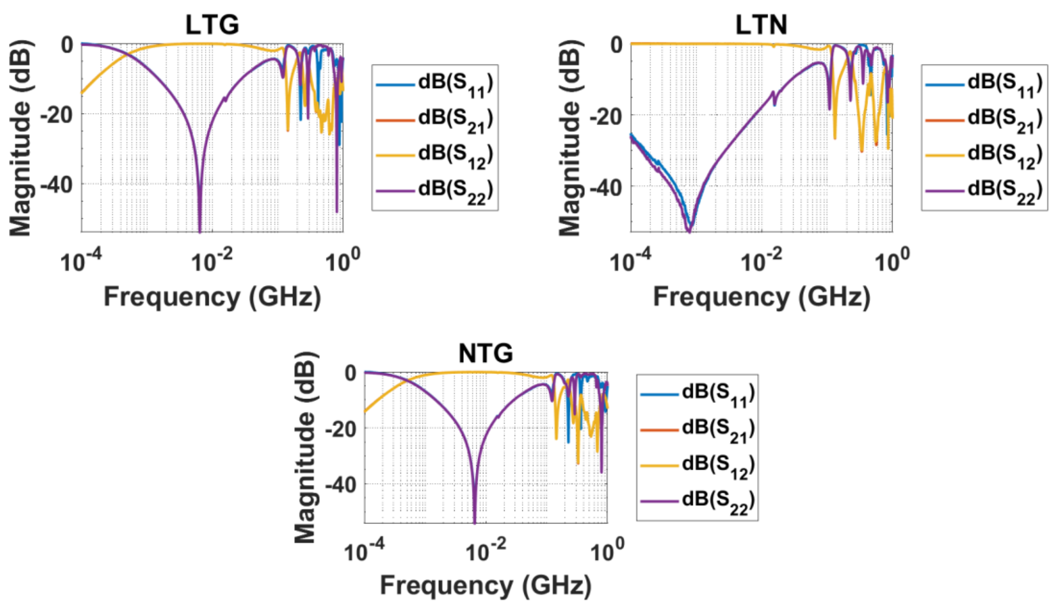

Figure C-41. DUT09 50 kV Network Parameters, Common Mode

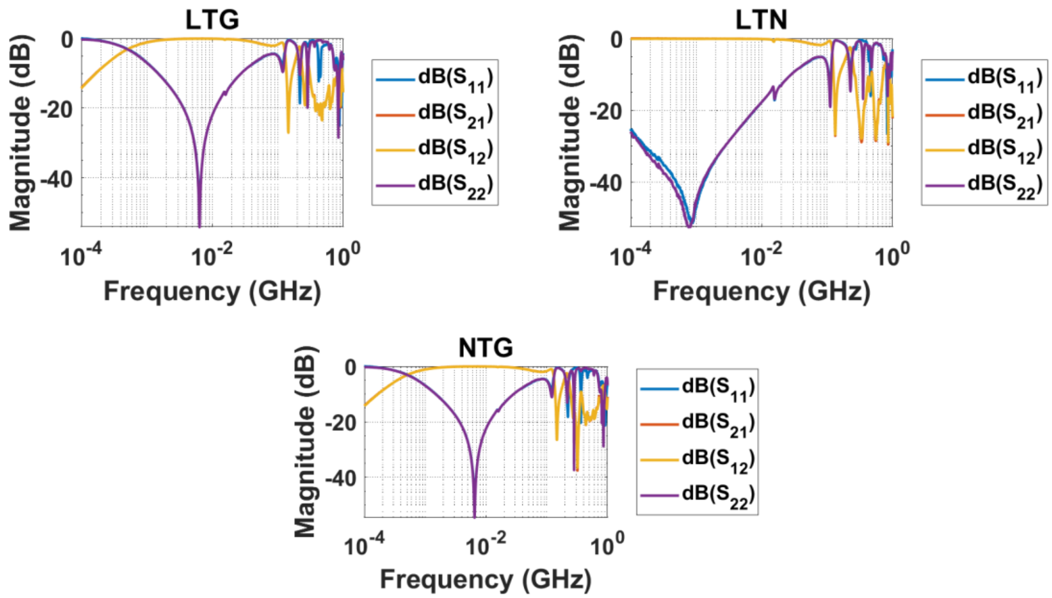

Figure C-42. DUT09 80 kV Network Parameters, Common Mode

C.8. DUT10

C.8.1. IV-Curve Trace

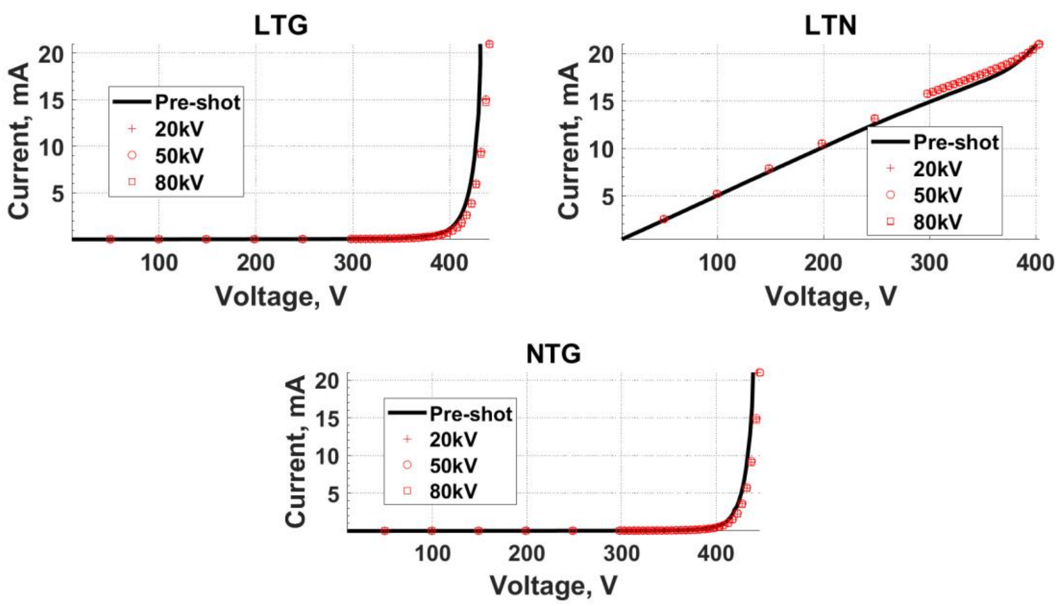

Figure C-43. DUT10 IV-Curves, Common Mode

C.8.2. Signal Distortion

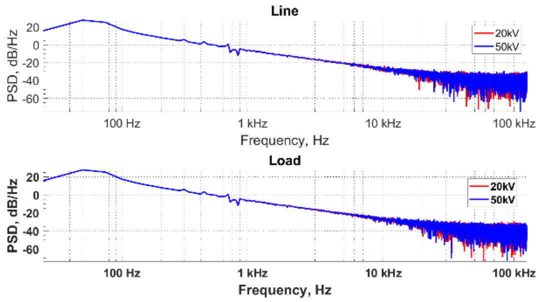

Figure C-44. DUT10 Power Spectral Density, Common Mode

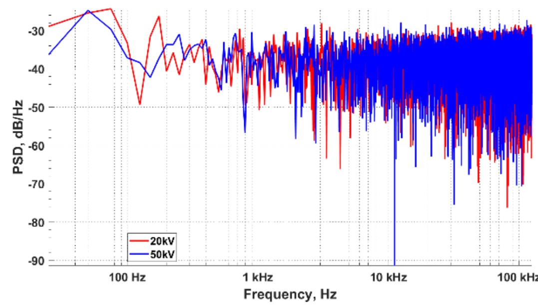

Figure C-45. DUT10 Power Spectral Density Difference, Common Mode

C.8.3. VNA Sweep

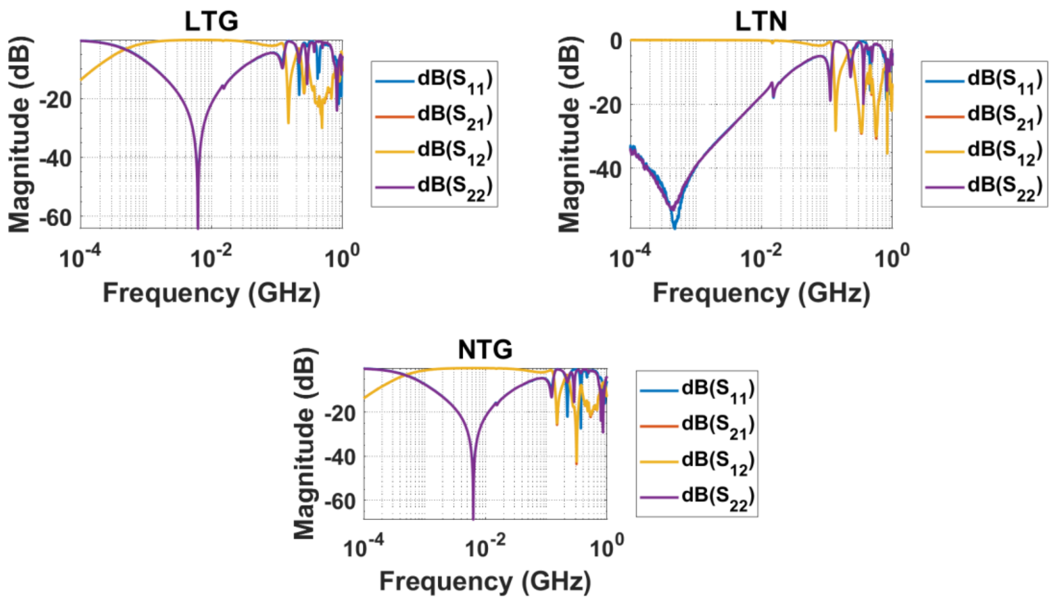

Figure C-46. DUT10 20 kV Network Parameters, Common Mode

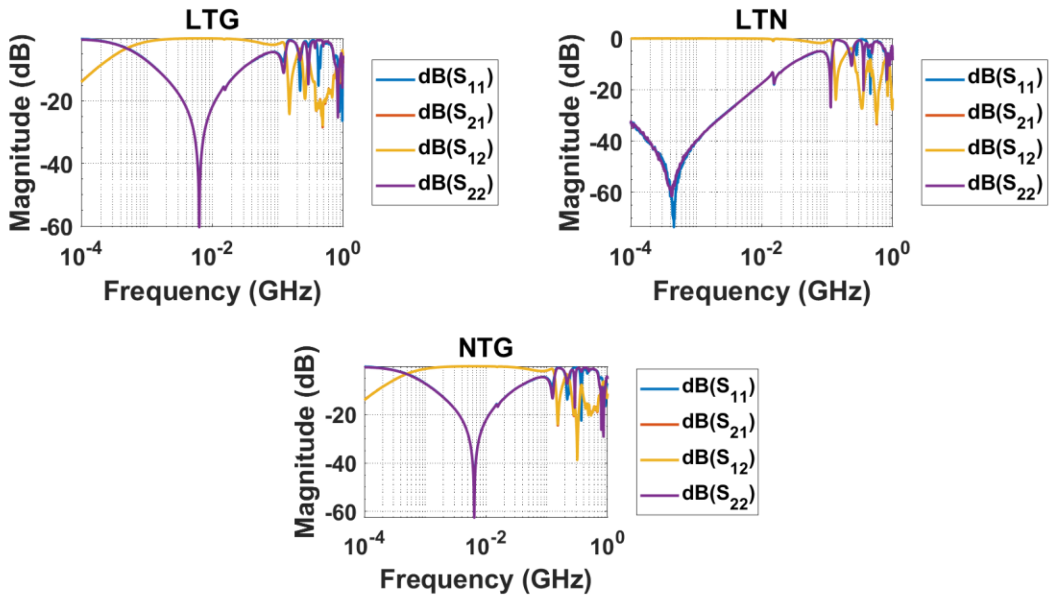

Figure C-47. DUT10 50 kV Network Parameters, Common Mode

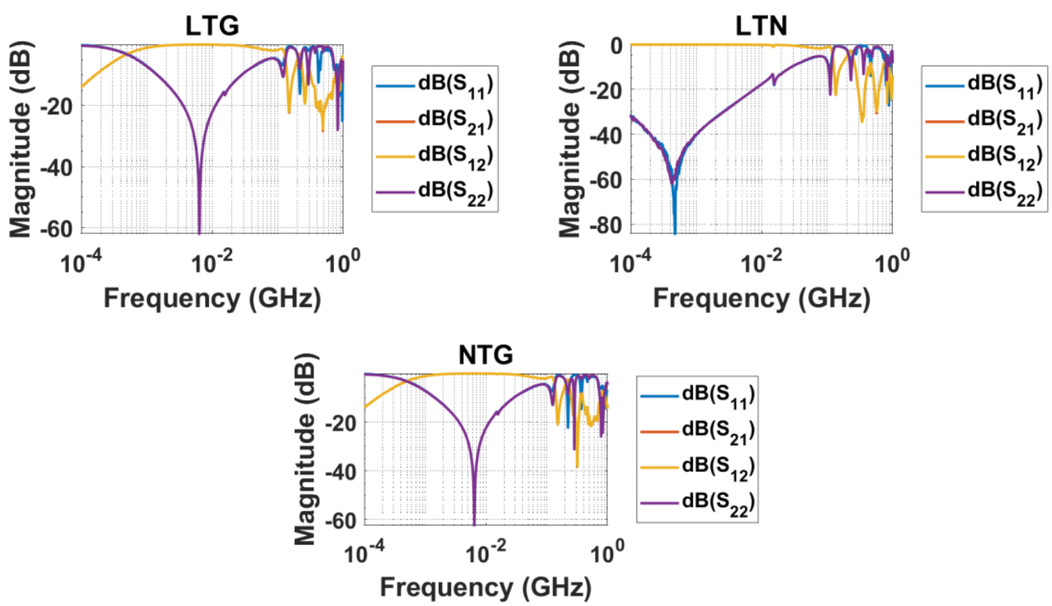

Figure C-48. DUT10 80 kV Network Parameters, Common Mode

APPENDIX D. SINGLE-ENDED CONFIGURATION STATE OF HEALTH DATA

D.1. DUT03

D.1.1. IV-Curve Trace

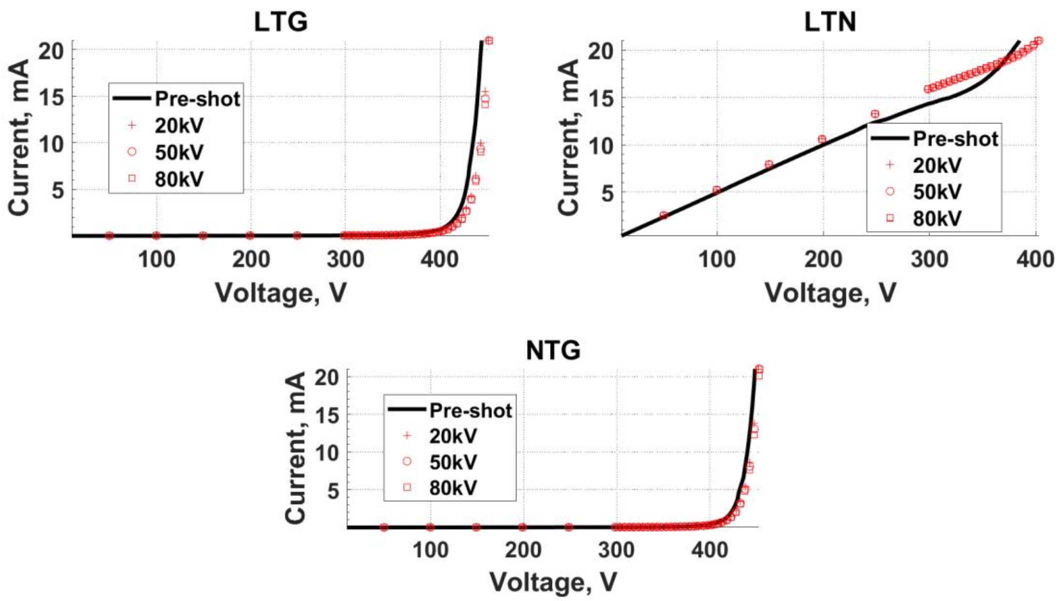

Figure D-1. DUT03 IV-Curves, Differential Mode Signal Distortion

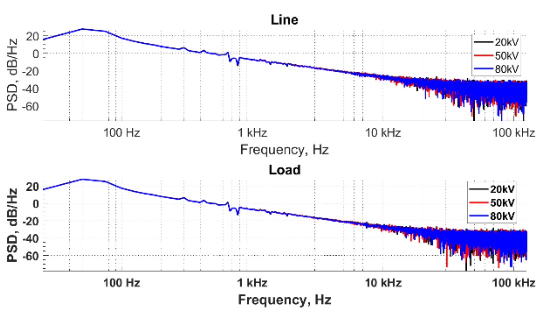

Figure D-2. DUT03 Power Spectral Density, Single-Ended Configuration

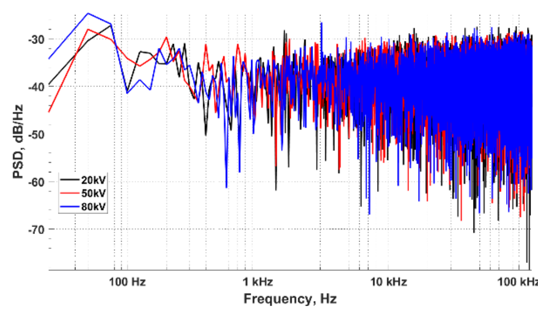

Figure D-3. DUT03 Power Spectral Density Difference, Single-Ended Configuration

D.1.2. VNA Sweep

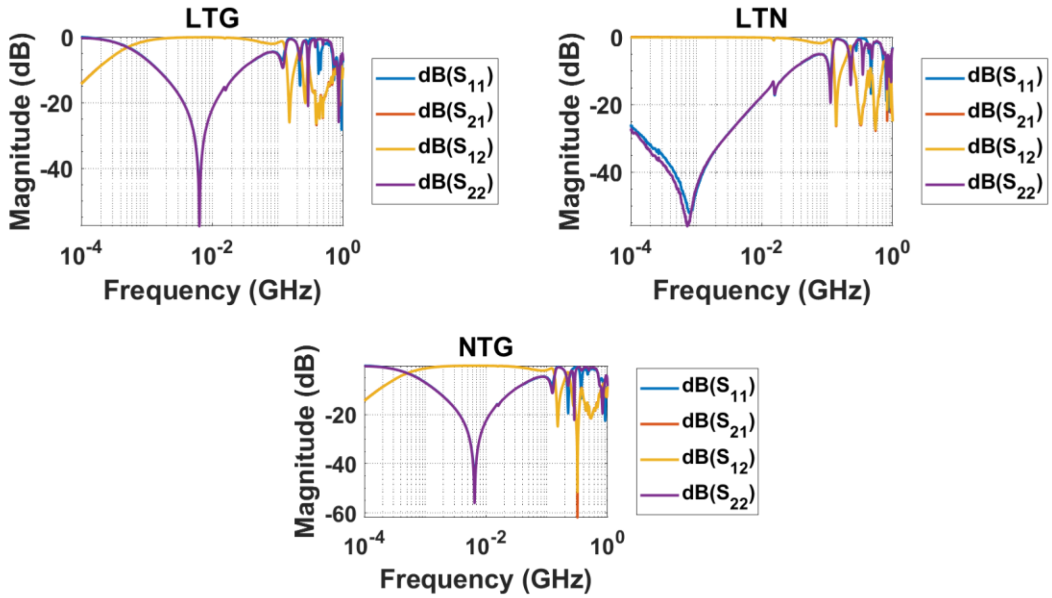

Figure D-4. DUT03 20 kV Network Parameters, Single-Ended Configuration

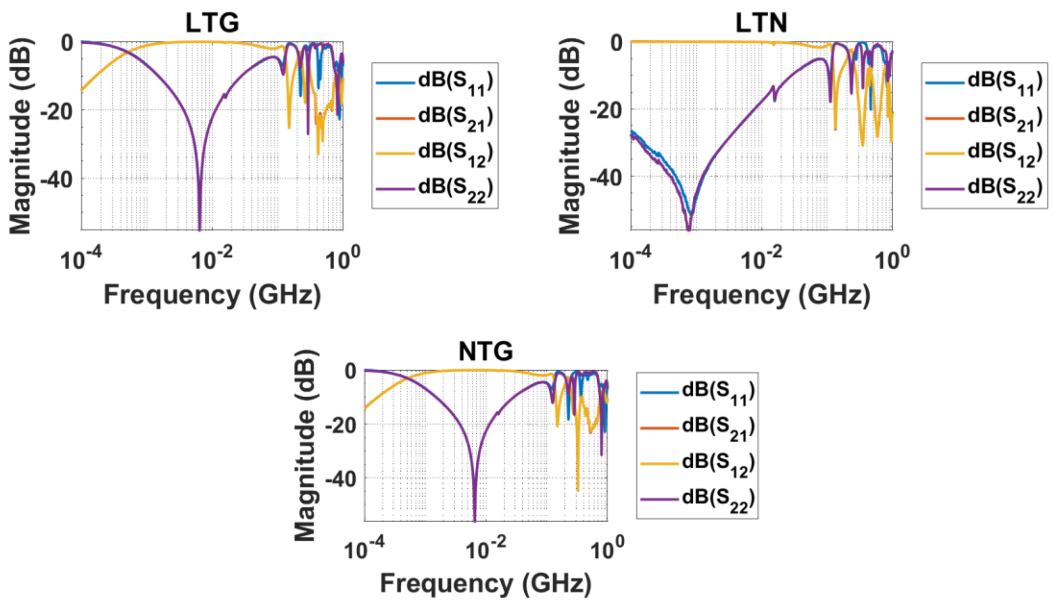

Figure D-5. DUT03 50 kV Network Parameters, Single-Ended Configuration

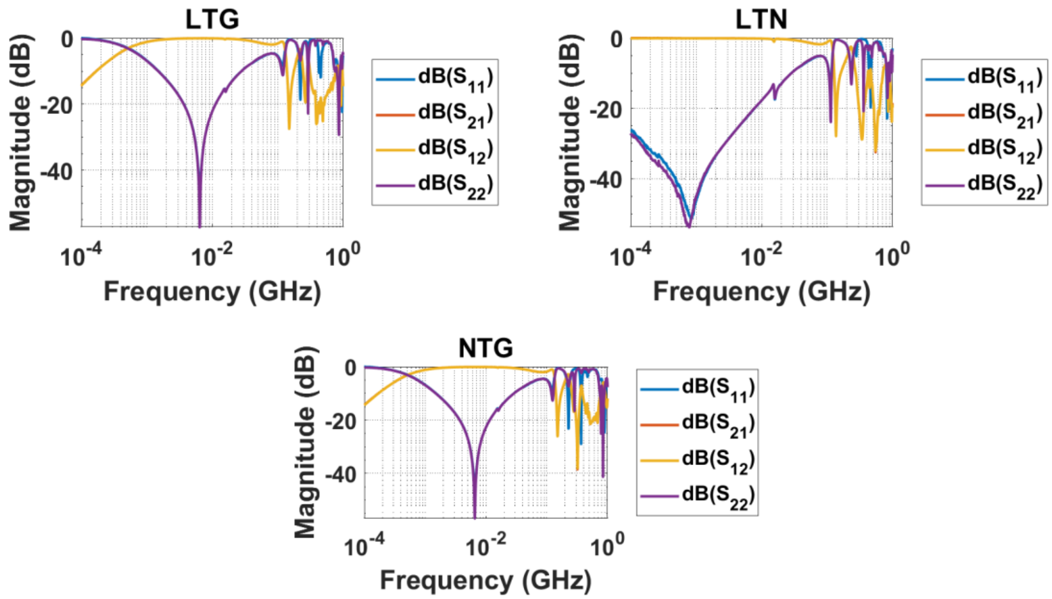

Figure D-6. DUT03 80 kV Network Parameters, Single-Ended Configuration

D.2. DUT04

D.2.1. IV-Curve Trace

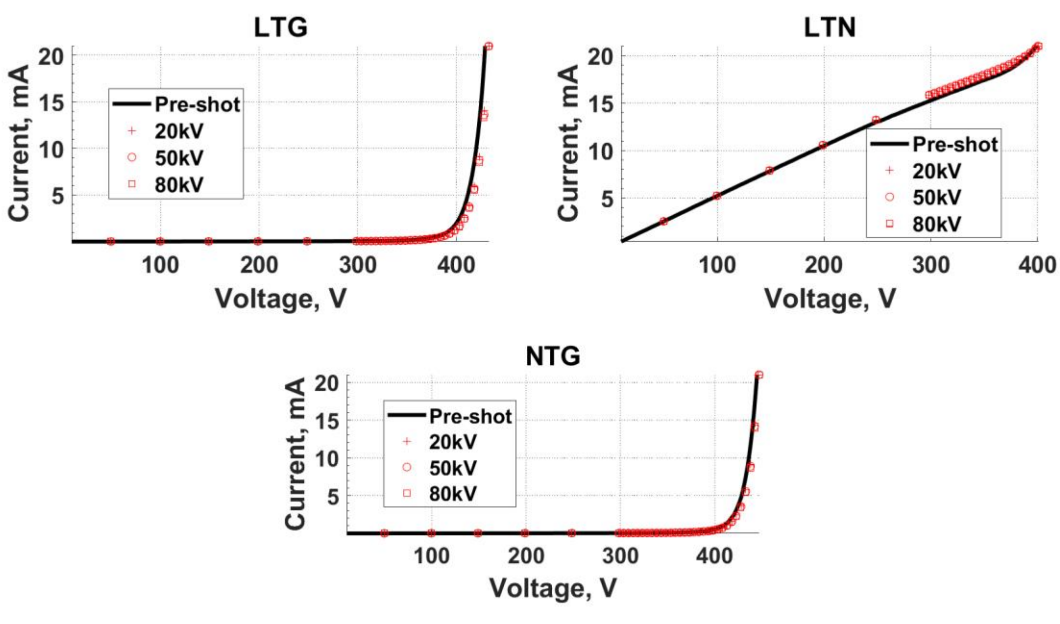

Figure D-7. DUT04 IV-Curves, Single-Ended Configuration

D.2.2. Signal Distortion

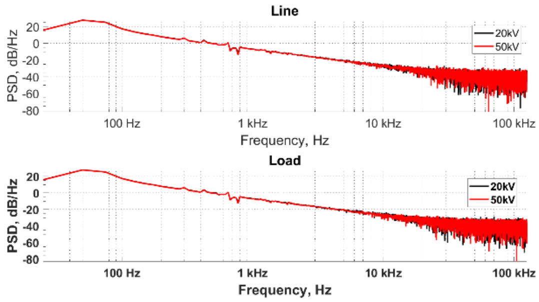

Figure D-8. DUT04 Power Spectral Density, Single-Ended Configuration

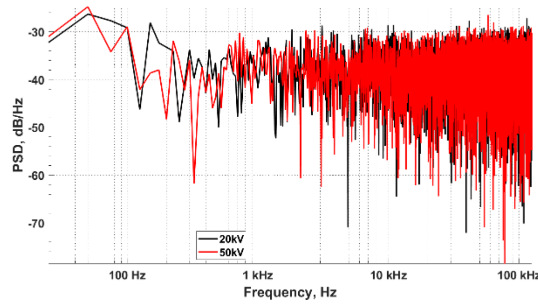

Figure D-9. DUT04 Power Spectral Density Difference, Single-Ended Configuration

Note: Due to oscilloscope error, signal distortion data is not available for DUT04, 80kV Single-Ended Configuration. However, results from other state of health measurements ensures that no damage was incurred to the device.

D.2.3. VNA Sweep

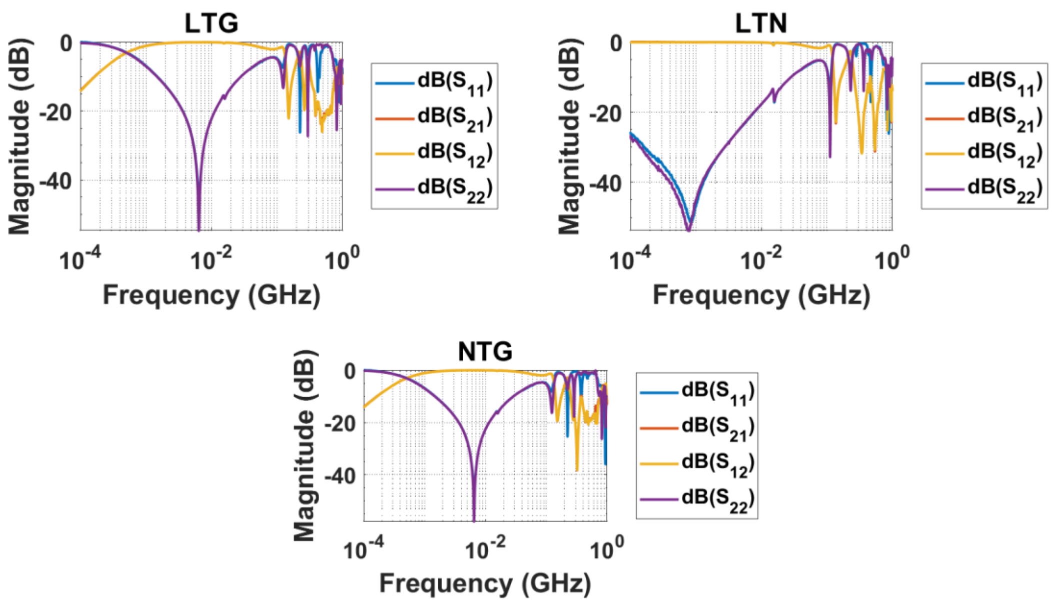

Figure D-10. DUT04 20 kV Network Parameters, Single-Ended Configuration

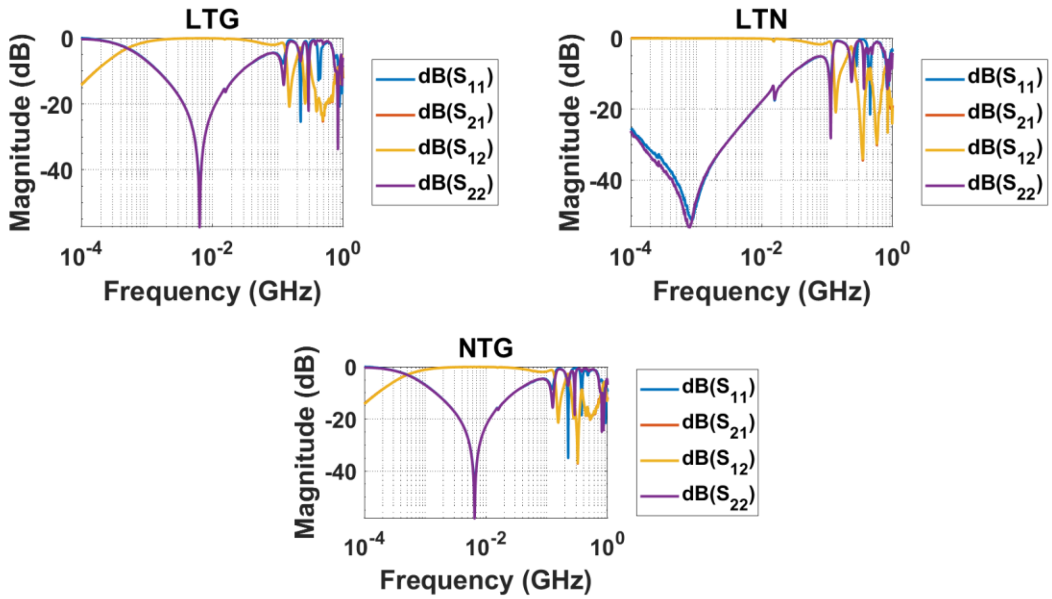

Figure D-11. DUT04 50 kV Network Parameters, Single-Ended Configuration

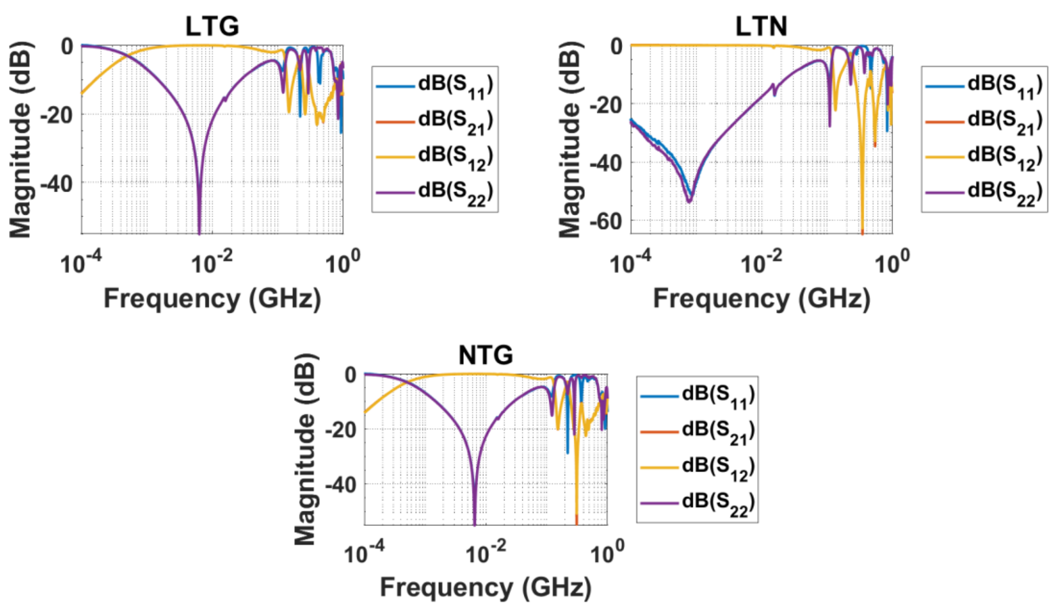

Figure D-12. DUT04 80 kV Network Parameters, Single-Ended Configuration

D.3. DUT05

D.3.1. IV-Curve Trace

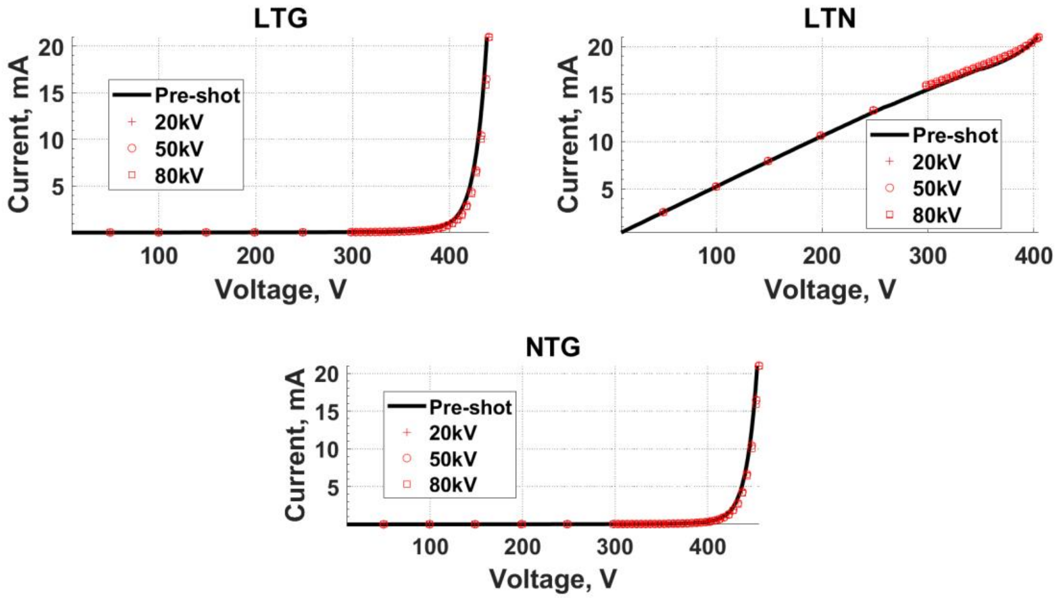

Figure D-13. DUT05 IV-Curves, Single-Ended Configuration

D.3.2. Signal Distortion

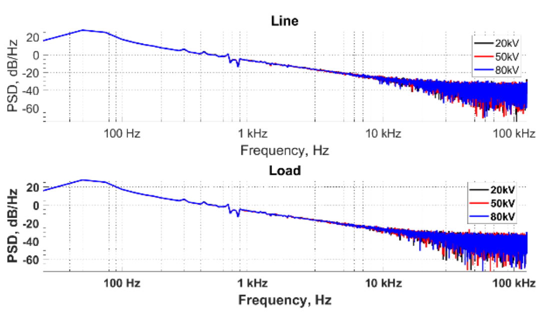

Figure D-14. DUT05 Power Spectral Density, Single-Ended Configuration

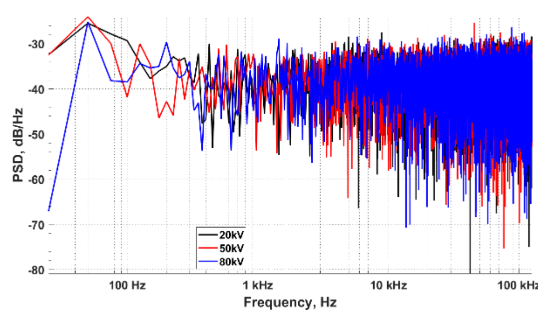

Figure D-15. DUT05 Power Spectral Density Difference, Single-Ended Configuration

D.3.3. VNA Sweep

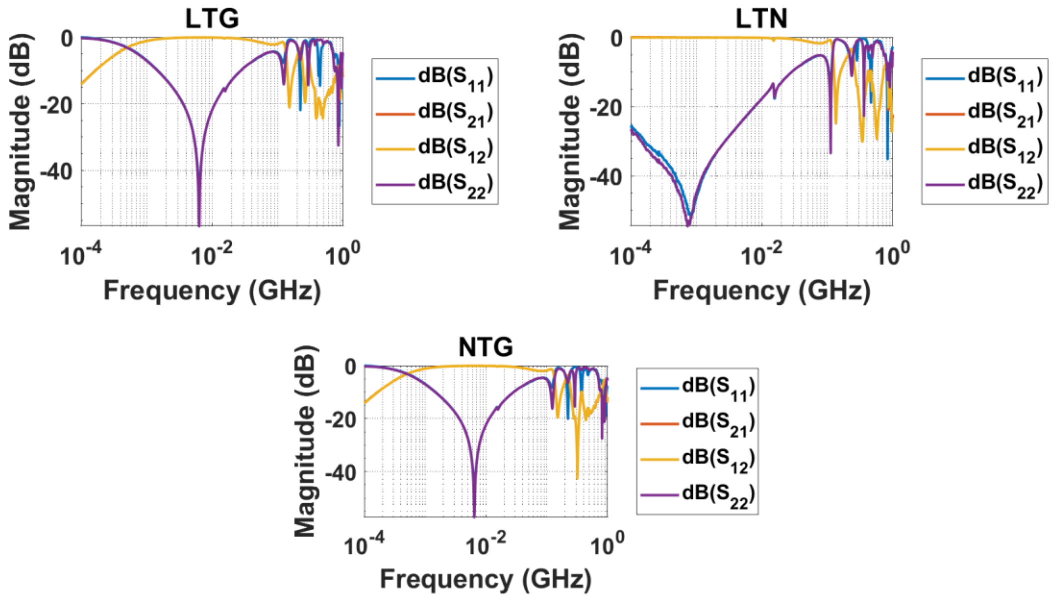

Figure D-16. DUT05 20 kV Network Parameters, Single-Ended Configuration

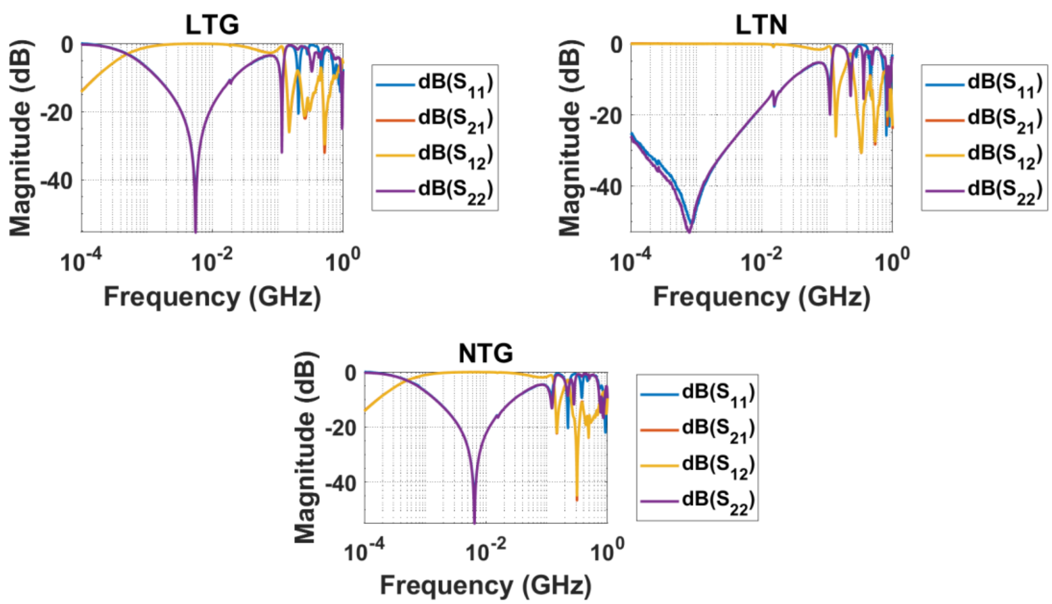

Figure D-17. DUT05 50 kV Network Parameters, Single-Ended Configuration

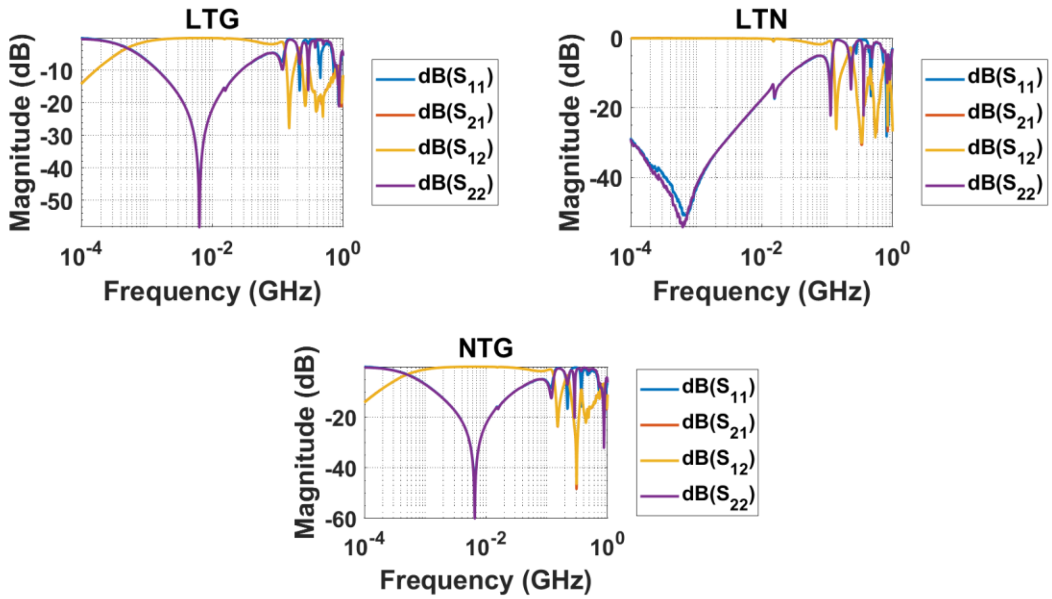

Figure D-18. DUT05 80 kV Network Parameters, Single-Ended Configuration

D.4. DUT06

D.4.1. IV-Curve Trace

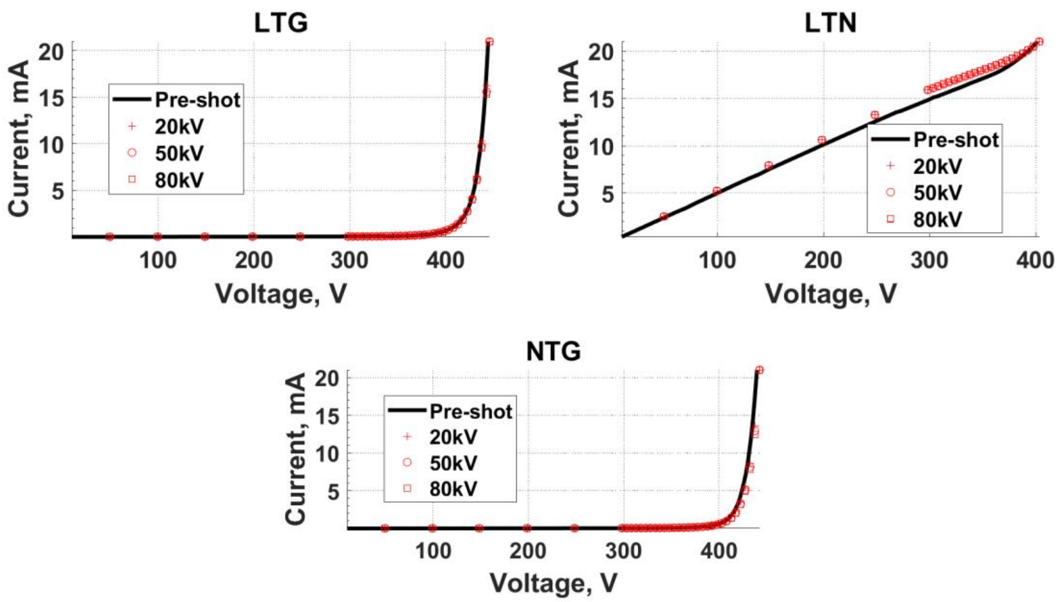

Figure D-19. DUT06 IV-Curves, Single-Ended Configuration

D.4.2. Signal Distortion

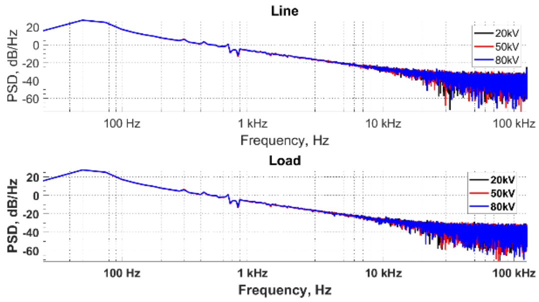

Figure D-20. DUT06 Power Spectral Density, Single-Ended Configuration

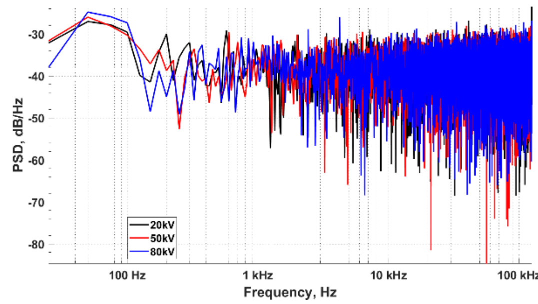

Figure D-21. DUT06 Power Spectral Density Difference, Single-Ended Configuration

D.4.3. VNA Sweep

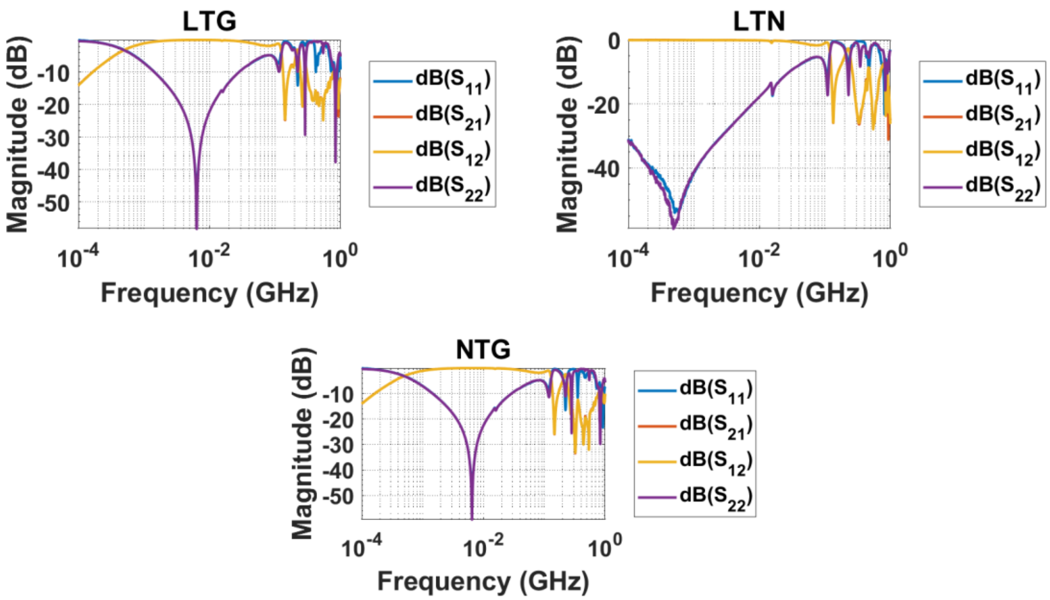

Figure D-22. DUT06 20 kV Network Parameters, Single-Ended Configuration

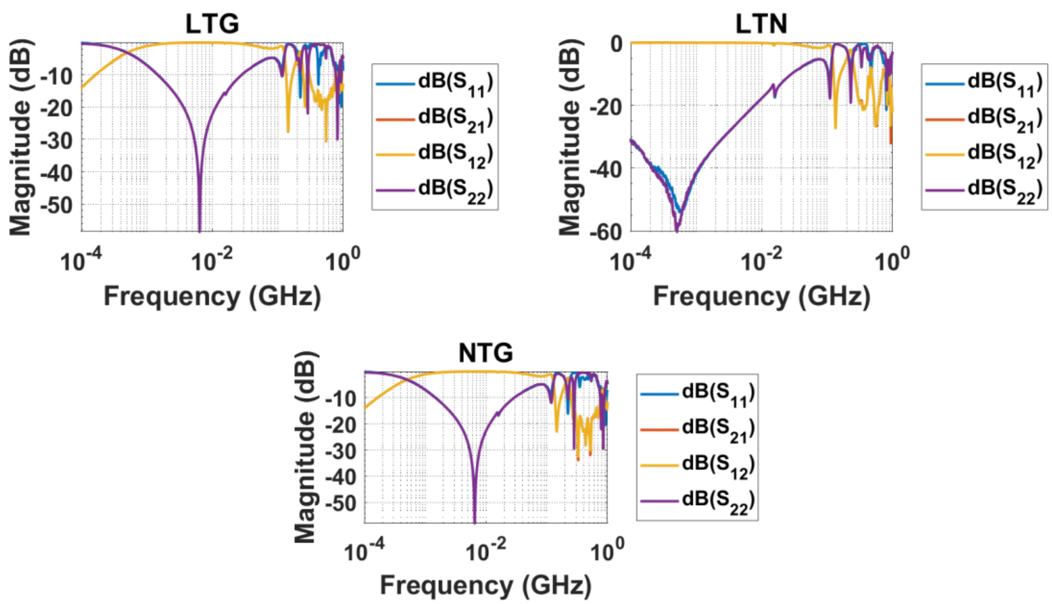

Figure D-23. DUT06 50 kV Network Parameters, Single-Ended Configuration

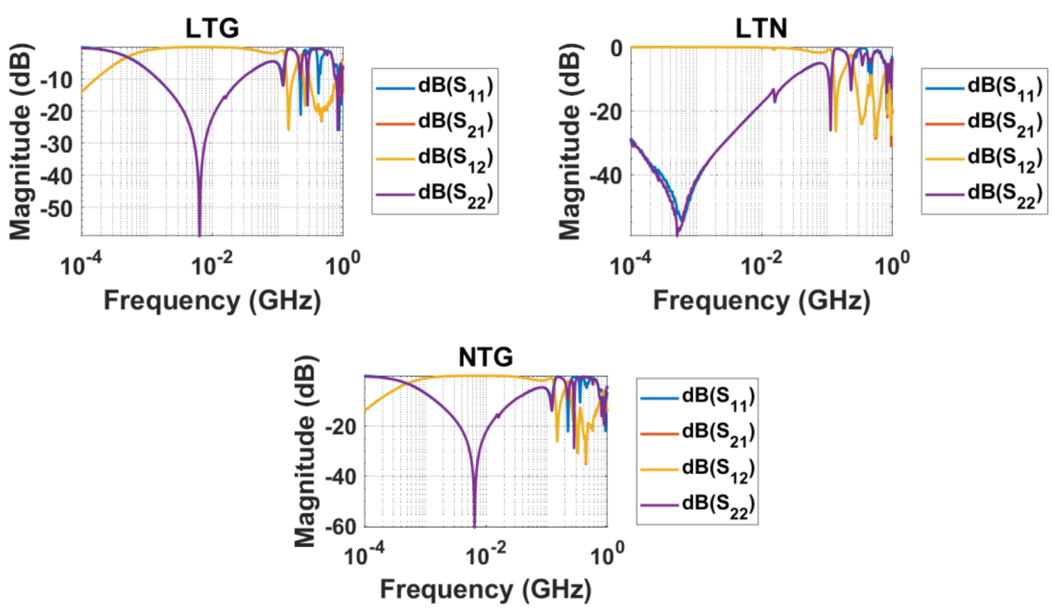

Figure D-24. DUT06 80 kV Network Parameters, Single-Ended Configuration

D.5. DUT07

D.5.1. IV-Curve Trace

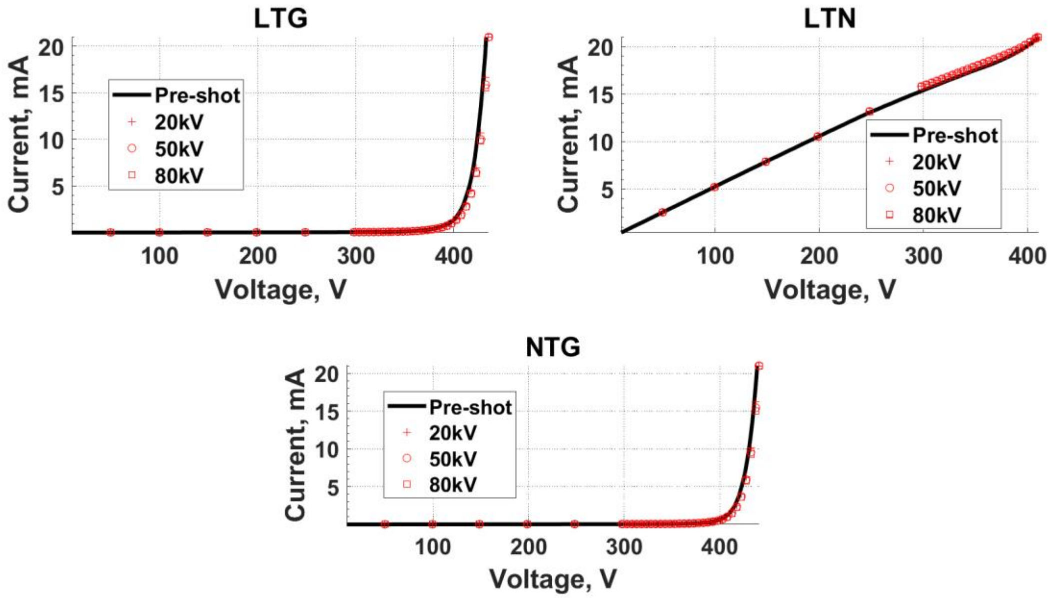

Figure D-25. DUT07 IV-Curves, Single-Ended Configuration

D.5.2. Signal Distortion

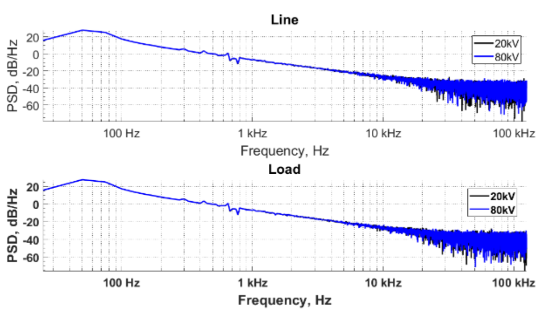

Figure D-26. DUT07 Power Spectral Density, Single-Ended Configuration

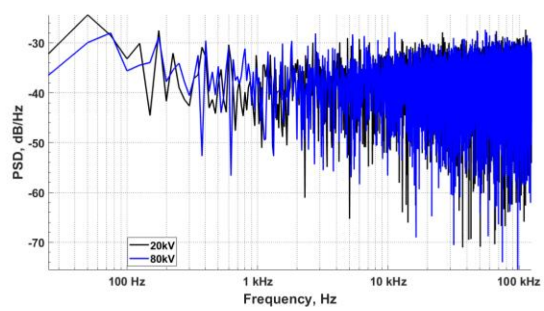

Figure D-27. DUT07 Power Spectral Density Difference, Single-Ended Configuration

Note: Due to oscilloscope error, signal distortion data is not available for DUT07, 50kV common mode configuration. However, results from other state of health measurements and results from the 80kV test ensures that no damage was incurred to the device.

D.5.3. VNA Sweep

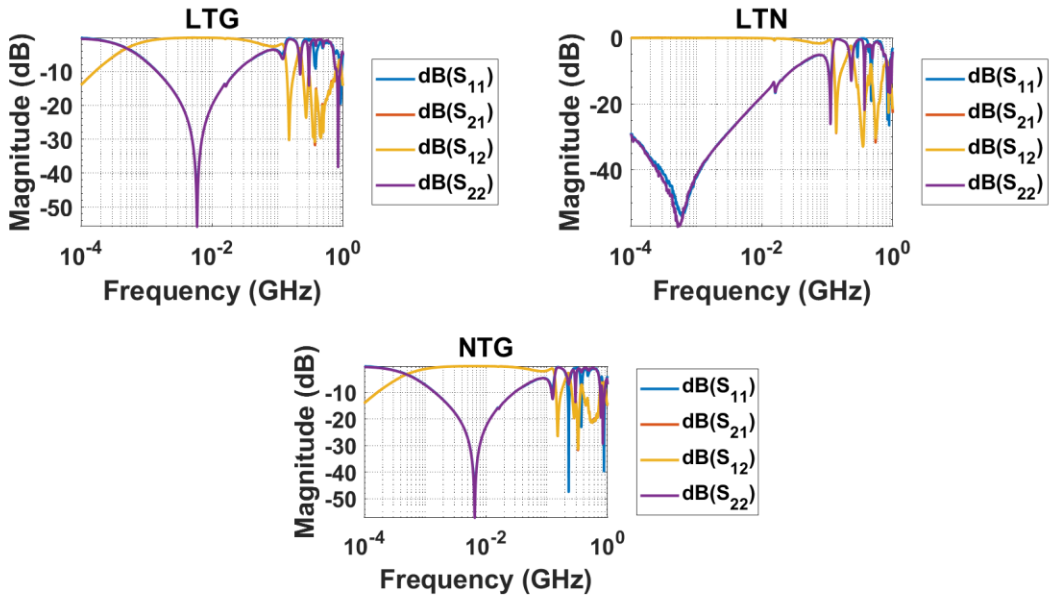

Figure D-28. DUT07 20 kV Network Parameters, Single-Ended Configuration

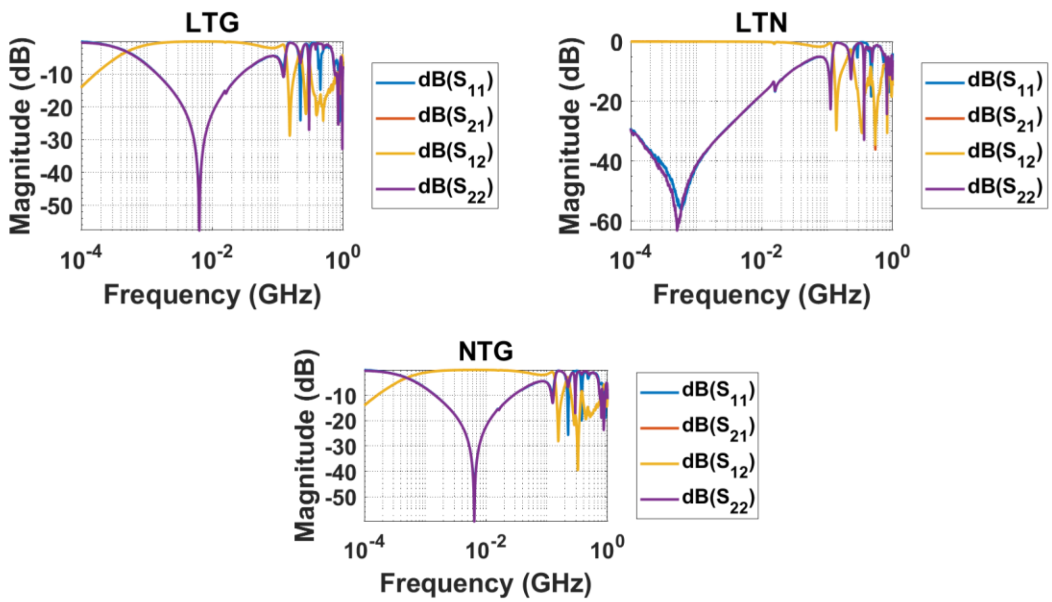

Figure D-29. DUT07 50 kV Network Parameters, Single-Ended Configuration

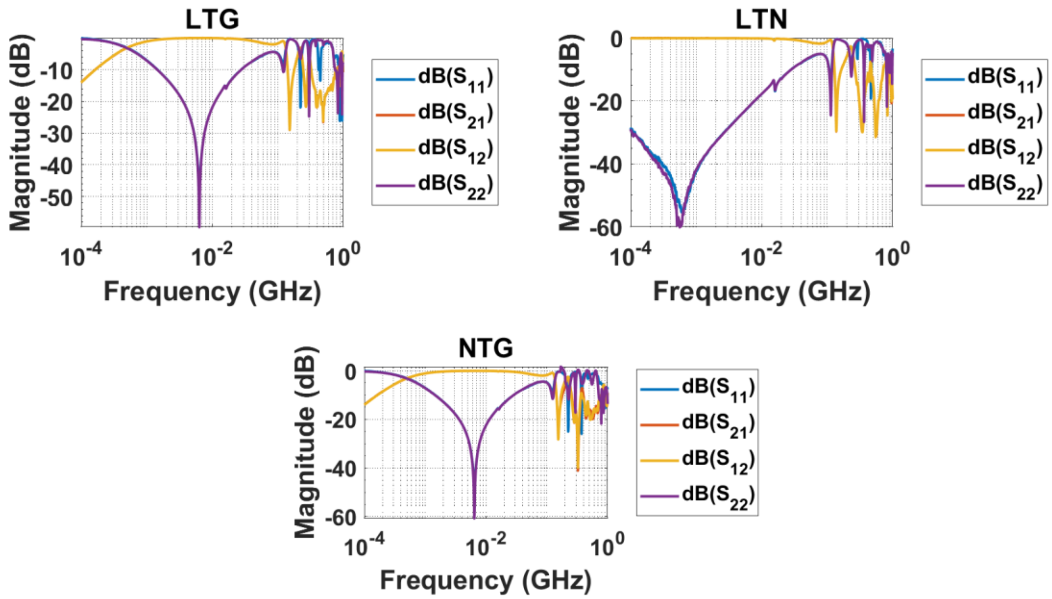

Figure D-30. DUT07 80 kV Network Parameters, Single-Ended Configuration

D.6. DUT09

D.6.1. IV-Curve Trace

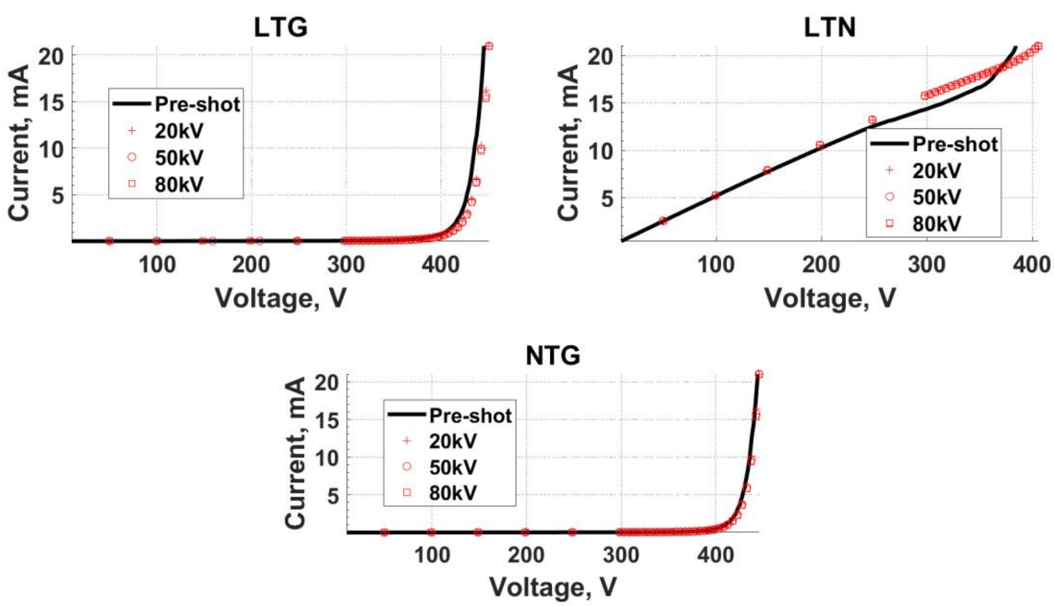

Figure D-31. DUT09 IV-Curves, Single-Ended Configuration

D.6.2. Signal Distortion

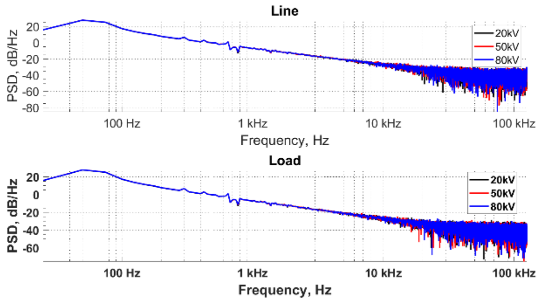

Figure D-32. DUT09 Power Spectral Density, Single-Ended Configuration

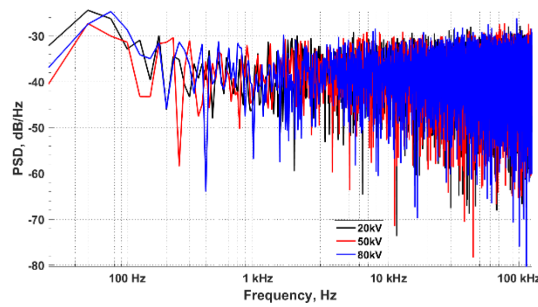

Figure D-33. DUT09 Power Spectral Density Difference, Single-Ended Configuration

D.6.3. VNA Sweep

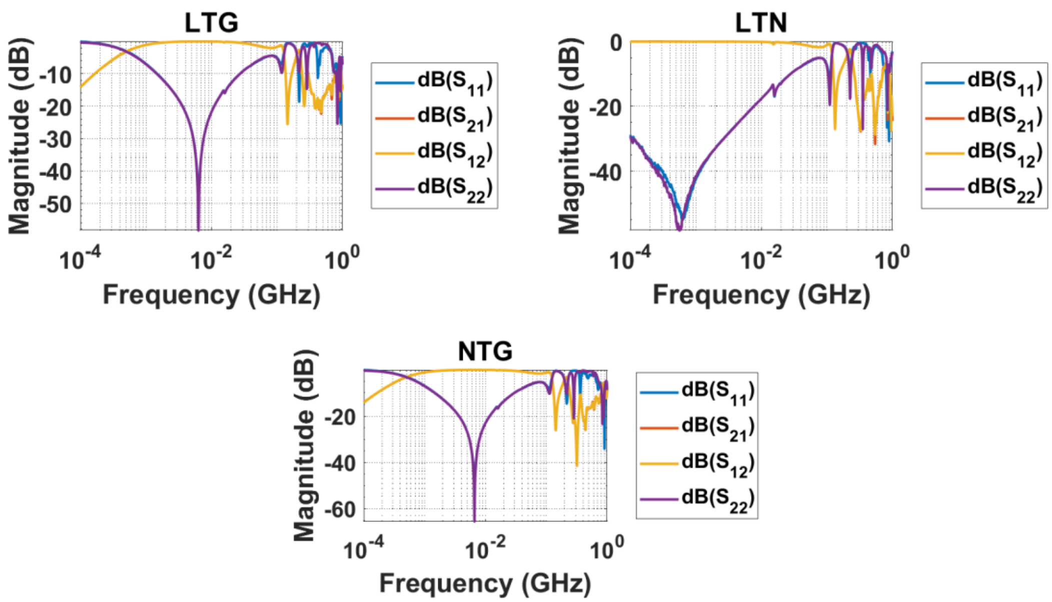

Figure D-34. DUT09 20 kV Network Parameters, Single-Ended Configuration

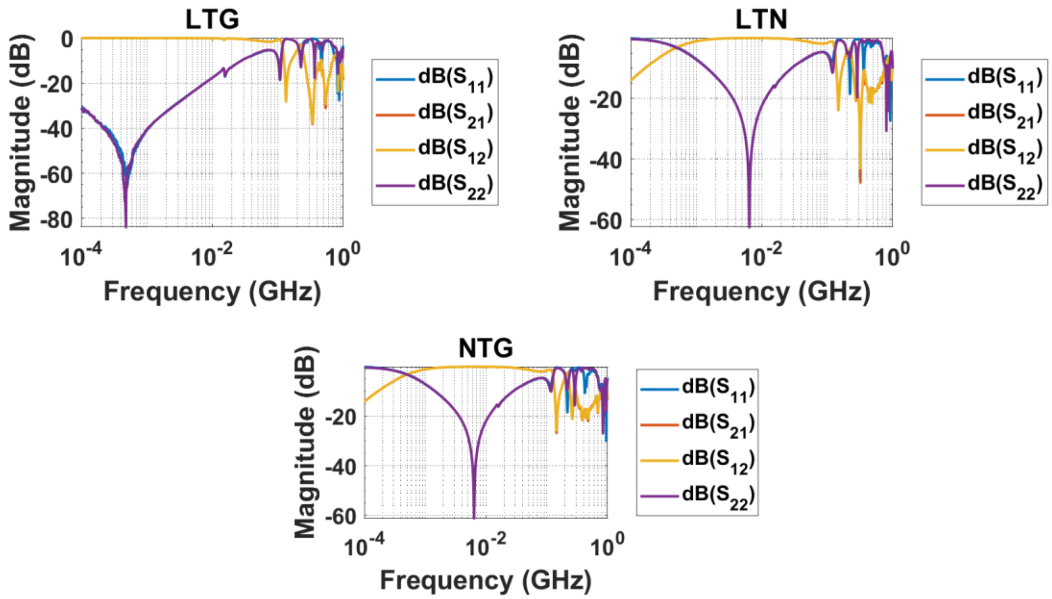

Figure D-35. DUT09 50 kV Network Parameters, Single-Ended Configuration

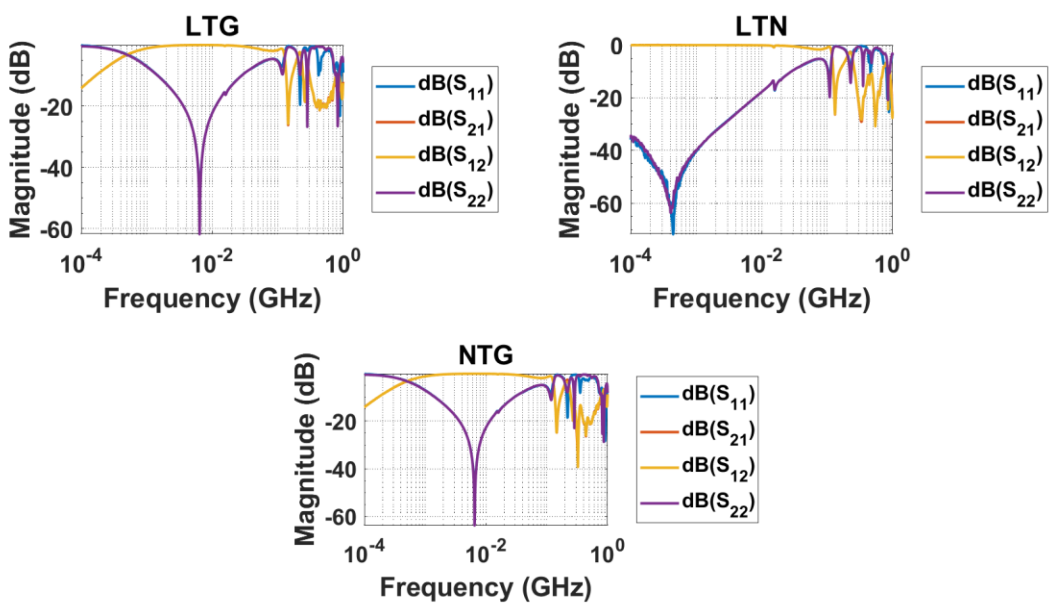

Figure D-36. DUT09 80 kV Network Parameters, Single-Ended Configuration

D.7. DUT10

D.7.1. IV-Curve Trace

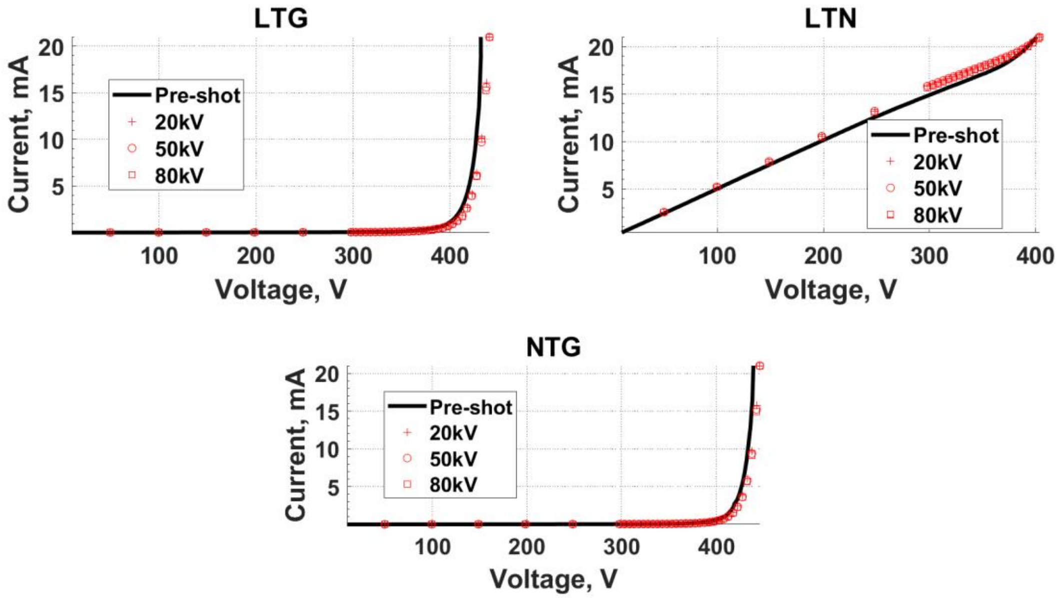

Figure D-37. DUT10 IV-Curves, Single-Ended Configuration

D.7.2. Signal Distortion

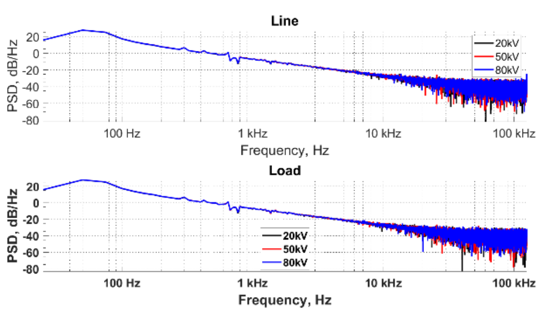

Figure D-38. DUT10 Power Spectral Density, Single-Ended Configuration

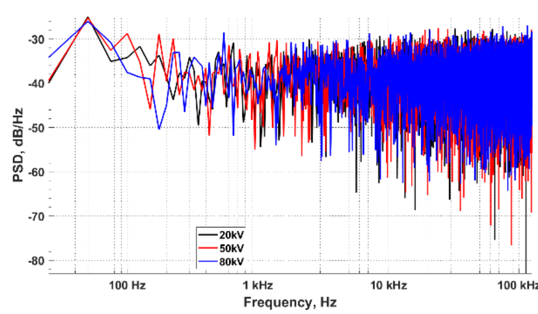

Figure D-39. DUT10 Power Spectral Density Difference, Single-Ended Configuration

D.7.3. VNA Sweep

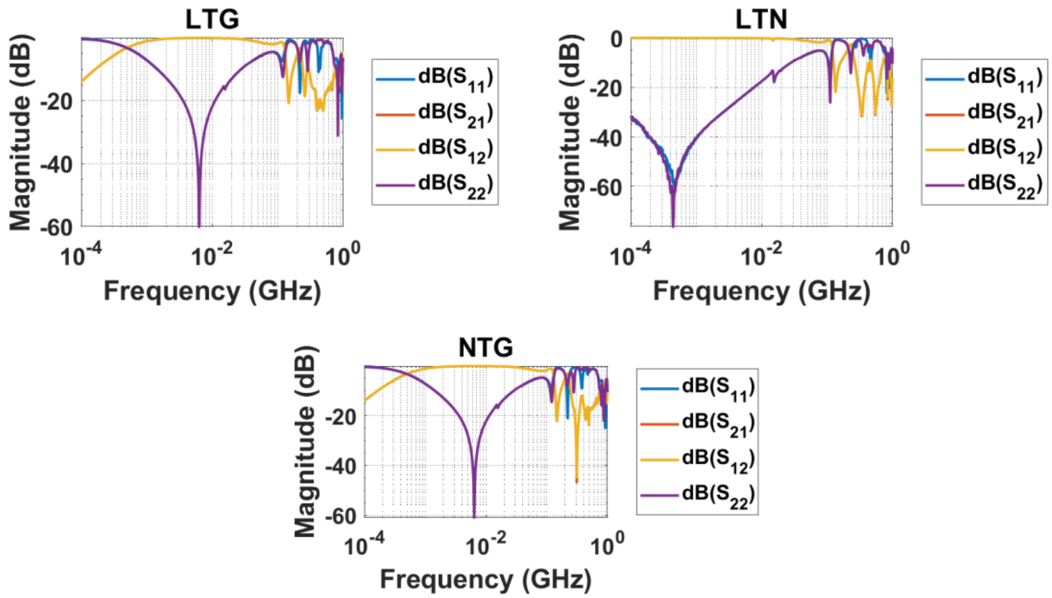

Figure D-40. DUT10 20 kV Network Parameters, Single-Ended Configuration

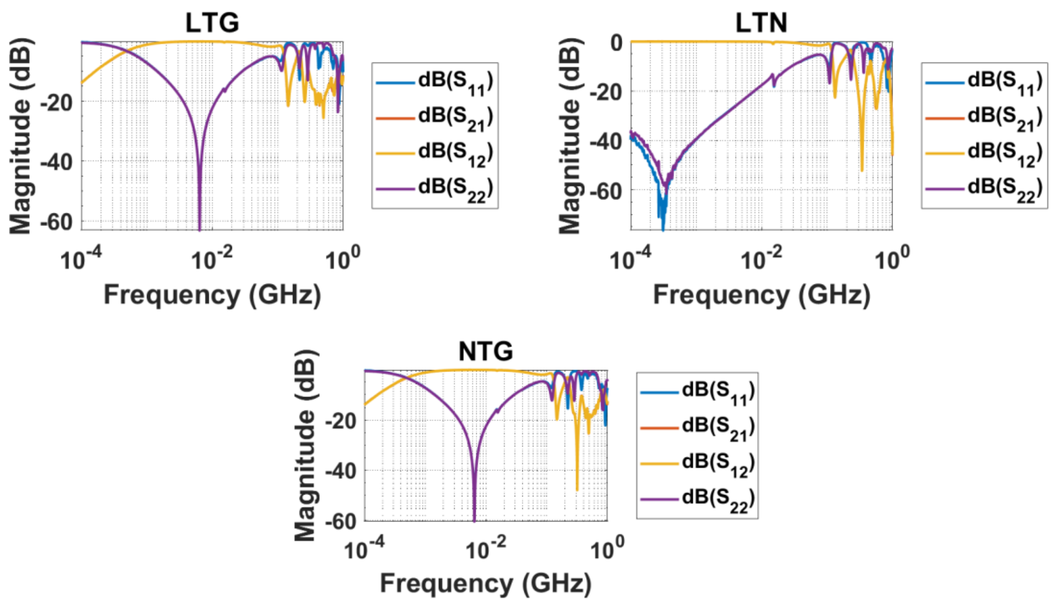

Figure D-41. DUT10 50 kV Network Parameters, Single-Ended Configuration

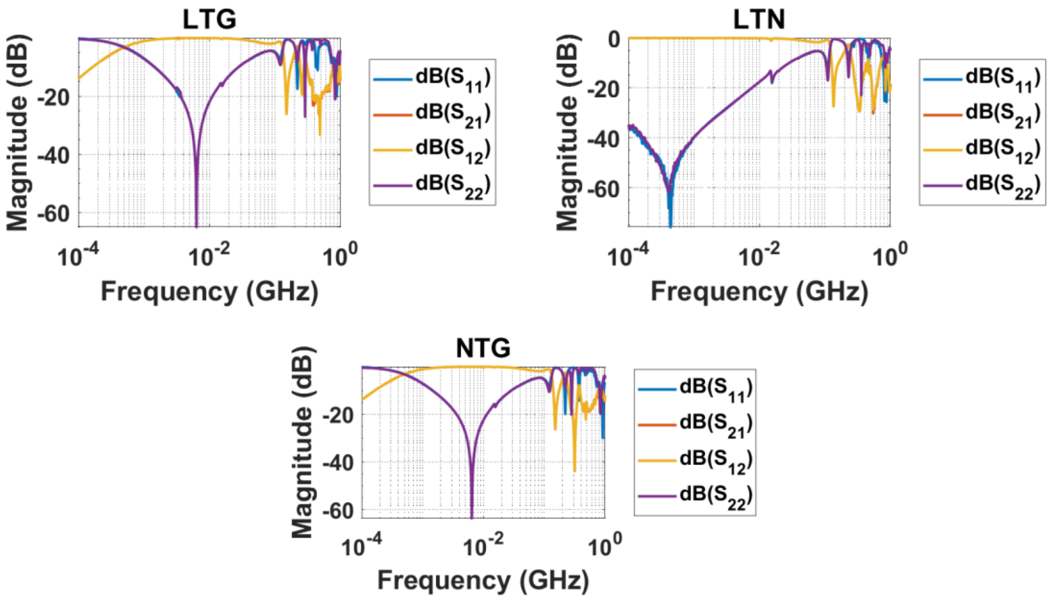

Figure D-42. DUT10 80 kV Network Parameters, Single-Ended Configuration

DISTRIBUTION

Email—Internal

Name	Org.	Sandia Email Address
Steve Glover	01353	sfglove@sandia.gov
Ross Guttromson	08812	rguttro@sandia.gov
Matt Halligan	01353	mhallig@sandia.gov
Craig Lawton	08141	crlawto@sandia.gov
Rodrigo Llanes	01353	rllanes@sandia.gov
Technical Library	01977	sanddocs@sandia.gov

Email—External (encrypt for OUO)

Name	Company Email Address	Company Name
Nikita Dougan	ndd@unm.edu	University of New Mexico
Ken Le	kvl@unm.edu	University of New Mexico
Jane Lehr	jmlehr@unm.edu	University of New Mexico
David Sanabria	desanabriad@unm.edu	University of New Mexico

This page left blank

This page left blank

Sandia National Laboratories is a multimission laboratory managed and operated by National Technology & Engineering Solutions of Sandia LLC, a wholly owned subsidiary of Honeywell International Inc. for the U.S. Department of Energy's National Nuclear Security Administration under contract DE-NA0003525.